

AEROSPACE INFORMATION REPORT

SAE,	AIR1168/2
------	-----------

REV. A

Issued Reaffirmed Stabilized 2001-08 2007-12 2011-07

Superseding AIR1168/2

Heat and Mass Transfer and Air-Water Mixtures

RATIONALE

This document has been determined to contain basic and stable technology which is not dynamic in nature.

STABILIZED NOTICE

This document has been declared "Stabilized" by the AC-9 Technical Committee and will no longer be subjected to periodic reviews for currency. Users are responsible for verifying references and continued suitability of technical requirements. Newer technology may exist.

PREFACE

This document is one of 14 Aerospace Information Reports (AIR) of the Third Edition of the SAE Aerospace Applied Thermodynamics Manual. The manual provides a reference source for thermodynamics, aerodynamics, fluid dynamics, heat transfer, and properties of materials for the aerospace industry. Procedures and equations commonly used for aerospace applications of these technologies are included.

In the Third Edition, no attempt was made to update material from the Second Edition nor were SI units added. However, all identified errata were corrected and incorporated and original figure numbering was retained, insofar as possible.

The SAE AC-9B Subcommittee originally created the SAE Aerospace Applied Thermodynamics Manual and, for the Third Edition, used a new format consisting of AIR1168/1 through AIR1168/10. AIR1168/11 through AIR1168/14 were created by the SAE SC-9 Committee.

The AIRs comprising the Third Edition are shown below. Applicable sections of the Second Edition are shown parenthetically in the third column.

AIR1168/1 Thermodynamics of Incompressible and

Compressible Fluid Flow

(1A,1B)

AIR1168/2

Heat and Mass Transfer and Air-Water

Mixtures

(1C,1D,1E)

AIR1168/3

Aerothermodynamic Systems Engineering

and Design

(3A,3B,3C,3D)

AIR1168/4

Ice, Rain, Fog, and Frost Protection

, , ,

(3F)

AIR1168/5

Aerothermodynamic Test Instrumentation

and Measurement

(3G)

SAE Technical Standards Board Rules provide that: "This report is published by SAE to advance the state of technical and engineering sciences. The use of this report is entirely voluntary, and its applicability and suitability for any particular use, including any patent infringement arising therefrom, is the sole responsibility of the user."

SAE reviews each technical report at least every five years at which time it may be reaffirmed, revised, or cancelled. SAE invites your written comments and suggestions. Copyright © 2011 SAE International

All rights reserved. No part of this publication may be reproduced, stored in a retrieval system or transmitted, in any form or by any means, electronic, mechanical, photocopying, recording, or otherwise, without the prior written permission of SAE.

TO PLACE A DOCUMENT ORDER:

SAE WEB ADDRESS:

877-606-7323 (inside USA and Canada) +1 724-776-4970 (outside USA)

Tel: +1 724-776-49 Fax: 724-776-0790

Email: CustomerService@sae.org

http://www.sae.org

Tel:

SAE values your input. To provide feedback on this Technical Report, please visit

http://www.sae.org/technical/standards/AIR1168/2A

PREFACE (Continued)

AIR1168/6	Characteristics of Equipment Components, Equipment Cooling System Design, and Temperature Control System Design	(3H,3J,3K)
AIR1168/7	Aerospace Pressurization System Design	(3E)
AIR1168/8	Aircraft Fuel Weight Penalty Due to Air Conditioning	(31)
AIR1168/9	Thermophysical Properties of the Natural Environment, Gases, Liquids, and Solids	(2A,2B,2C,2D)
AIR1168/10	Thermophysical Characteristics of Working Fluids and Heat Transfer Fluids Spacecraft Boost and Entry Heat Transfer	(2E,2F)
AIR1168/11	Spacecraft Boost and Entry Heat Transfer	(4A,4B)
AIR1168/12	Spacecraft Thermal Balance	(4C)
AIR1168/13	Spacecraft Equipment Environmental Control	(4D)
AIR1168/14	Spacecraft Life Support Systems	(4E)

F. R. Weiner, formerly of Rockwell International and past chairman of the SAE AC-9B Subcommittee, is commended for his dedication and effort in preparing the errata lists that were used in creating the Third Edition.

TABLE OF CONTENTS

SECTION 1C - HEAT TRANSFER

1.	INTRODUCTION	12
1.1	Scope	12
1.2	Nomenclature	
1.3	Common Abbreviations	14
2.	CONDUCTION	16
0.4	Mechanism of Heat Conduction Steady-State Heat Transfer Transient Heat Transfer General Energy Equation	40
2.1	Mechanism of Heat Conduction	10
2.1.1	Steady-State Heat Transfer	17
2.1.2	Transient Heat Transfer	17
2.2	General Energy Equation	18
2.2.1	Rectilinear Coordinates	18
2.2.2	Cylindrical Coordinates	19
2.2.3	Spherical Coordinates	20
2.2.4	Transient Heat Transfer General Energy Equation Rectilinear Coordinates Cylindrical Coordinates Spherical Coordinates Initial and Boundary Conditions Steady-State Heat Conduction in One Dimension	20
2.3	Steady-State Heat Conduction in One Dimension	21
2.3.1	Heat Flow Between Parallel Walls (Slab)	21
2.3.2	Heat Flow Through a Cylinder	22
2.3.3	Heat Flow Between Parallel Walls (Slab)	23
2.3.4	Heat Flow Through Composite Materials	23
2.4	Steady-State Heat Conduction in Two and Three Dimensions	
2.4.1	Conduction Shape Factors	
2.5	Steady-State Heat Conduction With Convection as a Boundary Condition	
2.6	Heat Transfer Through Fins in Steady State	
2.6.1	General Nomenclature	
2.6.2	Finite Length Rectangular Fin	
2.6.3	Annular Fin	
2.6.4	Finite Length Fin With Constant Heat Flux Near One End	
2.6.5	Finite Length Fin With Step Change in Convective Heating Near One End	
2.6.6	A Finite Length and an Infinitely Long Fin Welded Together Near One End	
2.6.7	Two Finite Length Fins Welded Together Near One End	
2.6.8	Fin Effectiveness of a Welded Double Skin	
2.6.9	Fin That is Heated by a Blanket and Loses Heat at One End	38
2.6.10	Fin Heated by a Blanket With a Linearly Varying Heat Flux	
2.7	Transient Heat Conduction	
2.7.1	Solid of Infinite Thermal Conductivity	
2.7.2	Semi-Infinite Solid With Known Surface Temperature	
2.7.3	Semi-Infinite Solid With Convection at the Surface	
2.7.4	Semi-Infinite Solid With Constant Heat Flux at the Surface	
2.7.5	Slab With Convection at the Faces	
_ · · · -		

TABLE OF CONTENTS (Continued)

2.7.6	Infinitely Long Cylinder With Convection Over the Surface	44
2.7.7	Solid Sphere With Convection Over the Surface	
2.7.8	Infinitely Long Fin	
2.7.9	Heat Flow in Two and Three Dimensions	47
2.8	Numerical Methods	
2.8.1	Conformal Mapping	
2.8.2	Relaxation	
2.8.3	Schmidt Plot	
2.8.4	Resistance - Capacitance Networks	61
	200	
3.	CONVECTION Heat Transfer Coefficient Dimensionless Parameters Basic Boundary Layer Concepts Boundary Layer Thickness	62
0.4	Heat Transfer Coefficient	00
3.1	Heat Transfer Coefficient	62
3.2	Dimensionless Parameters	63
3.3	Basic Boundary Layer Concepts	64
3.3.1	Boundary Layer Thickness	66
3.4	Free Convection Mechanism Free Convection in Open Spaces	67
3.4.1	Mechanism	67
3.4.2	Free Convection in Open Spaces	68
3.4.3	Free Convection in Enclosed Spaces	72
3.5	Forced Convection in Incompressible Flow	75
3.5.1	Laminar and Turbulent Flow	76
3.5.2		
3.5.3	Transition and Effective Turbulent Orgin	85
3.5.4	Nonisothermal Walls	
3.6	Forced Convection in Compressible Flow	
3.6.1	Definitions	
3.6.2	Evaluation of Fluid Properties	89
3.6.3	Flow Over Flat Plates	92
3.6.4	Wedges and Cones in Supersonic Flow	93
3.6.5	Blunt Body Heat Transfer	94
3.6.6	Surface Equilibrium Temperature	
3.7	Compact Heat Exchangers	99
4.	RADIATION	104
4.1	Definition	104
4.2	Kirchhoff's Law	
4.3	Planck's Law	
4.4	Stefan-Boltzmann Law	
4.5	Wien's Displacement Law	
4.6	Lambert's Cosine Law	

TABLE OF CONTENTS (Continued)

4.7	Radiation Between Solids	109
4.7.1	Elemental Black Surfaces	109
4.7.2	Finite Black Surfaces	110
4.7.3	Gray Body Radiation	111
4.7.4	Radiation Heat Transfer Coefficient	
4.7.5	Configuration Factors	113
4.7.6	Celestial Radiation	145
4.7.7	Radiation from Luminous Gases	
4.7.8	Radiation from Nonluminous Gases	146
	ე <u>ბ</u>	
5.	REFERENCES	147
	VOC.	
SECTION	1D - MASS TRANSFER	
	REFERENCES. 1D - MASS TRANSFER INTRODUCTION. Scope Relationship Between Convection and Evaporation.	4.40
1.	INTRODUCTION	149
1.1	Soons	140
1. 1 1.1.1	Polationship Retugen Convection and Evaporation	149 140
1. 1. 1	Trelationship between Convection and Evaporation	143
2.	SURFACE EVAPORATION INTO A GAS ATMOSPHERE	150
	XX.	
2.1	Diffusion	150
2.1.1	Nomenclature	150
2.1.2	Diffusion in Laminar Flow	152
2.1.3	Illustrative Example of Diffusion in Laminar Flow	154
2.1.4	Diffusion in Turbulent Flow	156
2.2	Diffusion and Convection	
2.2.1	Derivation of the Equations Relating Diffusion and Convection	157
_		
3.	SUBLIMATION	161
4.	CONDENSATION	162
4.4	N a va a va a libert. Va	460
4.1 4.1.1	NomenclatureGeneral	
4.2 4.2.1	Heat Transfer Coefficient for Condensing Pure Saturated Vapor Horizontal Tubes	
4.2.1 4.2.2	Vertical and Inclined Surfaces	
4.2.2 4.2.3	Film Thickness on a Vertical Surface	
4.2.3 4.2.4	Effect of Vapor Velocity	
4.2.4 4.3	Effect of Noncondensable Gas	
٦.٥	Lifect of Nortonide Isable Ods	100

TABLE OF CONTENTS (Continued)

168 169 170 170 171
169 170 170 171 173
170 170 171 173
170 171 173
171 173
173
474
174 174 175 176
174
175
175
176
179
180
180
181
181 183 183
100
103 103
103
184
104
185
189
190
192
193
193 193 194

LIST OF FIGURES

FIGURE 1	Curvilinear Orthogonal Coordinate System	. 18
FIGURE 2	Cylindrical Coordinates	. 19
FIGURE 3	Spherical Coordinates	. 20
FIGURE 4	Heat Flow Between Parallel Plates	22
FIGURE 5	Heat Flow Through a Cylinder	
FIGURE 6	Heat Flow Through a Sphere	. 23
FIGURE 7	Heat Transfer in a Slab	. 24
FIGURE 8	Heat Transfer in a Cylinder	
FIGURE 9	Heat Transfer in a Sphere	
FIGURE 10	Finite Length Rectangular Fin	
FIGURE 11	Annular Fin (No Temperature Drop Assumed Through Vertical Cylinder Wall)	
FIGURE 12	Efficiency of Annular Fins of Constant ThicknessFin With Constant Heat Flux Near One End	. 30
FIGURE 13	Fin With Constant Heat Flux Near One End	32
FIGURE 14	Fin With a Step Change in Convective Heating Near One End	. 33
FIGURE 15	Fins of Different Materials Joined at One End	. 34
FIGURE 16	Fins of Finite Length Joined Near One End	. 35
FIGURE 17	Effectiveness of Welded Double Skin	. 36
FIGURE 18	Loss of Heat at One End of Fin	. 38
FIGURE 19	Fin Heated With Blanket; Linear Varying Heat Flux	
FIGURE 20	Solid of Infinite Thermal Conductivity	
FIGURE 21	Semi-Infinite Solid With Known Surface Temperature	
FIGURE 22	Semi-Infinite Solid With Convection at the Surface	
FIGURE 23	Semi-Infinite Solid With Constant Heat Flux at the Surface	
FIGURE 24	Slab With Convection at the Faces	
FIGURE 25	Infinitely Long Cylinder With Convection Over the Surface	
FIGURE 26	Solid Sphere With Convection Over the Surface	
FIGURE 27	Transient Temperature Rise of Fin	
FIGURE 28	Region of a Long Vinder Near One End	
FIGURE 29	Finite Cylinder	
FIGURE 30	Region Near the Intersection of Two Perpendicular Faces of a Large Solid	
FIGURE 31	Region Near the Corner of Three Perpendicular Faces of a Large Solid	
FIGURE 32	Region of a Semi-Infinite Slab	
FIGURE 33	Region of a Quarter-Infinite Slab	
FIGURE 34	Infinite Rectangular Rod	
FIGURE 35	Semi-Infinite Rectangular Rod	. 53
FIGURE 36	Parallelopiped	
FIGURE 37	Conformal Mapping	
FIGURE 38	Steady Heat Transfer Into One, Two, or Three Dimensions	
FIGURE 39	A Nodes.	
FIGURE 40	B Nodes	
FIGURE 41	Initial Guess of Temperature Distribution	
FIGURE 42	Schmidt Plot	59

FIGURE 43	Boundary Layer Along a Flat Surface Parallel to Direction of Flow	64
FIGURE 44	Regions of Turbulent Bondary Layers	
FIGURE 45	Transition Region of Laminar to Turbulent Flow	66
FIGURE 46	Free Convection Heat Transfer Parameter $Y = (\rho g)^2 g \beta c_p / \mu k$	68
FIGURE 47	Sketch of a Vertical Plate or Cylinder	
FIGURE 48	Sketch of a Horizontal Cylinder	69
FIGURE 49	Horizontal Square Plate (Hot Face Up or Cooled Face Down)	
FIGURE 50	Horizontal Square Plate (Hot Face Down or Cooled Face Up)	
FIGURE 51	Sphere	
FIGURE 52	Vertical Parallel Plate	
FIGURE 53	Horizontal Parallel Plates Horizontal Annular Enclosed Space	73
FIGURE 54	Horizontal Annular Enclosed Space	74
FIGURE 55	Free Convection in Enclosed Space (Air at 70 °F)	/5
FIGURE 56	Flat Plate	77
FIGURE 57	Cylinder With External Flow Parallel to Axis	77
FIGURE 58	Duct Flow Skin Friction Coefficient Versus Reynolds Number at Edge	
	of Boundary LayerCylinder With External Flow Normal to Axis	78
FIGURE 59	Cylinder With External Flow Normal to Axis	79
FIGURE 60	Round Tube With Parabolic Velocity Distribution	79
FIGURE 61	Rectangular Tube With Parabolic Velocity Distribution	
FIGURE 62	SphereFlat Plate	80
FIGURE 63		
FIGURE 64	Cylinder With External Flow Parallel to Axis	81
FIGURE 65	Duct (Channel) With Flow Near Entrance	82
FIGURE 66	Channel Flow, Fully Developed	83
FIGURE 67	Laminar Heat Transfer on a Wedge (Subsonic Flow)	
FIGURE 68	Effective Turbulent Length as a Function of Turbulent Heat Transfer	
FIGURE 69	Typical Boundary Layer Temperature Profiles	
FIGURE 70	High Speed Flow Reference Temperature	
FIGURE 71	Surface Equilibrium Temperature	96
FIGURE 72	Wall Equitibrium Temperature for Aerodynamic Heating With Arbitrary	
	Heat Load	97
FIGURE 73	Stagnation Point Radiation Equilibrium Temperature, ϵ = 0.9, r = 2 ft	
	(ARDC 1956 Atmosphere)	
FIGURE 74	Counterflow Exchanger Performance	
FIGURE 75	Cross Flow Exchanger With Fluids Unmixed	
FIGURE 76	Multipass Cross Counterflow Exchanger; $C_{min}/C_{max} = 1$	
FIGURE 77	One to Two Parallel Counterflow Exchanger Performance	104
FIGURE 78	Monochromatic Radiation Intensity of a Black Body in the	
_	Direction Normal to the Surface. λ = Wavelength in Microns	
FIGURE 79	Directional Radiation of Typical Metals (a) and of Electrically Nonconducting	
	(Non-metal) Surfaces (b) Compared to a Lambert Surface	109

FIGURE 80	Sketch Showing Transfer of Energy From One Surface to Another	110
FIGURE 81	Three Body Radiation	
FIGURE 82	Radiation Heat Transfer Coefficient for Black Body Radiation	113
FIGURE 83	Plane Point Source and Plane Rectangle	
FIGURE 84	Plane Point Source and Plane Rectangle; Derivation of Equation 346	114
FIGURE 85	Plane Point Source and Plane Rectangle Intersecting at Angle φ	
FIGURE 86	Planes Intersecting at ϕ = 30°	
FIGURE 87	Planes Intersecting at ϕ = 60°	117
FIGURE 88	Planes Intersecting at ϕ = 90°	117
FIGURE 89	Planes Intersecting at ϕ = 120°	118
FIGURE 90	Planes Intersecting at φ = 150°	118
FIGURE 91	Spherical Point Source and Plane Rectangle With One Common Side	119
FIGURE 92	Two Angles Intersecting at ϕ = 90°; Derivation of Equations 360 and 361	
FIGURE 93	Plane Point Source and Plane Circular Disk	120
FIGURE 94	Plane Point Source and Plane Circular Disk; Derivation of Equation 366	121
FIGURE 95	Line Moving Parallel to Itself and Plane at Point Source dA ₁	121
FIGURE 96	Intersection of a Plane of Point Source dA ₁ and an Infinite Plane A ₂	122
FIGURE 97	Intersection of Planes of a Point Source and a Disk	122
FIGURE 98	Plane Point Source and Right Circular Cylinder	123
FIGURE 99	Plane Point Source and Right Circular Wlinder; Derivation of Equation 376	124
FIGURE 100	Concentric Cylinders With the Larger Having an Inside Point Source	124
FIGURE 101	Concentric Cylinders; Derivation of Equation 381	125
FIGURE 102	Plane Point Source and a Plane Trapezoid	126
FIGURE 103	Plane Point Source and a Plane Trapezoid; Derivation of	
	Equation 384; φ = 90°	127
FIGURE 104	Intersecting Planes of a Point Source and a Trapezoid	127
FIGURE 105	Intersecting Planes of a Point Source and a Trapezoid;	
	Derivation of Equation 390; ϕ = 90°	128
FIGURE 106	Parallel Line Source Plane and Rectangle Plane, With One Opposite Edge	129
FIGURE 107	Line Source and Rectangle Planes; Plot of Equation 396	130
FIGURE 108	Intersection of Planes of a Line Source and Rectangle	130
FIGURE 109	Line Source and Rectangle Planes; Intersection at $\phi = 30^{\circ}$	132
FIGURE 110	Line Source and Rectangle Planes; Intersection at $\phi = 60^{\circ}$	132
FIGURE 111	Line Source and Rectangle Planes; Intersection at ϕ = 90° (See Figure 108)	133
FIGURE 112	The Source and Rectangle Planes; Intersection at ϕ = 120° (See Figure 108)	133
FIGURE 113	Line Source and Rectangle Planes; Intersection at ϕ = 150° (See Figure 108)	134
FIGURE 114	Line Source and Right Circular Cylinder	134
FIGURE 115	Line Source and Right Circular Cylinder	
FIGURE 116	Concentric Cylinders With Line Source Inside the Larger One	135
FIGURE 117	Concentric Cylinders, One Inside Line Source	
FIGURE 118	Infinitely Long Cylinder and Infinite Plane, Mutually Parallel	137

FIGURE 119	Identically Parallel, Directly Opposed Rectangles	137
FIGURE 120	Parallel, Opposed Rectangles; Per Equation 413	
FIGURE 121	Two Rectangles With Common Edge and Included Angle	
FIGURE 122	Included Angle (Figure 121) φ = 30°	
FIGURE 123	Included Angle (Figure 121) $\phi = 60^{\circ}$	
FIGURE 124	Included Angle (Figure 121) ϕ = 90°	141
FIGURE 125	Included Angle (Figure 121) φ = 120°	142
FIGURE 126	Included Angle (Figure 121) φ = 150°	142
FIGURE 127	Parallel, Directly Opposed, Plane Circular Disks	142
FIGURE 128	Parallel, Opposed Plane Circular Disks; Per Equation 424	143
FIGURE 129	Parallel, Concentric Cylinders	143
FIGURE 130	Concentric Shapes	144
FIGURE 131	Parallel, Concentric Cylinders Concentric Shapes Cylinder Parallel to Plane of Rectangle	144
FIGURE 132	Diagram of a Liquid Evaporating Into a Gaseous Atmosphere	149
FIGURE 133	Dimensionless Relationship Between Evaporation and Convection	
	(Reference 1)	150
FIGURE 134	Relationship for KT/ ε_{AB} Versus f(θ) (Reference 20)	153
FIGURE 135	Relationship for Obtaining k _q from Table 6 (Reference 2)	157
FIGURE 136	P_BX as a Function of t_s and t_∞ with Water on the Surface	159
FIGURE 137	Altitude Versus Surface Temperature as a Function of P _s /P _B	
FIGURE 138	X (for Sublimation) Versus Surface Temperature	
FIGURE 139	P _B X as a Function of t _s and t _∞ for toe Subliming Into Air	
FIGURE 140	Recommended Data for Vertical Surfaces (Reference 3)	
FIGURE 141	Regimes of Boiling	
FIGURE 142	Nucleate Boiling Heat Flux for Saturated Liquids (Reference 3)	170
FIGURE 143	Peak Heat Flux Correlation for Forced Convection (Reference 32)	
	Note: 94% of the Points are Contained Within the ±33% Lines	172
FIGURE 144	Recovery Factor Versus Mass Transfer With a Laminar Boundary Layer	
	(Based on Theory of Reference 10)	176
FIGURE 145	Skin Friction Versus Mass Transfer With a Laminar Boundary Layer	
	(Based on Theory of Reference 10)	177
FIGURE 146	Analytic Curves for CO ₂ and Air With a Laminar Boundary Layer	
	(Based on Theory of Reference 10)	178
FIGURE 147	Effect of Reynolds Number on Heat Transfer Characteristics	
	Molecular Weight of Injectant = 29 (Based on Theory of Reference 11)	179
FIGURE 148	Effect of Mass Transfer Injectant Upon Heat Transfer for Turbulent	
	Boundary Layer	179
FIGURE 149	Effect of Mass Transfer Injectant Molecular Upon Weight Upon Heat	
51011DE :	Transfer for Turbulent Boundary Layer	
FIGURE 150	Psychrometric Chart, Sea Level	
FIGURE 151	Psychrometric Chart	
FIGURE 152	Adiabatic Humidification	189

FIGURE 153 FIGURE 154	Condensation From Supersaturated VaporCooling in the Absence of Liquid Water	
FIGURE 155 FIGURE 156	Heating a Saturated Vapor in the Absence of Liquid Water Heating a Saturated Vapor in the Presence of a Small Amount	
TIGORE 100	of Liquid Water	191
	LIST OF TABLES	
TABLE 1	Shape Factors Calculation Sheet Location of Transient Temperature Points for Schmidt Plot Estimates for Transition Reynolds Numbers Values of Diffusion Factors Turbulent Flow Factors Function $f(\alpha_1)$ Values of F_c and Δt	27
TABLE 2	Calculation Sheet	58
TABLE 3	Location of Transient Temperature Points for Schmidt Plot	60
TABLE 4	Estimates for Transition Reynolds Numbers	85
TABLE 5	Values of Diffusion Factors	154
TABLE 6	Turbulent Flow Factors	156
TABLE 7	Function $f(\alpha_1)$	165
TABLE 8	Values of F _c and Δt	166

Function f(\alpha_1) 165
Values of F_c and \(\Delta t \) 166
Surface-Liquid Combinations (Reference 6) 169

169

Circle to view the contract of the contract

TABLE 9

SECTION 1C - HEAT TRANSFER

1. INTRODUCTION:

1.1 Scope:

Heat transfer is the transport of thermal energy from one point to another. Heat is transferred only under the influence of a temperature gradient or temperature difference. The direction of heat transfer is always from the point at the higher temperature to the point at the lower temperature, in accordance with the second law of thermodynamics. The fundamental modes of heat transfer are conduction, convection, and radiation. Conduction is the net transfer of energy within a fluid or solid occurring by the collisions of molecules, atoms, or electrons. Convection is the transfer of energy resulting from fluid motion. Convection involves the processes of conduction, fluid motion, and mass transfer. Radiation is the transfer of energy from one point to another in the absence of a transporting medium. In practical applications several modes of heat transfer occur simultaneously. For example, aerodynamic heating of a vehicle surface includes convection to the surface, radiation away from the surface, and conduction through the surface structure. Since the three modes of heat transfer obey different laws, a real insight into such a problem can be gained only after they have been studied separately.

1.2 Nomenclature:

This list contains the nomenclature used in this section. There are additional symbols defined in certain paragraphs directly as they are used.

```
= Velocity of sound, ft/s
а
            = Area, ft<sup>2</sup>, in<sup>2</sup>
Α
            = Specific heat, Btu/lb-°F
С
            = Skin friction coefficient, dimensionless
C_f
            = Specific heat capacity at constant pressure, Btu/lb-°F
c_p
            = Specific heat capacity at constant volume, Btu/lb-°F
С
            = Speed of light, ft/s
D
            = Diameter, ft in
            = Self-diffusion coefficient (molecular diffusivity), ft<sup>2</sup>/s
D
            = Base of the Naperian (natural) logarithm, 2.718...
е
            = Exponent
exp
Ε
            = Electrical potential, volts
f
            = Friction factor, Darcy or Fanning, dimensionless
F
            = Configuration factor, dimensionless
            = Gravitational acceleration, ft/s<sup>2</sup>
g
            = Specific weight (density), lb/ft<sup>3</sup>
gρ
            = Weight flow rate per unit area, lb/h-ft<sup>2</sup>
G
            = Surface heat transfer coefficient, convection, Btu/h-ft<sup>2</sup>-°F
h
            = Planck's constant, dimensionless
h
```

1.2 (Continued):

```
h
             Specific enthalpy, Btu/lb
             = Enthalpy, Btu/lb
             = Current, amperes
             = Intensity of radiation, Btu/h-ft<sup>2</sup>
             = Mechanical equivalent of heat, 778 ft-lb/Btu
             = Colburn Modulus, (N<sub>St</sub>N<sub>Pr</sub><sup>2/3</sup>), dimensionless
             = Thermal conductivity, Btu-ft/h-ft<sup>2</sup>-°F
k
K
             = Boltzmann's constant, dimensionless
L
             = Length, ft, in
m
             = Mass, lb
             = Mach number, (V/a), dimensionless
Μ
N_{\text{Eu}}
             = Euler number, (g\Delta p/\rho gV^2), dimensionless
            = Grashof number, (\Delta tx^3(\rho g)^2g\beta/\mu^2), dimensionless
N_{Gr}
G_{Gz}
             = Graetz number, (Wc<sub>p</sub>/kx), dimensionless
N_{Kn}
             = Knudsen number, (\lambda_m/x), dimensionless
             = Lewis number, (N<sub>Sc</sub>/N<sub>Pr</sub>), dimensionless
N_{Le}
             = Nusselt number, (hD/k) or (hx/k), dimensionless
N_{Nu}
             = Prandtl number, (µgc<sub>p</sub>/k), dimensionless
N_{Pr}
             = Reynolds number, (VDρg/μ), dimensionless
N_{Re}
             = Schmidt number, (μ/ρgD), dimensionless
N_{Sc}
S_{St}
             = Stanton number (N_{Nu}/N_{Re}N_{Pr}) = (h/3600 \rho g V c_p), dimensionless (Note: The use of
               3600 depends on whether V is in ft/s or ft/h)
NTU
             = Number of transfer units, dimensionless
             = Pressure, psi, lb/ft<sup>2</sup>, in Hg
P or p
             = Rate of heat transfer, Btu/min, Btu/h
q
             = Radius, ft, in
r
             = Recovery factor, dimensionless
             = Resistance, ohms
R
R
             = Universal gas constant, ft-lb/lb-°R
             = Temperature, °F-
t
Т
             = Temperature, R
U
             = Overall conductance, Btu/h-ft-°F
             = Local velocity, ft/s, ft/min
٧
             = Specific volume, ft<sup>3</sup>/lb
V
٧
             = Velocity, ft/s, ft/min, ft/h
             = Weight flow rate, lb/h
W
             = Distance, ft
Х
             = Thermal diffusivity, k/ρgc<sub>p</sub>, ft<sup>2</sup>/h
α
             = Coefficient of volumetric expansion, °F-1
β
             = Emissivity, emittance, dimensionless
ε
             = Effectiveness, dimensionless
3
             = Efficiency, effectiveness, dimensionless
η
             = Absolute viscosity, lb/s-ft, lb/h-ft
             = Mass density, lb-s<sup>2</sup>/ft<sup>4</sup>
ρ
             = Specific weight (density), lb/ft<sup>3</sup>
ρg
```

1.2 (Continued):

9 = Partial

= Stefan-Boltzmann constant (0.173 x 10⁻⁸), Btu/h-ft²-°R⁴ σ

= Time, s, h τ

= Shearing stress, psi τ

= Transmissivity, dimensionless

λ = Wavelength, microns

= Molecular mean free path, ft = Sweep angle, degrees

Subscripts

= Average av = Adiabatic wall aw = Critical crit = Effective eff Т = Total

= Stagnation, static (as locally defined) s, S

= Local Х

1.3 Common Abbreviations:

= Argon Α Α = Ampere(s) abs = Absolute = Aeronautical aero

view the full PDF of air 168 28 = American Institute of Chemical Engineers AICHE

= Aerospace Information Report AIR

= American Amer.

= Argument (function) arg.

= American Society of Mechanical Engineers ASME

= Atmosphere atm = Average a۷ boil = Boiling

Btu (BTU) = British thermal units

Chem. = Chemical

CO = Carbon monoxide = Carbon dioxide CO_2 CH₄ = Methane = Conduction cond = Convection conv

= Cosine cos

= Hyperbolic cosine cosh coth = Hyperbolic cotangent

= Critical crit

1.3 (Continued):

ed. = Edition

eff = Efficiency, effectiveness, effective

Eng. = Engineering Engrs. = Engineers = Equation(s) Eq.(s) = Error function erf

erfc = Complementary error function

et al. = And others (Latin) = Etcetera (and more) etc.

evap = Evaporation exp = Exponent

= Degrees Fahrenheit °F

= Foot (feet) ft (FT) H_2 = Hydrogen He = Helium Hg = Mercury = Hour(s)h

= Institute of Mining Engineers (British), Institution of Mechanical Engineers (British) IME view the full

= Inch(es) in Inc. = Incorporated J. = Journal = Laminar lam lb (LB) = Pound(s)= Limit lim

= Natural logarithm to the base e ln

= Logarithm to the base 10 log

= Meter(s) m = Maximum max min = Minimum = Neon Ne N_2 = Nitrogen N_2O = Nitrogen oxide NO = Nitrous oxide = Number No., no.

NACA = National Advisory Committee for Aeronautics

02 = Oxygen = Page p. pp. = Pages = Progress Progr.

psi = Pounds per square inch

= Pounds per square inch, absolute psia = Pounds per square inch, gage psig

 $^{\circ}$ R = Degrees Rankine

= Radiation rad

1.3 (Continued):

Rev. = Review

RML = Research Memorandum (Lewis) SAE = Society of Automotive Engineers

= Second(s) S = Saturated sat Sci. = Sciences = September Sept.

SI = International System of Units (Système Internationale, France)

= Sine sin

sinh = Hyperbolic sine

Soc. = Society sub = Subcooled = Tangent tan

= Hyperbolic tangent tanh = Temperature temp TN = Technical Note TR = Technical Report

tot = Total

Trans. = Transactions = Turbulent turb

UAC = United Aircraft Corp.

= Volt(s)Vol (Vol.) = Volume W = Watt(s)

view the full PDF of air 168 28 = Wright Air Development Cente WADC

= Increment or difference Δ = Micron (10⁻⁶ meter) μ = Partial derivative 9

2. CONDUCTION:

2.1 Mechanism of Heat Conduction:

The study of conductive heat transfer within a system (body) includes a study of the effect of the surroundings, or boundary conditions, upon the system. These boundary conditions may consist of convective, conductive, or radiant heat transfer or an arbitrary heat input rate. The system will react by transferring heat within itself by conduction, which is the flow of heat from a hotter to a cooler area by a kinetic interchange between colliding particles (molecules, atoms, or electrons) or by a change in the thermal storage, or both, which is the absorption of internal energy (molecule vibration) accompanied by a change in temperature or of the state of the system. All these effects may be related mathematically through a series of differential equations, and the solutions may be divided broadly into steady and unsteady state (transient) heat transfer problems.

2.1.1 Steady-State Heat Transfer: A steady-state condition may be defined to exist when the flow of heat and the temperature distribution within the system are functions of position only and are independent of time. Under these circumstances, heat may be transferred by conduction only (in the absence of internal radiation or convective currents). It has been established empirically that the rate of heat flow by conduction, q, in Btu/h, between two parallel planes of area A a distance x apart and at temperatures t₁ and t₂ may be expressed as

$$q = \frac{kA (t_1 - t_2)}{x}$$
 (Eq. 1)

where:

k = Proportionality factor known as the thermal conductivity, a material property

Usually, it is taken to be independent of the direction of heat flow (isotropic medium) and of temperature, so that heat flow is linear with temperature differential. The heat conduction equation (Fourier's law of conduction) may also be expressed in differential form as

$$\frac{q}{A} = -k \frac{dt}{dx}$$
 (Eq. 2)

where:

q/A = Heat flux and is in the direction of negative temperature gradient, dt/dx

2.1.2 Transient Heat Transfer: The unsteady state (transient) condition implies that the heat transfer is time variant, and therefore that energy storage must be considered in addition to heat conduction. This may be expressed in differential form as

$$q = mc \frac{dt}{d\tau}$$
 (Eq. 3)

where:

q = Net heat flow into or out of storage

m = Elemental mass

c = Specific heat per unit mass

 $dt/d\tau = Rate$ of temperature change

It is noted here that mc is a material property and is usually assumed to be independent of temperature.

2.2 General Energy Equation:

The laws of heat conduction and storage expressed in 2.1.1 and 2.1.2 may be combined into what is known as the Fourier-Poisson heat conduction equation. For a generalized, curvilinear orthogonal coordinate system (see Figure 1) with internal heat generation and conductivity allowed to be a function of temperature, this is

$$\frac{1}{\mu\nu\lambda} \left[\frac{\partial}{\partial\eta} \left\{ k \left(\frac{\gamma\lambda}{\mu} \right) \frac{\partial t}{\partial\eta} \right\} + \frac{\partial}{\partial\rho} \left\{ k \left(\frac{\lambda\mu}{\nu} \right) \frac{\partial t}{\partial\rho} \right\} \right]
+ \frac{\partial}{\partial\xi} \left\{ k \left(\frac{\mu\nu}{\lambda} \right) \frac{\partial t}{\partial\xi} \right\} + q' = \rho g c \frac{\partial t}{\partial\tau}$$
(Eq. 4)

where:

 μ dη, λ dξ, and ν dρ = Length of sides of the elemental volume (see Figure 1) μ , λ , and ν = Unit vectors

q' = Time rate of energy generation in the fluid per unit volume, Btu/h-ft³

2.2.1 Rectilinear Coordinates: These are:

$$\mu = \lambda = \nu = (Eq. 5)$$

$$d\xi = dx; d\eta = dy; d\rho = dz$$
 (Eq. 6)

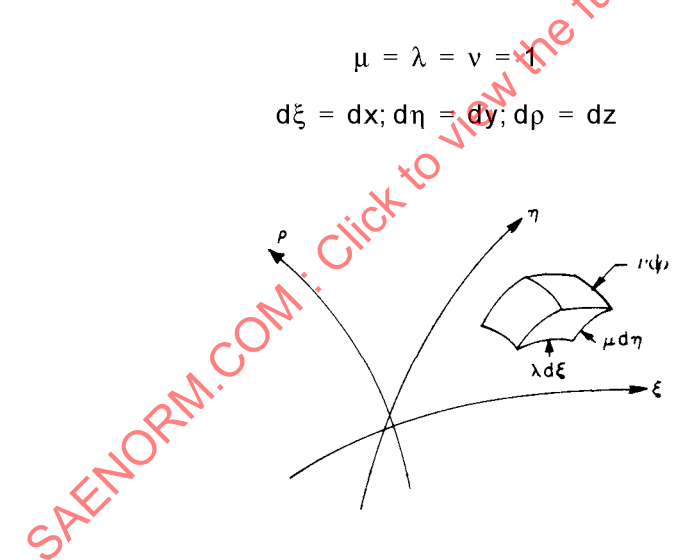


FIGURE 1 - Curvilinear Orthogonal Coordinate System

2.2.1 (Continued):

and for constant conductivity and no internal heat generation:

$$\frac{\partial t}{\partial \tau} = \alpha \left(\frac{\partial^2 t}{\partial x^2} + \frac{\partial^2 t}{\partial y^2} + \frac{\partial^2 t}{\partial z^2} \right)$$
 (Eq. 7)

where:

 $\alpha = k/\rho gc = thermal diffusivity$

2.2.2 Cylindrical Coordinates: Refer to Figure 2.

$$\lambda = 1$$
 $\mu = r$ (Eq. 8)

$$v = 1 d\xi = dz (Eq. 9)$$

$$d\eta = d\phi \qquad d\rho = dr$$
 (Eq. 10)

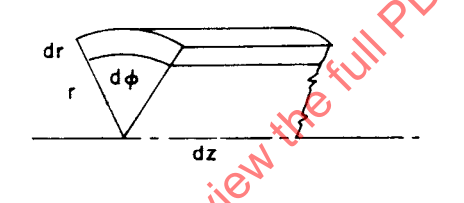


FIGURE 2 - Cylindrical Coordinates

For constant conductivity and no internal heat generation,

$$\frac{\partial t}{\partial r} = \alpha \left(\frac{\partial^2 t}{\partial r^2} + \frac{1}{r} \frac{\partial t}{\partial r} + \frac{1}{r^2} \frac{\partial^2 t}{\partial \phi^2} + \frac{\partial^2 t}{\partial z^2} \right)$$
 (Eq. 11)

For no heat flow in the and z directions (radial flow only),

$$\frac{\partial t}{\partial \tau} = \alpha \left(\frac{\partial^2 t}{\partial r^2} + \frac{1}{r} \frac{\partial t}{\partial r} \right)$$
 (Eq. 12)

2.2.3 Spherical Coordinates: Refer to Figure 3.

$$\mu = 1 \qquad \lambda = r \tag{Eq. 13}$$

$$v = r \sin \phi$$
 $d\eta = dr$ (Eq. 14)

$$d\xi = d\phi$$
 $d\rho = d\psi$ (Eq. 15)

For constant conductivity and no internal heat generation,

$$\frac{\partial t}{\partial \tau} = \frac{\alpha}{r^2} \left(r^2 \frac{\partial^2 t}{\partial r^2} + 2r \frac{\partial t}{\partial r} + \frac{1}{\sin^2 \phi} \frac{\partial^2 t}{\partial \psi^2} + \frac{\partial^2 t}{\partial \phi^2} + \frac{1}{\tan \phi} \frac{\partial t}{\partial \phi} \right)$$
 (Eq. 16)

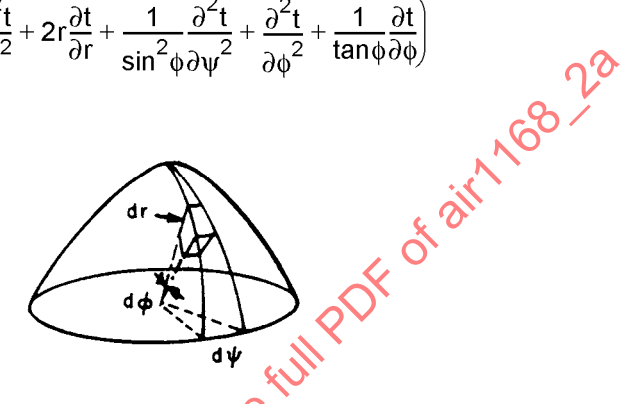


FIGURE 3 - Spherical Coordinates

For radial heat flow only,

$$\frac{\partial t}{\partial r} \propto \left(\frac{\partial^2 t}{\partial r^2} + \frac{2}{r} \frac{\partial t}{\partial r} \right)$$
 (Eq. 17)

2.2.4 Initial and Boundary Conditions: Before the preceding differential equations can be solved for a unique solution of the temperature distribution or heat flow rate, it is necessary to introduce subsidiary equations, which may be described as the temperature distribution at time zero and the conditions at the boundaries of the system which affect the heat flow into or out of the system. From the nature of the equations, it is apparent that it is necessary to specify one initial condition and two boundary conditions for each dimension considered. The specification of the initial condition is self-evident [t(0,x,y,z),etc.], whereas the specification of the boundary condition may take several forms, depending upon the type of heat flow. The most common boundary conditions for the x axis are:

2.2.4 (Continued):

(a) Specified wall temperature:

$$t(\tau, x, y, z) = t_1 \tag{Eq. 18}$$

(b) Insulated wall:

$$\frac{\partial t(\tau, x, y, z)}{\partial x} = 0$$
 (Eq. 19)

(c) Convection:

$$-k\frac{\partial t(\tau,0)}{\partial x} = h(t_0 - t)$$
 (Eq. 20)

(d) Radiation:

$$-k\frac{\partial t(\tau,0)}{\partial x} = \sigma F_{12}[t_0^4 - t^4]$$
coefficient
or

One Dimension:

conduction is that for steady state $(\partial t/\partial \tau = 0)$ and one-dimensional

where:

h = Local heat transfer coefficient

 F_{12} = Configuration factor

2.3 Steady-State Heat Conduction in One Dimension:

> The simplest solution of the heat conduction is that for steady state $(\partial t/\partial \tau = 0)$ and one-dimensional flow with specified wall temperature at each boundary.

Heat Flow Between Parallel Walls (Slab): Refer to Figure 4. 2.3.1

$$ct(0) = t_1$$
 (Eq. 22)

$$t(L) = t_2 (Eq. 23)$$

$$t_x = t_1 - (t_1 - t_2) \frac{x}{L}$$
 (Eq. 24)

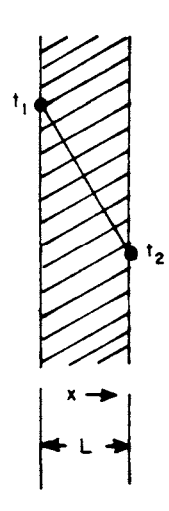


FIGURE 4 - Heat Flow Between Parallel Plates vilinder: Refer to Figure 5. $t(r_1) = t_1$

2.3.2 Heat Flow Through a Cylinder: Refer to Figure 5.

$$t(r_1) = t_1$$
 (Eq. 26)

$$t(r_2) = t_2 \tag{Eq. 27}$$

$$t_r = t_1 - (t_1 - t_2) \frac{\ln(r/r_1)}{\ln(r_2/r_1)}$$
 (Eq. 28)

$$\frac{q}{\text{Unit length}} = \frac{2\pi k(t_1 - t_2)}{\ln(r_2/r_1)}$$
 (Eq. 29)

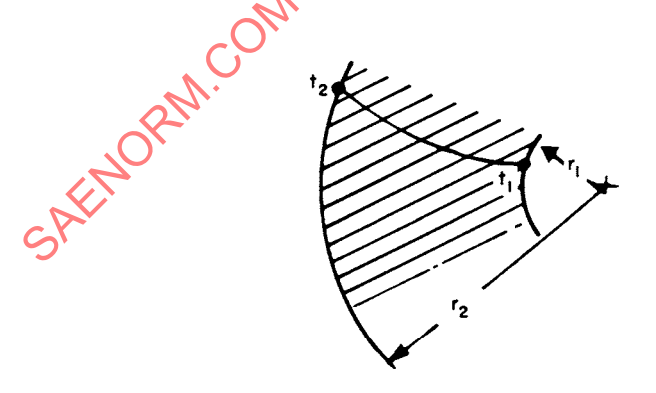


FIGURE 5 - Heat Flow Through a Cylinder

2.3.3 Heat Flow Through a Sphere: Refer to Figure 6.

$$t(r_1) = t_1$$
 (Eq. 30)

$$t(r_2) = t_2$$
 (Eq. 31)

$$t_{r} = t_{1} - \frac{t_{1} - t_{2}}{1 - (r_{1}/r_{2})} + \frac{t_{1} - t_{2}}{[(1/r_{1}) - (1/r_{2})]r}$$
 (Eq. 32)

$$q = \frac{4\pi k(t_1 - t_2)}{(1/r_1) - (1/r_2)}$$
 (Eq. 33)

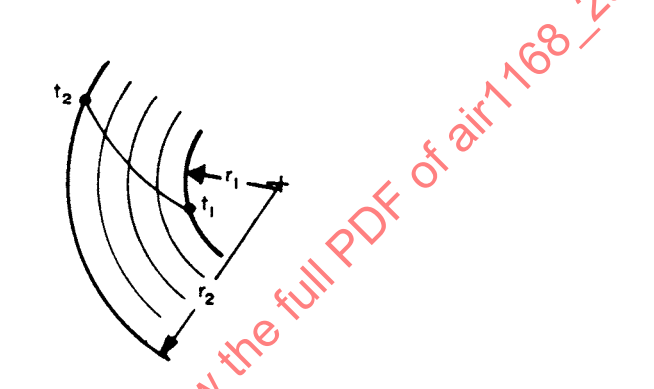


FIGURE 6 - Heat Flow Through a Sphere

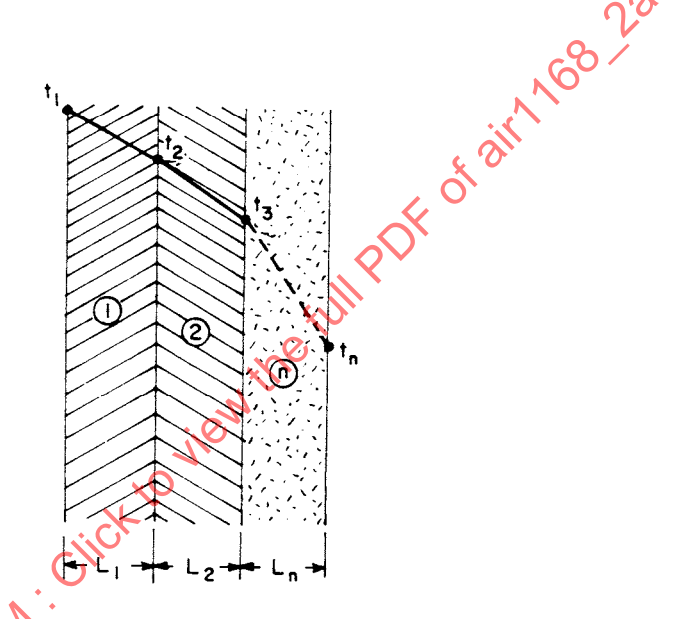
- 2.3.4 Heat Flow Through Composite Materials: When considering the flow of heat through materials of different thermal properties, or perhaps of varying geometrical properties, it is valuable to consider two concepts:
 - (a) Thermal Resistance This is analogous to electrical resistance and permits the use of the well-known electrical laws for adding resistances in series for the flow of heat through composite materials (or adding conductances in parallel when heat flows through several parallel paths). This concept often will permit the writing of complicated heat flow equations by inspection.
 - (b) Overall Conductance This is the reciprocal of the total resistance to heat flow. The overall conductance, when multiplied by the overall temperature difference, results in heat flow per unit area across the system being considered.

Slab: Refer to Figure 7. Materials 1,2,...n have conductivities $k_1,k_2,...k_n$, and lengths $L_1,L_2,...L_n$, respectively.

$$t(0) = t_0 (Eq. 34)$$

$$t (L_1 + L_2 + ... L_n) = t_n$$
 (Eq. 35)

$$t_{x} = t_{1} - (t_{1} - t_{n}) \bullet \frac{[(L_{1}/k_{1}) + (L_{2}/k_{2}) + ...(\Delta x/k_{x})]}{\sum_{1}^{n} (L_{n}/k_{n})}$$
 (Eqs. 36, 37)



$$= \frac{A(t_1 - t_n)}{(L_1/k_1) + (L_2/k_2) + ...(L_n/k_n)} = UA(t_1 - t_n)$$
 (Eq. 38)

where:

FIGURE 7 - Heat Transfer in a Slab
$$\frac{A(t_1 - t_n)}{(L_1/k_1) + (L_2/k_2) + ...(L_n/k_n)} = UA(t_1 - t_n)$$

$$U = \frac{1}{(L_1/k_1) + (L_2/k_2) + ...(L_n/k_n)} = \text{Overall conductance}$$
(Eq. 39)

2.3.4.2 Cylinder: Refer to Figure 8.

$$t(r_1) = t_1$$
 (Eq. 40)

$$t(r_n) = t_n (Eq. 41)$$

$$t_{r} = t_{1} - (t_{1} - t_{n}) \left[\frac{\left(\frac{1}{k_{1}}\right) \ln\left(\frac{r_{2}}{r_{1}}\right) + \dots \left(\frac{1}{k_{i}}\right) \ln\left(\frac{r}{r_{i}}\right)}{\sum_{1}^{n} \left(\frac{1}{k_{n}}\right) \ln\left(\frac{r_{n+1}}{r_{n}}\right)} \right]$$
(Eq. 42)

$$\frac{q}{\text{Unit length}} = \frac{2\pi (t_1 - t_n)}{\sum_{1}^{n} \left(\frac{1}{k_n}\right) \ln \left(\frac{r_{n+1}}{r_n}\right)}$$
 (Eq. 43)

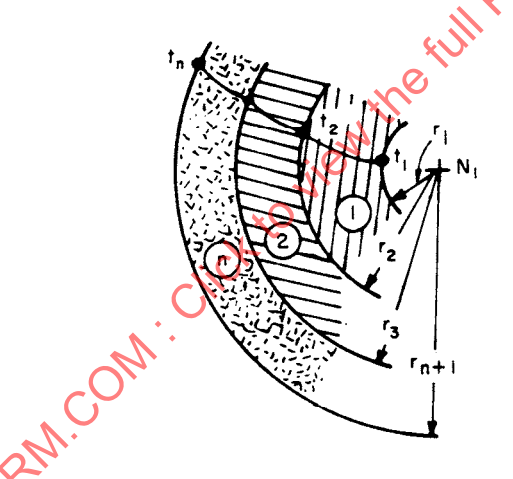


FIGURE 8 - Heat Transfer in a Cylinder

2.3.4.3 Sphere: Refer to Figure 9.

$$t(r_1) = t_1$$
 (Eq. 44)

$$t(r_n) = t_n (Eq. 45)$$

$$t_{r} = t_{1} - (t_{1} - t_{n}) \left[\frac{\frac{1}{k_{1}} \left(\frac{1}{r_{1}} - \frac{1}{r_{2}} \right) + \dots \frac{1}{k_{i}} \left(\frac{1}{r_{i}} - \frac{1}{r} \right)}{\sum_{1}^{n} \frac{1}{k_{n}} \left(\frac{1}{r_{n}} + \frac{1}{r_{n+1}} \right)} \right]$$
(Eq. 46)

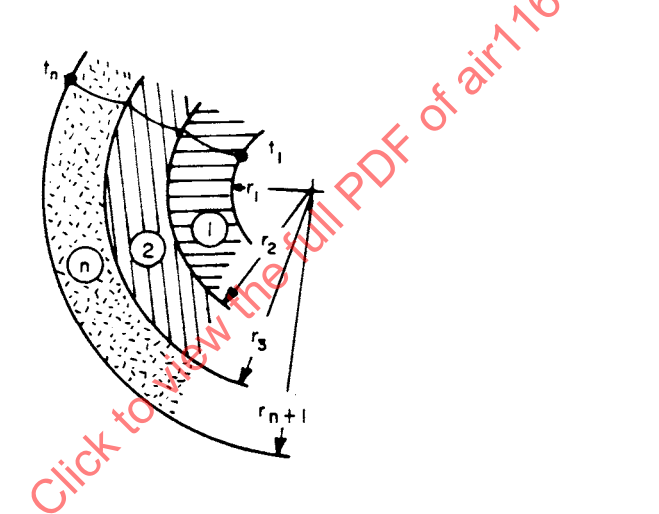


FIGURE 9 - Heat Transfer in a Sphere
$$q = \frac{4\pi(t_1 - t_n)}{\sum_{1}^{n} \frac{1}{k_n} \left(\frac{1}{r_n} - \frac{1}{r_{n+1}}\right)}$$
 (Eq. 47)

- 2.4 Steady-State Heat Conduction in Two and Three Dimensions:
- 2.4.1 Conduction Shape Factors: The general equation is

$$q = \phi \Delta T k \tag{Eq. 48}$$

Table 1 is adapted from Reference 17.

TABLE 1 - Shape Factors

D				ე ტ
L/D	1/φ	1/φ	1/φ	68/
1	0	0	0	10
2	0.10	0.12	0.13	
3	0.16	0.17	0.13 0.18	
4	0.20	0.22	0.23	
5	0.23	0.24	0.25	
		- 1	1	-

2.5 Steady-State Heat Conduction With Convection as a Boundary Condition:

The solution to all preceding geometries, with convection as a boundary condition, may easily be written by inspection if it is remembered that

$$q = \frac{\Delta T_{\text{overall}}}{\text{Sum of Thermal resistances}}$$
 (Eq. 49)

where the thermal resistance for convection = 1/hA.

- 2.6 Heat Transfer Through Fins in Steady State:
- 2.6.1 General Nomenclature: A fin may be described as a material of finite thermal conductivity, which is heated or cooled convectively from a fluid flowing over its surface and which transfers a finite quantity of heat or cooling by conduction through its base into the material to which it is connected. For all fins described herein, the conductivity through the thickness of the fin (in the direction of δ) will be considered infinite; that is, the temperature will be uniform at any point x. Also, the material conductivity will be assumed independent of temperature. In describing the thermodynamic performance of a fin, the significant performance factor is a term called the "fin effectiveness," ϵ , which is a ratio expressing the fraction of the surface area that is effective in transferring heat through the base of the fin in terms of the base temperature of the fin; that is,

$$\varepsilon = \frac{q_0}{Ah(t_1 - t_0)}$$
 (Eq. 50)

The following nomenclature will be standard for all solutions, with additional nomenclature being added as required for particular solutions.

A = Total fin surface area, ft^2 (both sides)

h = Heat transfer coefficient between fin and fluid (h₁ for interface 1, h₂ for interface 2, etc.), Btu/h-ft²-°F

k = Thermal conductivity of fin, Btu/h-ft-°F

t_m = Temperature of fin if there is no fin effect, °F

t_o = Temperature at base of fin (surface to which fin is connected), °F

t_x = Temperature of fin at point x, °F

 $t_1, t_2, ... t_n$ = Fluid temperature over area 1,2 Ω , °F

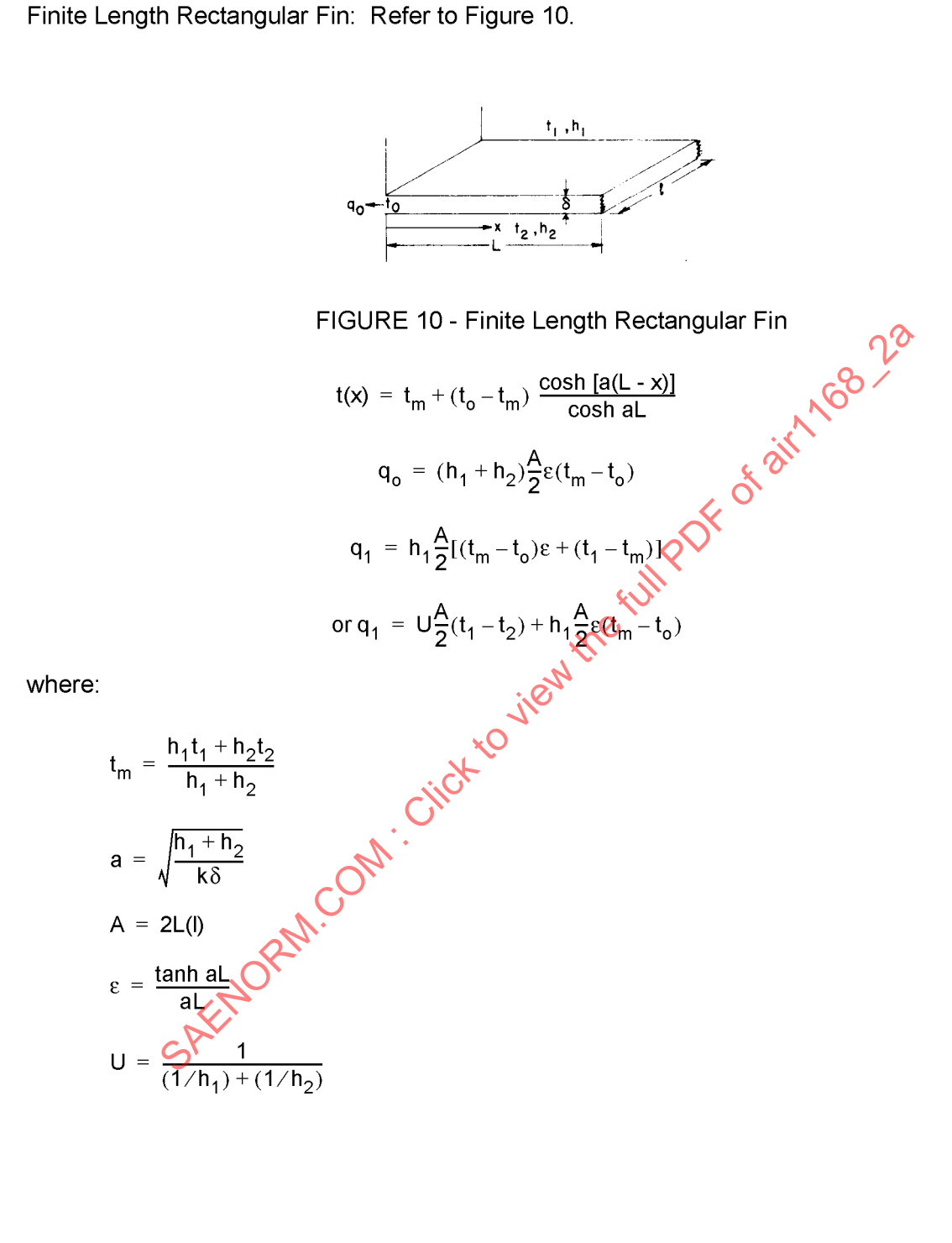
q_o = Heat transferred out of fin to connecting surface, Btu/h

 q_1,q_1 , or q_n = Heat entering fin from fluid 1,2,...,n, Btu/h

x = Distance from origin, ft

 δ = Fin thickness, ft

Finite Length Rectangular Fin: Refer to Figure 10. 2.6.2



$$t(x) = t_m + (t_o - t_m) \frac{\cosh [a(L - x)]}{\cosh aL}$$
 (Eq. 51)

$$q_o = (h_1 + h_2) \frac{A}{2} \varepsilon (t_m - t_o)$$
 (Eq. 52)

$$q_1 = h_1 \frac{A}{2} [(t_m - t_0)\varepsilon + (t_1 - t_m)]$$
 (Eq. 53)

or
$$q_1 = U_2^A(t_1 - t_2) + h_1^A \epsilon (t_m - t_0)$$
 (Eq. 54)

$$t_{m} = \frac{h_{1}t_{1} + h_{2}t_{2}}{h_{1} + h_{2}}$$
 (Eq. 55)

$$a = \sqrt{\frac{h_1 + h_2}{k\delta}}$$
 (Eq. 56)

$$A = 2L(I)$$
 (Eq. 57)

$$\varepsilon = \frac{\tanh aL}{aL}$$
 (Eq. 58)

$$U = \frac{1}{(1/h_1) + (1/h_2)}$$
 (Eq. 59)

2.6.3 Annular Fin: Refer to Figures 11 and 12. This is a problem in radial heat flow, where a circular disk of radius L + L' surrounds a heat sink of radius L' and temperature t_0 . Convection from temperature t_1 and film coefficient t_1 surrounds the fin.

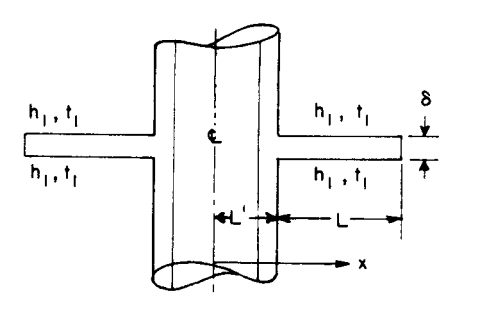


FIGURE 11 - Annular Fin (No Temperature Drop Assumed Through Vertical Cylinder Wall)

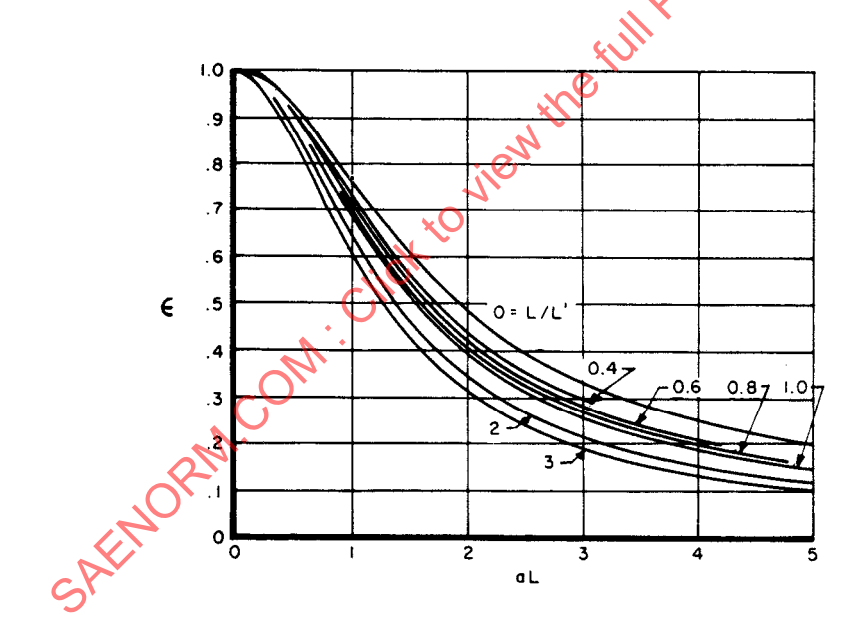


FIGURE 12 - Efficiency of Annular Fins of Constant Thickness

$$\frac{t_{x}-t_{1}}{t_{o}-t_{1}} = \frac{(1)+(2)}{(3)+(4)}$$
 (Eq. 60)

2.6.3 (Continued):

where:

$$(1) = I_1[(L + L')a]K_0(ax)$$
 (Eq. 61)

$$(2) = K_1[(L + L')a]I_0(ax)$$
 (Eq. 62)

$$(3) = I_1[(L + L')a]K_0(aL')$$
 (Eq. 63)

$$(4) = K_1[(L + L')a]I_0(aL')$$
 (Eq. 64)

$$q_{o} = 2\pi L'k\delta a \left(\frac{(5)-(6)}{(7)+(8)}(t_{o}-t_{1})\right)$$

$$= \pi [(L+L')^{2}-L'^{2}]h_{1}\epsilon(t_{o}-t_{1})$$
(Eq. 65)
$$(Eq. 66)$$

$$(Eq. 66)$$

$$(Eq. 67)$$

$$(Eq. 68)$$

$$(Eq. 69)$$

$$(Eq. 69)$$

where:

$$(5) = I_1[(L + L')a]K_1(aL')$$
 (Eq. 66)

$$(6) = K_1[(L + L')a]I_1(aL')$$
 (Eq. 67)

$$(7) = I_1[(L + L')a]K_0(aL')$$
 (Eq. 68)

$$(8) = K_1[(L + L')a]I_0(aL')$$
 (Eq. 69)

(see Figure 12).

where:

I_o(arg) = Modified Bessel Function, first kind, zero order I₁(arg) = Modified Bessel Function, first kind, first order K_o(arg) = Modified Bessel Function, second kind, zero order $K_1(arg) = Modified Bessel Function, second kind, first order$

$$a = \sqrt{h_1/(k\delta)}$$
 (Eq. 70)

2.6.4 Finite Length Fin With Constant Heat Flux Near One End: Refer to Figure 13. This is the case of a convectively cooled surface of finite length I_2 , in the positive x direction; the boundary condition at $x = I_2$ is $dt_{x2}/dx=0$.

For x > 0,

$$\frac{t_{x2} - t_{m}}{t_{q} - t_{m}} = \frac{\cosh a_{2} (l_{2} - x)}{(a_{2}/a_{1})\sinh a_{2}l_{2} \cdot \coth a_{1}l_{1} + \cosh a_{2}l_{2}}$$
(Eq. 71)

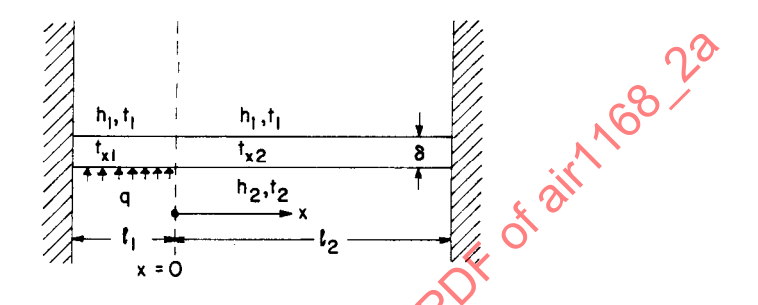


FIGURE 13 - Fin With Constant Heat Flux Near One End

For x < 0,

$$\frac{t_{q} - t_{x1}}{t_{q} - t_{m}} = \frac{(a_{2}/a_{1})\cosh a_{1} (l_{1} + x)}{(a_{2}/a_{1})\cosh a_{1} l_{1} + \sinh a_{1} l_{1} \cdot \coth a_{2} l_{2}}$$
(Eq. 72)

where:

$$t_{q} = (h_{1}t_{1} + q)/h_{1}$$
 (Eq. 73)

$$a_1 = \sqrt{h_1/(k\delta)}$$
 (Eq. 74)

$$a_2 = \sqrt{(a_1 + h_2)/(k\delta)}$$
 (Eq. 75)

2.6.5 Finite Length Fin With Step Change in Convective Heating Near One End: Refer to Figure 14. The surface is of finite length I_2 in the positive x direction, and the boundary condition at $x = I_2$ is $(dt_{x/2}/dx) = 0$.

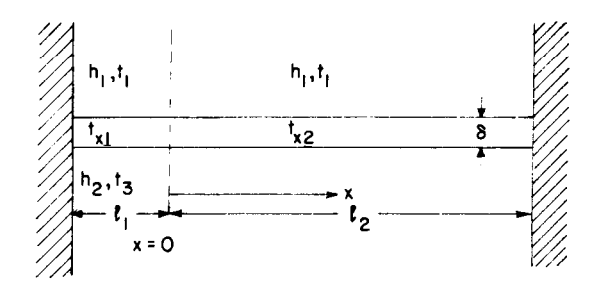


FIGURE 14 - Fin With a Step Change in Convective Heating Near One End

For x > 0,

$$\frac{t_{x2} - t_{m2}}{t_{m1} - t_{m2}} = \frac{\cosh a_2 (l_2 - x)}{(a_2/a_1)\sinh a_2 l_2 \cdot \coth a_1 l_2 + \cosh a_2 l_2}$$
 (Eq. 76)

For x < 0,

$$\frac{t_{m1} - t_{x1}}{t_{m1} - t_{m2}} = \frac{(a_2/a_1)\cosh a_1 (l_1 + x)}{(a_2/a_1)\cosh a_1 l_1 + \sinh a_1 l_1 \cdot \coth a_2 l_2}$$
(Eq. 77)

2.6.6 A Finite Length and an Infinitely Long Fin Welded Together Near One End: Refer to Figure 15. This is the case of two fins of different materials joined together near one end for a length I₁ so that there is perfect thermal contact in that area, with homogeneous thermal properties. One fin is very long and the other is of length I₃. The convective heating and cooling over the various surfaces is noted in Figure 15.

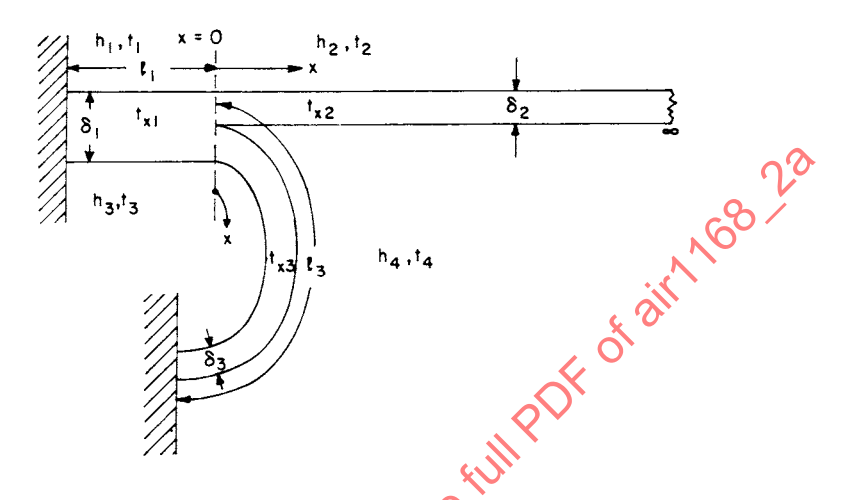


FIGURE 15 - Fins of Different Materials Joined at One End

For x > 0,

$$\frac{t_{x2} - t_{m2}}{t_{m1} - t_{m2}} = \begin{bmatrix} \frac{k_1 \delta_1 a_1}{k_2 \delta_2 a_2} & \tanh a_1 I_1 + \frac{t_{m3} - t_{m2}}{t_{m1} - t_{m2}} & \frac{k_3 \delta_3 a_3}{k_2 \delta_2 a_2} & \tanh a_3 I_3 \\ 1 + \frac{k_1 \delta_1 a_1}{k_2 \delta_2 a_2} & \tanh a_1 I_1 + \frac{k_3 \delta_3 a_3}{k_2 \delta_2 a_2} & \tanh a_3 I_3 \end{bmatrix} e^{-a} 2^x$$
 (Eq. 78)

$$\frac{t_{x3} - t_{m3}}{t_{m1} - t_{m2}} = \left[\frac{\frac{t_{m1} - t_{m3}}{t_{m4}} \left(1 + \frac{k_1 \delta_1 a_1}{k_2 \delta_2 a_2} \tanh a_1 I_1 \right) - 1}{\frac{k_1 \delta_1 a_1}{k_2 \delta_2 a_2} \tanh a_1 I_1 + \frac{k_3 \delta_3 a_3}{k_2 \delta_2 a_2} \tanh a_3 I_3} \right] \left[\cosh a_3 x - \tanh a_3 I_3 \cdot \sinh a_3 x \right]$$
 (Eq. 79)

For x < 0

$$\frac{t_{m1} - t_{x1}}{t_{m1} - t_{m2}} = \left[\frac{1 + \frac{t_{m1} - t_{m3}}{t_{m1} - t_{m2}} \frac{k_3 \delta_3 a_3}{k_2 \delta_2 a_2} \tanh a_3 I_3}{1 + \frac{k_1 \delta_1 a_1}{k_2 \delta_2 a_2} \tanh a_1 I_1 + \frac{k_3 \delta_3 a_3}{k_2 \delta_2 a_2} \tanh a_3 I_3} \right] [\cosh a_1 x + \tanh a_1 I_1 \cdot \sinh a_1 x]$$
 (Eq. 80)

2.6.6 (Continued):

where:

$$a_1 = \sqrt{\frac{h_1 + h_3}{k_1 \delta_1}}$$
 (Eq. 81)

$$a_2 = \sqrt{\frac{h_2 + h_4}{k_2 \delta_2}}$$
 (Eq. 82)

$$a_{3} = \sqrt{\frac{h_{3} + h_{4}}{k_{3}\delta_{3}}}$$

$$t_{m1} = \frac{h_{1}t_{1} + h_{3}t_{3}}{h_{1} + h_{3}}$$

$$(Eq. 84)$$

$$t_{m2} = \frac{h_{2}t_{2} + h_{4}t_{4}}{h_{2} + h_{4}}$$

$$(Eq. 85)$$

$$t_{m3} = \frac{h_{3}t_{3} + h_{4}t_{4}}{h_{3} + h_{4}}$$
(Eq. 86)

$$t_{m1} = \frac{h_1 t_1 + h_3 t_3}{h_1 + h_3}$$
 (Eq. 84)

$$t_{m2} = \frac{h_2 t_2 + h_4 t_4}{h_2 + h_4}$$
 (Eq. 85)

$$t_{m3} = \frac{h_3 t_3 + h_4 t_4}{h_3 + h_4} \tag{Eq. 86}$$

Two Finite Length Fins Welded Together Near One End: Refer to Figure 16. This is the same 2.6.7 case as that in 2.6.6 except that the boundary condition at $x = I_2$ is $dt_{\chi 2}/dx = 0$.

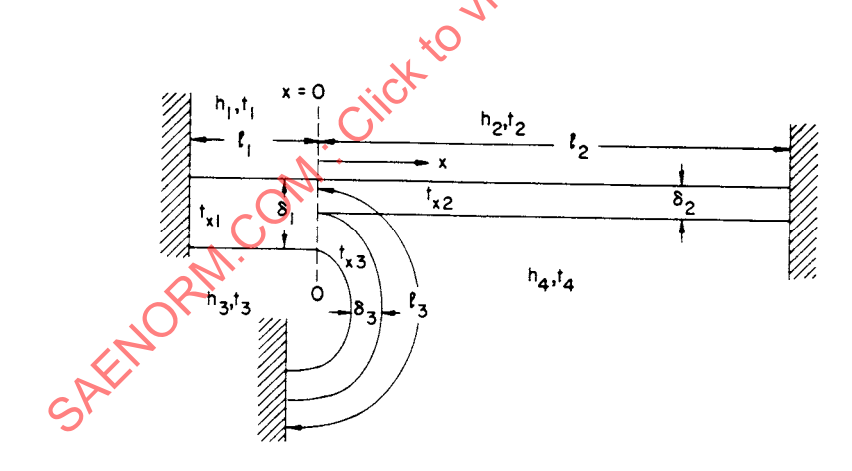


FIGURE 16 - Fins of Finite Length Joined Near One End

2.6.7 (Continued):

For x < 0,

$$\frac{t_{m1} - t_{x1}}{t_{m1} - t_{m2}} = \begin{bmatrix} \frac{1 + \frac{t_{m1} - t_{m3}}{t_{m1} - t_{m2}} & \frac{k_3 \delta_3 a_3}{k_2 \delta_2 a_2} & \frac{tanh \ a_3 l_3}{tanh \ a_2 l_2} \\ \frac{1 + \frac{k_1 \delta_1 a_1}{t_{m1} - t_{m2}} & \frac{tanh \ a_1 l_1}{t_{m1} - t_{m2}} & \frac{k_3 \delta_3 a_3}{k_2 \delta_2 a_2} & \frac{tanh \ a_3 l_3}{tanh \ a_2 l_2} \\ \frac{1 + \frac{k_1 \delta_1 a_1}{k_2 \delta_2 a_2} & \frac{tanh \ a_1 l_1}{tanh \ a_2 l_2} & \frac{k_3 \delta_3 a_3}{k_2 \delta_2 a_2} & \frac{tanh \ a_3 l_3}{tanh \ a_2 l_2} \\ \frac{1 + \frac{k_1 \delta_1 a_1}{k_2 \delta_2 a_2} & \frac{tanh \ a_1 l_1}{tanh \ a_2 l_2} & \frac{k_3 \delta_3 a_3}{k_2 \delta_2 a_2} & \frac{tanh \ a_3 l_3}{tanh \ a_2 l_2} \\ \frac{1 + \frac{k_1 \delta_1 a_1}{k_2 \delta_2 a_2} & \frac{tanh \ a_1 l_1}{tanh \ a_2 l_2} & \frac{k_3 \delta_3 a_3}{k_2 \delta_2 a_2} & \frac{tanh \ a_3 l_3}{tanh \ a_2 l_2} \\ \frac{1 + \frac{k_1 \delta_1 a_1}{k_2 \delta_2 a_2} & \frac{tanh \ a_2 l_2}{tanh \ a_2 l_2} & \frac{tanh \ a_3 l_3}{k_2 \delta_2 a_2} & \frac{tanh \ a_3 l_3}{tanh \ a_2 l_2} \\ \frac{1 + \frac{k_1 \delta_1 a_1}{k_2 \delta_2 a_2} & \frac{tanh \ a_2 l_2}{tanh \ a_2 l_2} & \frac{tanh \ a_3 l_3}{k_2 \delta_2 a_2} & \frac{tanh \ a_3 l_3}{tanh \ a_2 l_2} \\ \frac{1 + \frac{k_1 \delta_1 a_1}{k_2 \delta_2 a_2} & \frac{tanh \ a_2 l_2}{tanh \ a_2 l_2} & \frac{tanh \ a_3 l_3}{k_2 \delta_2 a_2} & \frac{tanh \ a_3 l_3}{tanh \ a_2 l_2} \\ \frac{1 + \frac{k_1 \delta_1 a_1}{k_2 \delta_2 a_2} & \frac{tanh \ a_2 l_2}{tanh \ a_2 l_2} & \frac{tanh \ a_3 l_3}{k_2 \delta_2 a_2} & \frac{tanh \ a_3 l_3}{tanh \ a_2 l_2} \\ \frac{1 + \frac{k_1 \delta_1 a_1}{k_2 \delta_2 a_2} & \frac{tanh \ a_3 l_3}{tanh \ a_2 l_2} & \frac{tanh \ a_3 l_3}{k_2 \delta_2 a_2} & \frac{tanh \ a_3 l_3}{tanh \ a_2 l_2} \\ \frac{1 + \frac{k_1 \delta_1 a_1}{k_2 \delta_2 a_2} & \frac{tanh \ a_3 l_3}{tanh \ a_2 l_2} & \frac{tanh \ a_3 l_3}{k_2 \delta_2 a_2} & \frac{tanh \ a_3 l_3}{tanh \ a_3 l_3} \\ \frac{1 + \frac{k_1 \delta_1 a_1}{k_2 \delta_2 a_2} & \frac{tanh \ a_3 l_3}{tanh \ a_3 l_3} & \frac{tanh \ a_3 l_3}{tanh \ a_3 l_3} \\ \frac{1 + \frac{k_1 \delta_1 a_1}{k_2 \delta_2 a_2} & \frac{tanh \ a_3 l_3}{tanh \ a_3 l_3} & \frac{tanh \ a_3 l_3}{tanh \ a_3 l_3} \\ \frac{1 + \frac{k_1 \delta_1 a_1}{k_2 \delta_2 a_3} & \frac{tanh \ a_3 l_3}{tanh \ a_3 l_3} & \frac{tanh \ a_3 l_3}{tanh \ a_3 l_3} \\ \frac{1 + \frac{k_1 \delta_1 a_1}{k_2 \delta_2 a_3} & \frac{tanh \ a_3 l_3}{tanh \ a_3 l_3} & \frac{tanh \ a_3 l_3}{tanh \ a_3 l_3} & \frac{tanh \ a_3 l_3}{tanh \ a_3 l_3} \\ \frac{1 + \frac{k_1 \delta_1 a_1}{k_$$

For x > 0,

$$\frac{t_{x2}-t_{m2}}{t_{m1}-t_{m2}} = \begin{bmatrix} \frac{k_1\delta_1a_1}{k_2\delta_2a_2} \frac{\tanh a_1l_1}{\tanh a_2l_2} + \frac{t_{m3}-t_{m2}}{t_{m1}-t_{m2}} \frac{k_3\delta_3a_3}{k_2\delta_2a_2} \frac{\tanh a_3l_3}{\tanh a_2l_2} \\ 1 + \frac{k_1\delta_1a_1}{k_2\delta_2a_2} \frac{\tanh a_1l_1}{\tanh a_2l_2} + \frac{k_3\delta_3a_3}{k_2\delta_2a_2} \frac{\tanh a_3l_3}{\tanh a_2l_2} \end{bmatrix} [\cosh a_2x - \tanh a_2x] \quad \text{(Eq. 88)}$$

$$\frac{t_{x3} - t_{m3}}{t_{m1} - t_{m2}} = \left[\frac{\frac{t_{m1} - t_{m3}}{t_{m1} - t_{m2}} \left(1 + \frac{k_1 \delta_1 a_1}{k_2 \delta_2 a_2} \frac{\tanh a_1 l_1}{\tanh a_2 l_2} \right) - 1}{1 + \frac{k_1 \delta_1 a_1}{k_2 \delta_2 a_2} \frac{\tanh a_1 l_1}{\tanh a_2 l_2} + \frac{k_3 \delta_3 a_3}{k_2 \delta_2 a_2} \frac{\tanh a_3 l_3}{\tanh a_2 l_2}} \right]$$
(Eq. 89)

2.6.8 Fin Effectiveness of a Welded Double Skin: Refer to Figure 17. Fin effectiveness for this case may be defined as the ratio of the heat that is transferred out of the surface 1 plus 2 to that which would be transferred in the absence of conduction (through surface 2 only) and is equal to ε_{oa} .

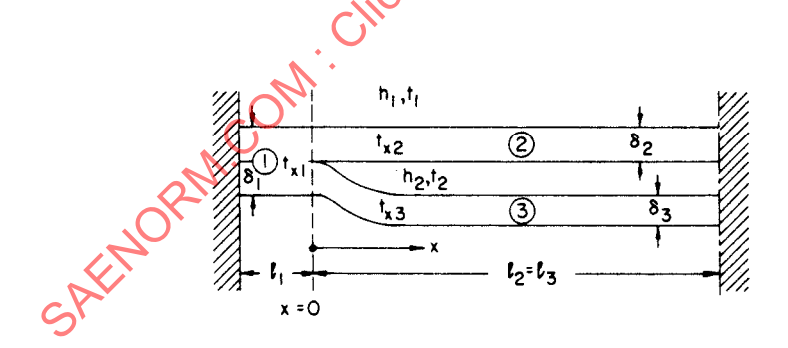


FIGURE 17 - Effectiveness of Welded Double Skin

SAE AIR1168/2A Page 37 of 194

2.6.8 (Continued):

$$\varepsilon_{0a} = \frac{q_{fin}}{q_{no\,fin}}$$

$$= \int_{0}^{1} h_{1}(t_{x2} - t_{1}) \, dx + \int_{-t_{1}}^{0} h_{1}(t_{x1} - t_{1}) \, dx$$

$$= \int_{0}^{1} h_{1}(t_{x2} - t_{1}) \, dx + \int_{-t_{1}}^{0} h_{1}(t_{x1} - t_{1}) \, dx$$

$$= 1 + \frac{U_{1}\varepsilon_{1}}{h_{1}t_{2}} + \frac{U_{1}\varepsilon_{1}}{h_{1}} + \frac{U_{1}\varepsilon_{1}}{t_{2}\varepsilon_{2}} + \varepsilon_{3}$$

$$1 + \frac{U_{1}\varepsilon_{1}}{h_{2}\varepsilon_{2}} + \frac{U_{1}\varepsilon_{3}}{h_{1}\varepsilon_{2}}$$

$$\varepsilon_{1} = \frac{t_{1}}{t_{1}} + \frac{t_{1}}{t_{2}} + \frac{U_{1}\varepsilon_{2}}{t_{2}} + \frac{U_{1}\varepsilon_{3}}{t_{2}} + \frac{U_{1}\varepsilon_{3}}{t_{2}}$$

$$\varepsilon_{2} = \frac{t_{1}}{t_{2}} + \frac{t_{1}}{t_{2}} + \frac{U_{1}\varepsilon_{3}}{t_{2}} + \frac{U_{1}\varepsilon_{3}$$

where:

$$U = \frac{1}{(1/h_1) + (1/h_2)}$$
 (Eq. 91)

$$\varepsilon_1 = \frac{\tanh a_1 l_1}{a_1 l_1} \tag{Eq. 92}$$

$$\varepsilon_2 = \frac{\tanh a_2 l_2}{a_2 l_2} \tag{Eq. 93}$$

$$\varepsilon_3 = \frac{\tanh a_3 I_3}{a_3 I_3} \tag{Eq. 94}$$

$$a_1 = \sqrt{\frac{h_1}{k_1 \delta_1}}$$
 (Eq. 95)

$$a_2 = \sqrt{\frac{h_1 + h_2}{k_2 \delta_2}}$$
 (Eq. 96)

$$a_3 = \sqrt{\frac{b_2}{k_3 \delta_3}}$$
 (Eq. 97)

2.6.9 Fin That is Heated by a Blanket and Loses Heat at One End: Refer to Figure 18. This is the case of a fin heated by a constant flux q_H , which is located in a "blanket" wrapped over the outside of the fin. A thermal resistance R_2 separates the heat source from the fin, and another R_1 separates the heat source from ambient temperature t_1 . One end of the fin (x = 1) has a finite thermal conductance UA (per unit width) to temperature t_2 , and the other end of the fin (x = 0) is insulated.

$$\frac{t_{x}-t_{1}}{(t_{x}-t_{1})_{o}} = 1 + \left[\frac{\frac{t_{2}-t_{1}}{(t_{x}-t_{1})_{o}} - 1}{1 + \frac{k\delta a}{UA} \tanh al} \right] \frac{\cosh ax}{\cosh al}$$
 (Eq. 98)

where:

$$a = \sqrt{\frac{[1/(R_1 + R_2)] + h_3}{k\delta}}$$
 (Eq. 99)

 $(t_x - t_1)_0$ = Temperature difference between fin and ambient of there were no fin effect

$$= \frac{h_3 t_3 + \frac{q_H + (t_1/R_1)}{1 + (R_2/R_1)}}{h_3 + \frac{1}{R_1 + R_2}}$$
(Eq. 100)

FIGURE 18 - Loss of Heat at One End of Fin

2.6.10 Fin Heated by a Blanket With a Linearly Varying Heat Flux: Refer to Figure 19. This case is the same as the preceding one except that the heat flux is constant for X < 0, and varies linearly for X > 0.

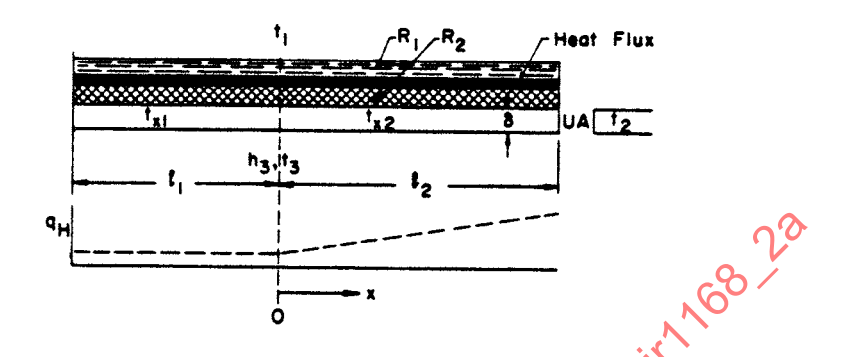


FIGURE 19 - Fin Heated With Blanket; Linear Varying Heat Flux

For X < 0,

$$\frac{t_{x1} - t_1}{(t_{x1} - t_1)_0} = \left[\frac{(ac/d) + b}{a[\tanh al_1 + (e/d)]} \right] [\cosh ax + \tanh al_1 \sinh ax] + 1$$
 (Eq. 101)

For X > 0,

$$\frac{t_{x2} - t_1}{(t_{x2} - t_1)_0} = \left[\frac{(ac/d) + b}{a[\tanh a_1 + (e/d)]} \right]$$
(Eq. 102)

 \cdot [cosh ax + tanh al \rightarrow sinh ax] + [- (b/a) sinh ax + bx + 1]

where:

$$a = \sqrt{\frac{h_3 + [1/(R_1 + R_2)]}{R\delta}}$$
 (Eq. 103)

$$b = \frac{[R_1(dq_H/dx)](R_1 + R_2)}{[R_1(dq_H/dx)](R_1 + R_2)} \frac{1}{(t_x - t_1)_0}$$
 (Eq. 104)

$$c = \left[\frac{UA}{k\delta a} \left(1 - \frac{t_2 - t_1}{(t_x - t_1)_o} \right) + \left(\frac{UA}{k\delta a} I_2 + \frac{1}{a} \right) b \right]$$
 (Eq. 105)

$$d = \frac{UA}{k\delta a} \sinh al_2 + \cosh al_2$$
 (Eq. 106)

2.6.10 (Continued):

$$e = \frac{UA}{k\delta a} \cosh al_2 + \sinh al_2$$
 (Eq. 107)

$$(t_x - t_1)_0 = h_3 t_3 + \frac{q_H + (t_1/R_1)}{1 + (R_2/R_1)} - t_1$$
 (Eq. 108)

2.7 Transient Heat Conduction:

This section treats solutions to the general heat conduction equation when the term $\partial t/\partial \tau \neq 0$; that is, the temperature distribution through the system is a function of time as well as distance. For simplicity, solutions will be presented only for those cases where there is a step change in the boundary conditions at time zero and where the initial temperature is uniform. For other assumptions and the conversion of the step change to an arbitrary time dependent input, see Reference 2.

2.7.1 Solid of Infinite Thermal Conductivity: In this case the temperature of the body is uniform throughout at each instant of time, and the body, whose thermal capacity is mc, receives heat from the surrounding fluid of temperature, t_m, by convection. See Figure 20.

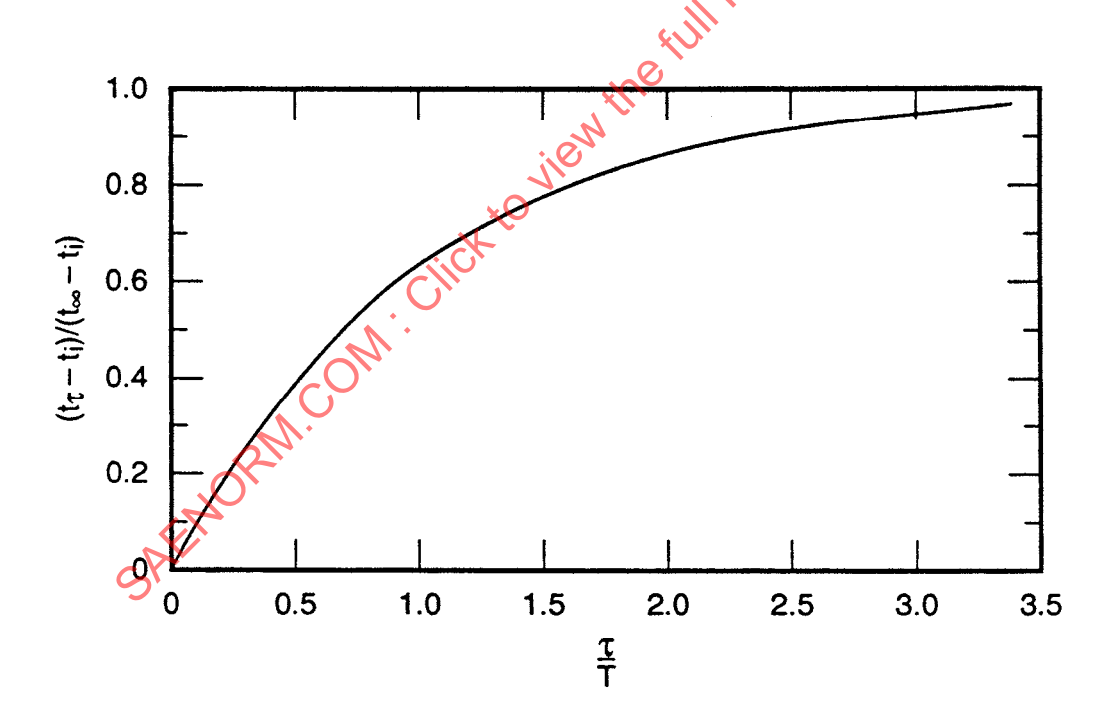


FIGURE 20 - Solid of Infinite Thermal Conductivity

$$\frac{t_{\tau} - t_{i}}{t_{\infty} - t_{i}} = 1 - e^{-\tau/T}$$
 (Eq. 109)

where:

 t_{τ} = Body temperature at time τ , °F

t_i = Body temperature at time 0, °F

t = Temperature of surrounding fluid, °F

 τ = Time after initiation of step change, h

T = Time constant of body

$$=\frac{mc}{hA}$$
, h

m = Mass of body, lb

c = Specific heat of body, Btu/lb-°F

h = Heat transfer coefficient over body from surrounding fluid, Btu/h-ft²-°F

A = Surface heat transfer area of body, ft^2

2.7.2 Semi-Infinite Solid With Known Surface Temperature: See Figure 21. This is the case of a very thick slab whose initial temperature is t_i and whose surface at x = 0 is suddenly changed to temperature t_0 at time zero.

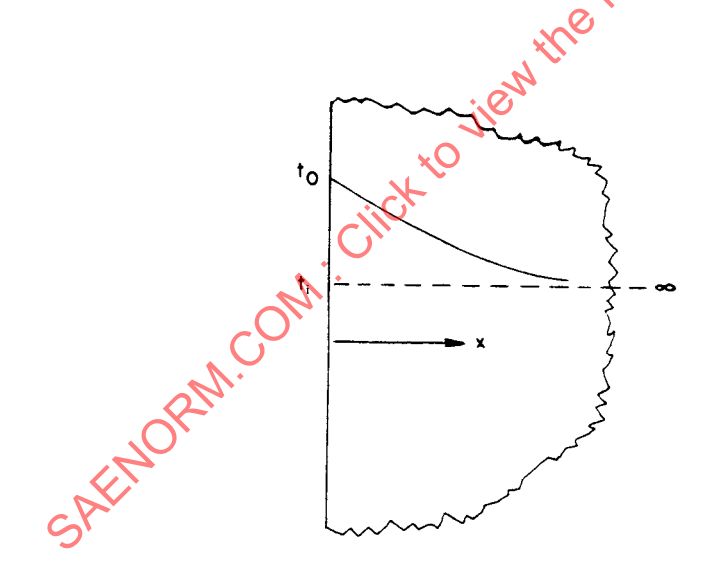


FIGURE 21 - Semi-Infinite Solid With Known Surface Temperature

$$\frac{t_{x,\tau} - t_{i}}{t_{o} - t_{i}} = 1 - \text{erf} \frac{x}{2\sqrt{\alpha\tau}}$$

$$= \text{erfc} \frac{x}{2\sqrt{\alpha\tau}}$$
(Eq. 110)

where:

 $\begin{array}{l} t_{x,\,\tau} = \text{Body temperature at distance } x \text{ and after time } \tau,\,\,^\circ F \\ \alpha = \text{Thermal diffusivity of material, } k/\rho g c_p \\ \tau = \text{Time after initiation of step change, h} \\ \text{erf } (\xi) = \text{Gauss error function defined as erf } (\xi) = \frac{2}{\sqrt{\pi}} \int\limits_0^{\xi} e^{-\eta^2} d\eta \, \text{where } \eta \, \text{ is a dummy variable} \\ \text{erfc } (\xi) = \text{Complementary error function defined as erfc } (\xi) = 1 - \text{erf}(\xi) \end{array}$

This equation is plotted in Figure 22 for the case of $hx/k = \infty$.

2.7.3 Semi-Infinite Solid With Convection at the Surface: This is the same as the preceding case except that the surface at x = 0 is heated from the surrounding fluid of temperature t_{∞} by film coefficient h. This solution is presented in graphical form in Figure 22 for various values of the dimensionless parameter hx/k.

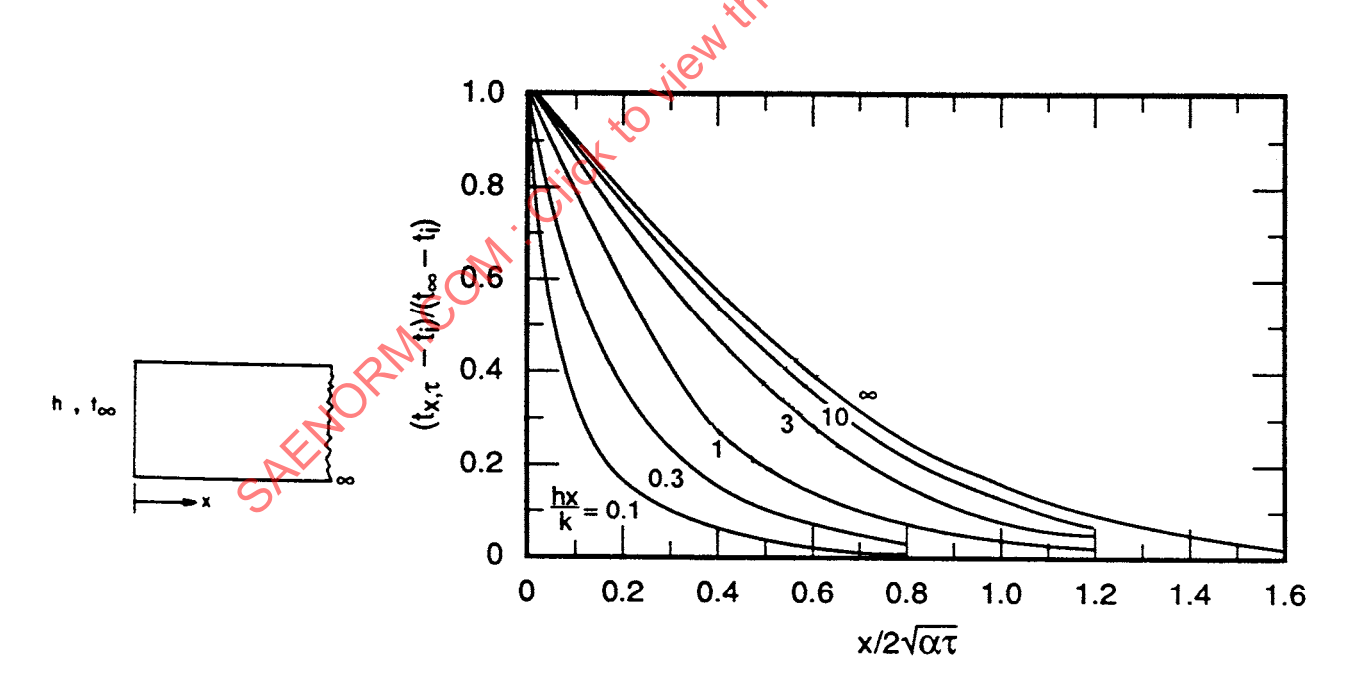


FIGURE 22 - Semi-Infinite Solid With Convection at the Surface

$$\frac{t_{x,\tau} - t_1}{t_{\infty} - t_i} = \operatorname{erfc} \frac{x}{2\sqrt{\alpha\tau}} - \left[\operatorname{e} \exp\left(\frac{hx}{k} + \frac{h^2}{k^2}\alpha\tau\right) \right] \left[\operatorname{erfc}\left(\frac{x}{2\sqrt{\alpha\tau}} + \frac{h}{k}\sqrt{\alpha\tau}\right) \right]$$
 (Eq. 111)

2.7.4 Semi-Infinite Solid With Constant Heat Flux at the Surface: This is the same case as above except that the surface x = 0 is heated by a flux of Q_0 , Btu/h-ft². Refer to Figure 23.

$$\frac{t_{x,\tau} - t_i}{Q_0 x/k} = \frac{2}{x} \sqrt{\frac{\alpha \tau}{\pi}} e \exp\left(\frac{-x^2}{4\alpha \tau}\right) - erfc\left(\frac{x}{2\sqrt{\alpha \tau}}\right)$$
 (Eq. 112)

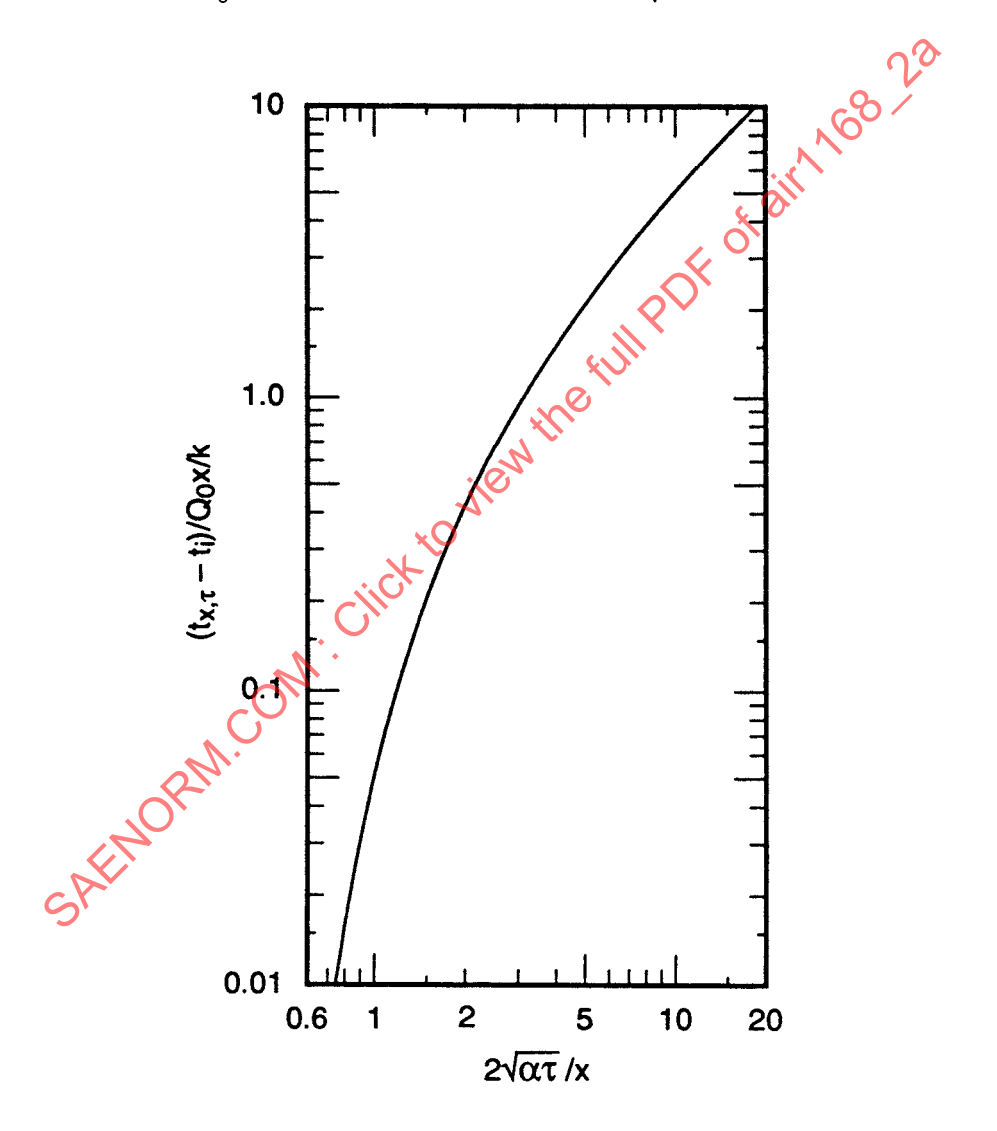


FIGURE 23 - Semi-Infinite Solid With Constant Heat Flux at the Surface

- Slab With Convection at the Faces: This is the case of a slab of thickness 2L of initial temperature t_i which is heated by convection on both faces by a fluid at temperature t_{_} and film coefficient h. Since the equation expressing this case is an infinite series that is tedious to calculate, only the graphical solution of Figure 24 will be presented.
- 2.7.6 Infinitely Long Cylinder With Convection Over the Surface: Refer to Figure 25.
- 2.7.7 Solid Sphere With Convection Over the Surface: Refer to Figure 26.
- 2.7.8 Infinitely Long Fin: Refer to Figure 27.

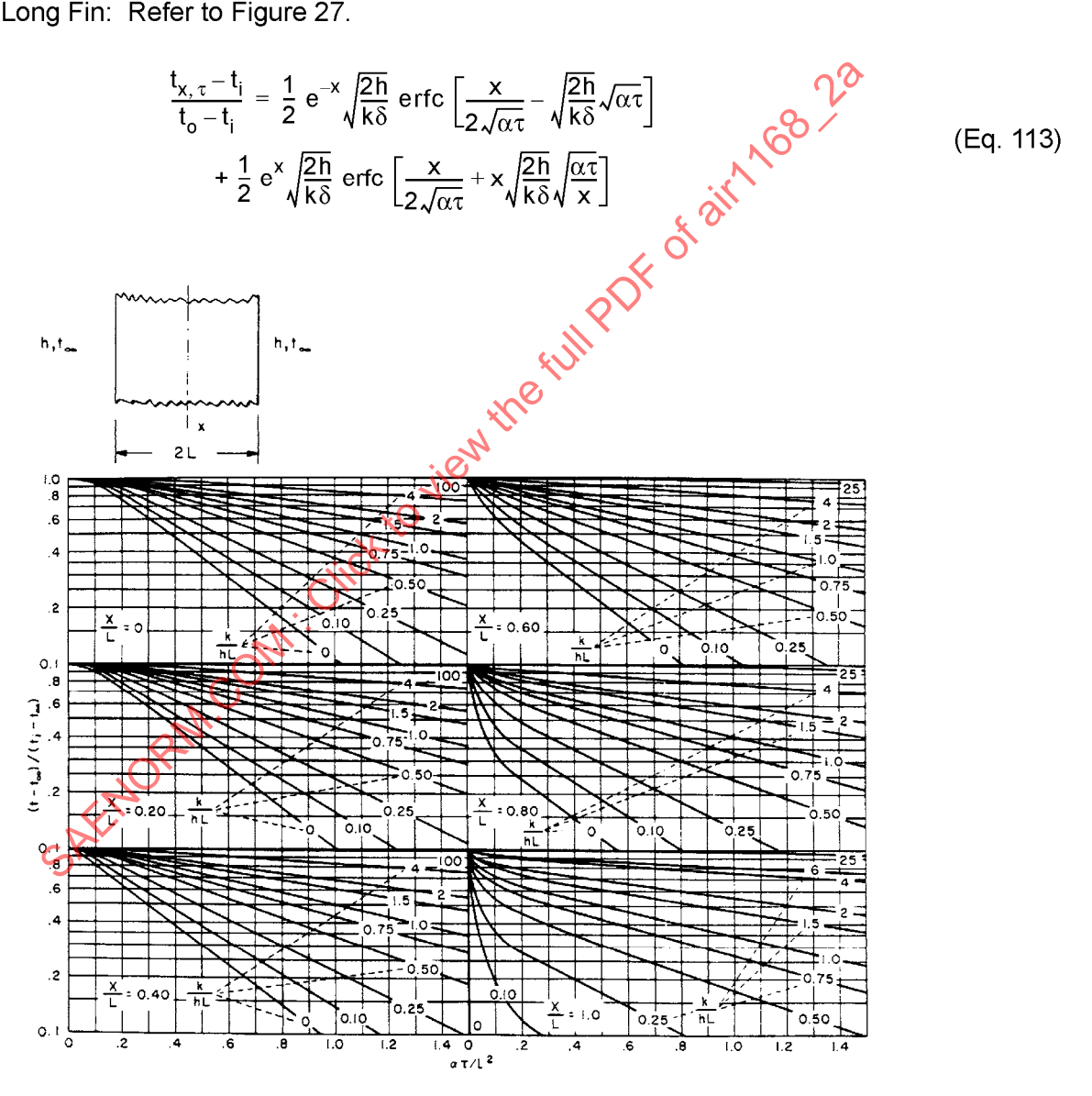


FIGURE 24 - Slab With Convection at the Faces

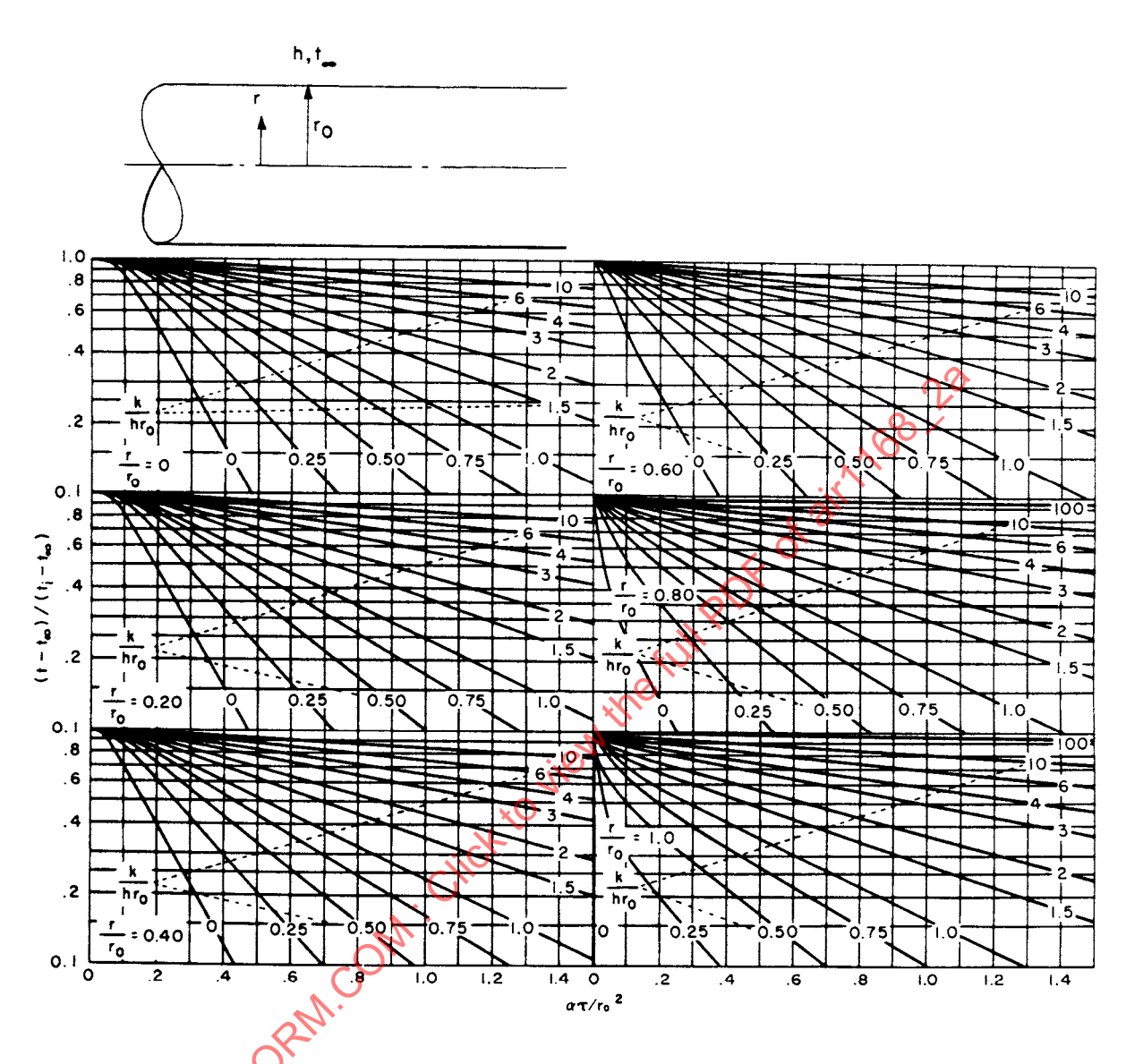
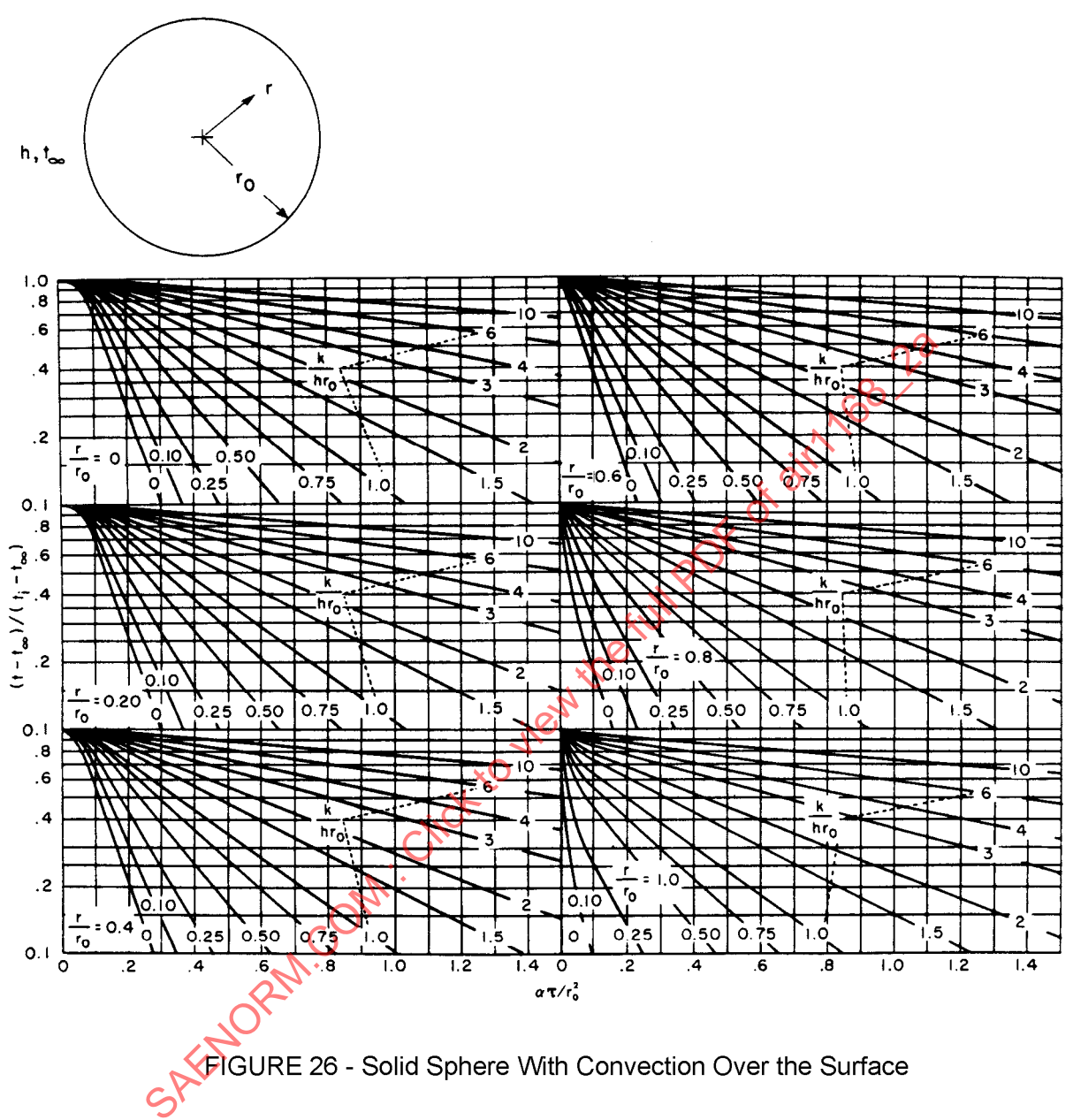


FIGURE 25 - Infinitely Long Cylinder With Convection Over the Surface



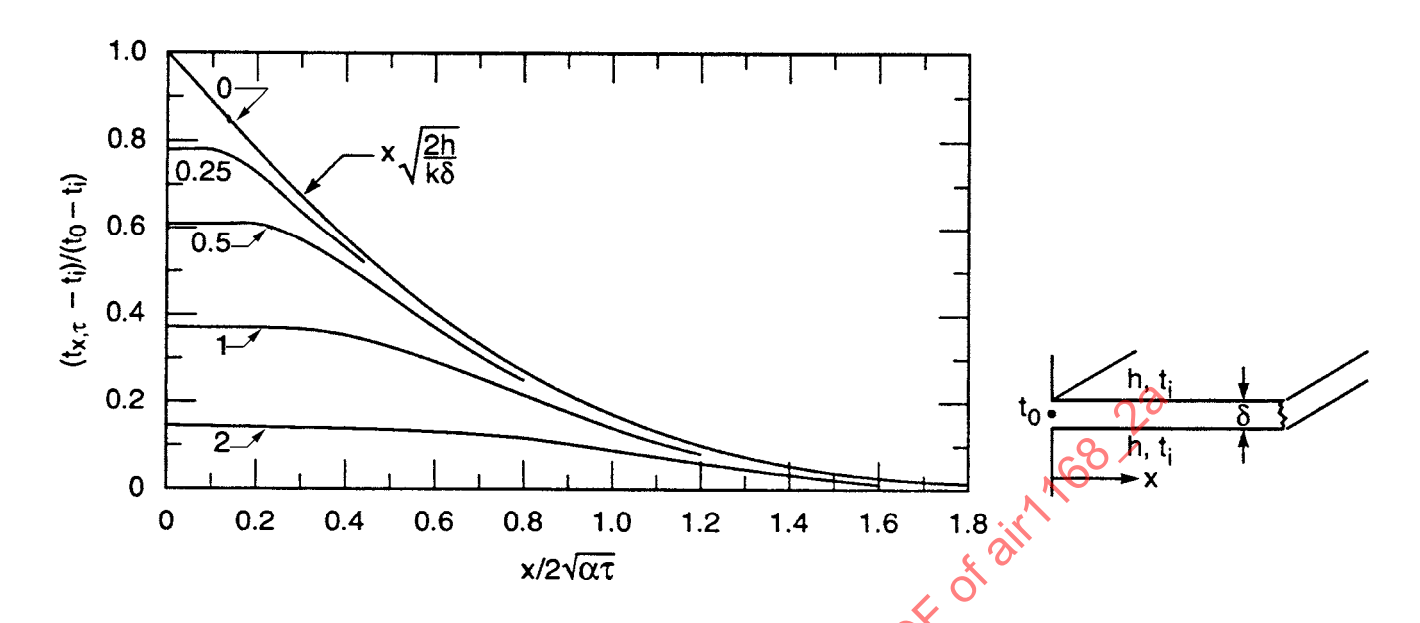


FIGURE 27 - Transient Temperature Rise of Fin

2.7.9 Heat Flow in Two and Three Dimensions: The general solution to the heat conduction equation presented in 2.2 often may be obtained as the product of the solution for each dimension:

$$t(x,y,z,\tau) = t(x,\tau) \cdot t(y,\tau) \cdot t(z,\tau)$$
 (Eq. 114)

This may be solved for the case of uniform initial temperature and either fixed surface temperatures or convection to the surrounding fluid. Typical examples of the application of this principle are given in the following paragraphs.

CASE 1. Semi-Infinite Cylinder This is the region of a long cylinder near one end, shown in Figure 28.

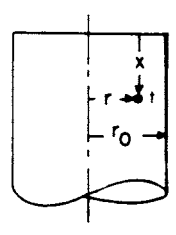


FIGURE 28 - Region of a Long Cylinder Near One End

Solution:

$$\frac{t-t_{\infty}}{t_{i}-t_{\infty}} = \left[\frac{t_{r,\,\tau}-t_{\infty}}{t_{i}-t_{\infty}}\right] \left[1 - \frac{t_{x,\,\tau}-t_{i}}{t_{\infty}-t_{i}}\right] \tag{Eq. 115}$$

where from Figure 25,

$$\frac{t_{r,\tau} - t_{\infty}}{t_i - t_{\infty}} = f\left(\frac{r}{r_o}, \frac{\alpha\tau}{r_o^2}, \frac{k}{hr_o}\right)$$
 (Eq. 116)

and, from Equation 111,

$$1 - \frac{t_{x,\tau} - t_i}{t_{\infty} - t_i} = f\left(\frac{x}{2\sqrt{\alpha\tau}}, \frac{hx}{k}\right)$$
 (Eq. 117)

where f means "function of".

CASE 2. Finite Cylinder - This cylinder, with length 2L, is of the same order of magnitude as its diameter. See Figure 29.

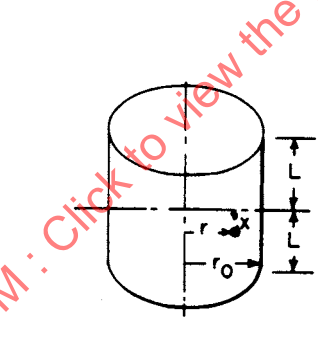


FIGURE 29 - Finite Cylinder

Solution:

$$\frac{t - t_{\infty}}{t_i - t_{\infty}} = \left[\frac{t_{r, \tau} - t_{\infty}}{t_i - t_{\infty}}\right] \left[\frac{t_{x\tau} - t_{\infty}}{t_i - t_{\infty}}\right]$$
 (Eq. 118)

where, from Figure 25,

$$\frac{t_{r,\tau} - t_{\infty}}{t_{i} - t_{\infty}} = f\left(\frac{r}{r_{o}}, \frac{\alpha\tau}{r_{o}^{2}}, \frac{k}{hr_{o}}\right)$$
 (Eq. 119)

and, from Figure 24,

$$\frac{t_{x,\tau} - t_{\infty}}{t_i - t_{\infty}} = f\left(\frac{x}{L}, \frac{\alpha \tau}{L^2}, \frac{k}{hL}\right)$$
 (Eq. 120)

CASE 3. Quarter-Infinite Solid - This is the region near the edge or intersection of two perpendicular faces of a large solid, as shown in Figure 30.



FIGURE 30 - Region Near the Intersection of Two Perpendicular Faces of a Large Solid

Solution:

$$\frac{t - t_{\infty}}{t_i - t_{\infty}} = \left[1 - \frac{t_{x1, \tau} - t_i}{t_{\infty} - t_i}\right] \left[1 - \frac{t_{x2, \tau} - t_i}{t_{\infty} - t_i}\right]$$
 (Eq. 121)

where, from Equation 111,

$$1 - \frac{t_{x1,\tau}}{t_{\infty}} = f\left(\frac{x_1}{2\sqrt{\alpha\tau}}, \frac{hx_1}{k}\right)$$
 (Eq. 122)

$$t_{x2,\tau}^{-t_i} = f\left(\frac{x_2}{2\sqrt{\alpha\tau}}, \frac{hx_2}{k}\right)$$
 (Eq. 123)

CASE 4. Eighth-Infinite solid - This region is near the corner or intersection of three mutually perpendicular faces of a large solid. See the sketch shown in Figure 31.

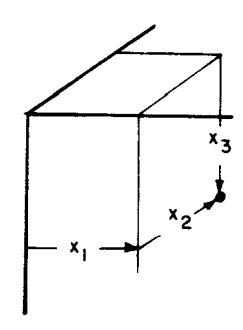


FIGURE 31 - Region Near the Corner of Three Perpendicular Faces of a Large Solid

$$\frac{t - t_{\infty}}{t_{i} - t_{\infty}} = \left[1 - \frac{t_{x1, \tau} - t_{i}}{t_{\infty} - t_{i}}\right] \left[1 - \frac{t_{x2, \tau} - t_{i}}{t_{\infty} - t_{i}}\right] \left[1 - \frac{t_{x3, \tau} - t_{i}}{t_{\infty} - t_{i}}\right]$$
(Eq. 124) on 111,

where, from Equation 111,

$$1 - \frac{t_{x1,\tau} - t_i}{t_{\infty} - t_i} = f\left(\frac{x_1}{2\sqrt{\alpha\tau}}, \frac{hx_1}{k}\right)$$
 (Eq. 125)

$$1 - \frac{t_{x2,\tau} - t_i}{t_m - t_i} = f(\frac{x_2}{2\sqrt{\alpha\tau}}, \frac{hx_2}{k})$$
 (Eq. 126)

$$1 - \frac{t_{x_1, \tau} - t_i}{t_{\infty} - t_i} = f\left(\frac{x_1}{2\sqrt{\alpha\tau}}, \frac{hx_1}{k}\right)$$

$$1 - \frac{t_{x_2, \tau} - t_i}{t_{\infty} - t_i} = f\left(\frac{x_2}{2\sqrt{\alpha\tau}}, \frac{hx_2}{k}\right)$$

$$1 - \frac{t_{x_3, \tau} - t_i}{t_{\infty} - t_i} = f\left(\frac{x_3}{2\sqrt{\alpha\tau}}, \frac{hx_3}{k}\right)$$
(Eq. 125)
$$1 - \frac{t_{x_3, \tau} - t_i}{t_{\infty} - t_i} = f\left(\frac{x_3}{2\sqrt{\alpha\tau}}, \frac{hx_3}{k}\right)$$
(Eq. 127)

CASE 5. Semi-Infinite Slab - This is the region of a large slab near one plane surface perpendicular to the faces of the slab. See Figure 32.

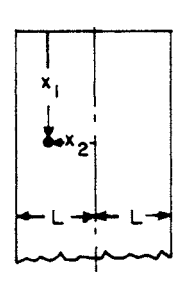


FIGURE 32 - Region of a Semi-Infinite Slab

Solution:

$$\frac{t - t_{\infty}}{t_i - t_{\infty}} = \left(1 - \frac{t_{x1, \tau} - t_i}{t_{\infty} - t_i}\right) \left(\frac{t_{x2, \tau} - t_{\infty}}{t_i - t_{\infty}}\right) \tag{Eq. 128}$$

where, from Equation 111,

$$1 - \frac{t_{x1,\tau} - t_i}{t_{\infty} - t_i} = f\left(\frac{x_1}{2\sqrt{\alpha\tau}}, \frac{hx_1}{k}\right)$$
 (Eq. 129)

and, from Figure 24,

$$\frac{t_{x2,\tau} - t_{\infty}}{t_i - t_{\infty}} = f\left(\frac{x_2}{L}, \frac{\alpha\tau}{L^2}, \frac{hL}{k}\right)$$
 (Eq. 130)

CASE 6. Quarter-Infinite Slab - This is the region of a large slab near the intersection of two perpendicular surfaces, each of which is perpendicular to the faces of the slab. See Figure 33.

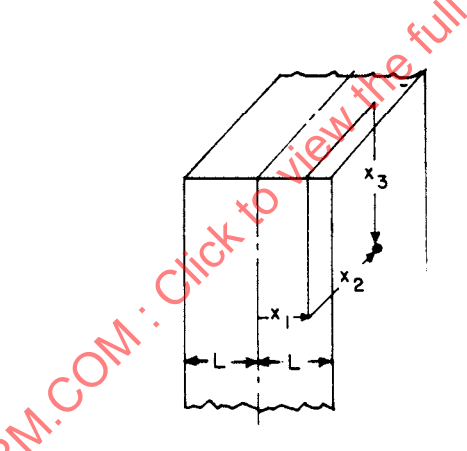


FIGURE 33 - Region of a Quarter-Infinite Slab

Solution:

$$\frac{t-t_{\infty}}{t_i-t_{\infty}} = \left(\frac{t_{x1,\,\tau}-t_{\infty}}{t_i-t_{\infty}}\right) \left(1 - \frac{t_{x2,\,\tau}-t_i}{t_{\infty}-t_i}\right) \left(1 - \frac{t_{x3,\,\tau}-t_i}{t_{\infty}-t_i}\right) \tag{Eq. 131}$$

where, from Figure 24,

$$\frac{t_{x1,\tau} - t_{\infty}}{t_i - t_{\infty}} = f\left(\frac{x_1}{L}, \frac{\alpha \tau}{L^2}, \frac{hL}{k}\right)$$
 (Eq. 132)

and, from Equation 111,

$$1 - \frac{t_{x2,\tau} - t_i}{t_{\infty} - t_i} = f\left(\frac{x_2}{2\sqrt{\alpha\tau}}, \frac{hx_2}{k}\right)$$
 (Eq. 133)

$$1 - \frac{t_{x3,\tau} - t_i}{t_m - t_i} = f\left(\frac{x_3}{2\sqrt{\alpha\tau}}, \frac{hx_3}{k}\right)$$
 (Eq. 134)

CASE 7. Infinite Rectangular Rod - This is the region of a long rod of rectangular cross section (width $2L_1$, and thickness $2L_2$) remote from both ends or a rectangular rod with insulated ends. Refer to Figure 34.

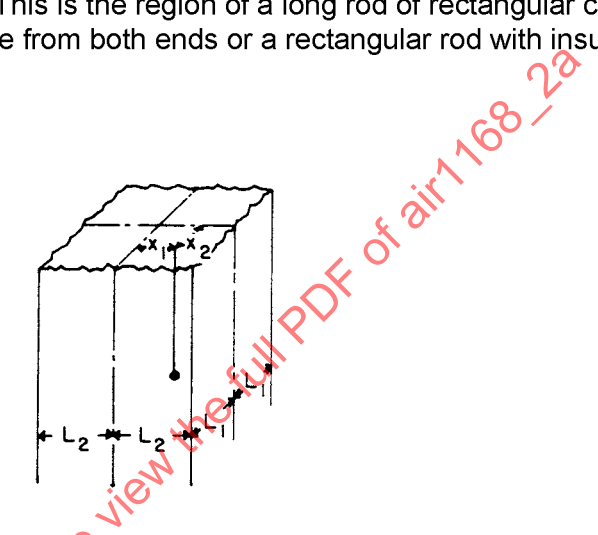


FIGURE 34 Infinite Rectangular Rod

Solution:

$$C_{t_{i}-t_{\infty}}^{t} = \left(\frac{t_{x1,\tau}-t_{\infty}}{t_{i}-t_{\infty}}\right) \left(\frac{t_{x2,\tau}-t_{i}}{t_{i}-t_{\infty}}\right)$$
 (Eq. 135)

where, from Figure 24.

$$\frac{t_{x1,\tau} - t_{\infty}}{t_i - t_{\infty}} = f\left(\frac{x_1}{L_1}, \frac{\alpha \tau}{L_1^2}, \frac{hL_1}{k}\right)$$
 (Eq. 136)

$$\frac{t_{x2,\tau} - t_{\infty}}{t_{i} - t_{\infty}} = f\left(\frac{x_{2}}{L_{2}}, \frac{\alpha\tau}{L_{2}^{2}}, \frac{hL_{2}}{k}\right)$$
 (Eq. 137)

CASE 8. Semi-Infinite Rectangular Rod - This is the region of a long rod of rectangular cross section near one end, illustrated in Figure 35.

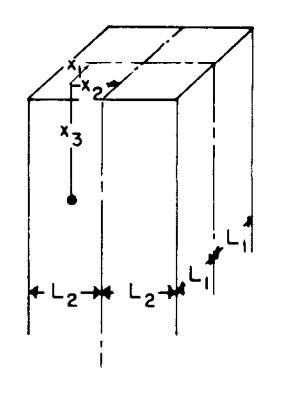


FIGURE 35 - Semi-Infinite Rectangular Rod

Solution:

$$\frac{\mathbf{t} - \mathbf{t}_{\infty}}{\mathbf{t}_{i} - \mathbf{t}_{\infty}} = \left(\frac{\mathbf{t}_{x1, \tau} - \mathbf{t}_{\infty}}{\mathbf{t}_{i} - \mathbf{t}_{\infty}}\right) \left(\frac{\mathbf{t}_{x2, \tau} - \mathbf{t}_{\infty}}{\mathbf{t}_{i} - \mathbf{t}_{\infty}}\right) \left(\frac{\mathbf{t}_{x2, \tau} - \mathbf{t}_{\infty}}{\mathbf{t}_{i} - \mathbf{t}_{i}}\right)$$
(Eq. 138)

where, from Figure 24,

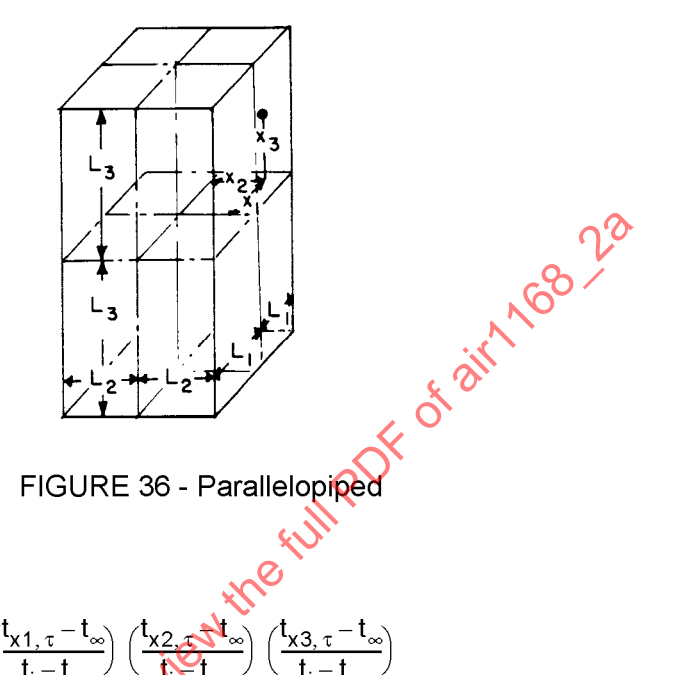
$$\frac{\mathbf{t}_{\mathbf{x}_{1},\tau}}{\mathbf{t}_{i}} = \mathbf{f}\left(\frac{\mathbf{x}_{1}}{\mathsf{L}_{1}}, \frac{\alpha\tau}{\mathsf{L}_{1}^{2}}, \frac{\mathsf{hL}_{1}}{\mathsf{k}}\right) \tag{Eq. 139}$$

$$\frac{t_{x2,\tau} - t_{\infty}}{t_i - t_{\infty}} = f\left(\frac{x_2}{L_2}, \frac{\alpha \tau}{L_2^2}, \frac{hL_2}{k}\right)$$
 (Eq. 140)

and, from 2.7.3,

$$1 - \frac{t_{x3,\tau} - t_i}{t_m - t_i} = f\left(\frac{x_3}{2\sqrt{\alpha\tau}}, \frac{hx_3}{k}\right)$$
 (Eq. 141)

CASE 9. Brick - This case applies to a parallelopiped, or brick of dimensions $2L_1$, $2L_2$, and $2L_3$, all dimensions being of the same order of magnitude. Refer to Figure 36.



Solution:

$$\frac{t - t_{\infty}}{t_{i} - t_{\infty}} = \left(\frac{t_{X1, \tau} - t_{\infty}}{t_{i} - t_{\infty}}\right) \left(\frac{t_{X2, \tau} + t_{\infty}}{t_{i} - t_{\infty}}\right) \left(\frac{t_{X3, \tau} - t_{\infty}}{t_{i} - t_{\infty}}\right)$$
(Eq. 142)

where, from Figure 24,

$$\frac{t_{x1,\tau}-t_{\infty}}{t_1-t_{\infty}} = f\left(\frac{x_1}{L_1}, \frac{\alpha\tau}{L_2^2}, \frac{hL_1}{k}\right)$$
 (Eq. 143)

$$\frac{t_{x2,\tau}-t_{\infty}}{t_{i}-t_{\infty}} = f\left(\frac{x_{2}}{L_{2}}, \frac{\alpha\tau}{L_{2}^{2}}, \frac{hL_{2}}{k}\right)$$
 (Eq. 144)

$$\frac{t_{x3,\tau} - t_{\infty}}{t_i - t_{\infty}} = f\left(\frac{x_3}{L_3}, \frac{\alpha \tau}{L_3^2}, \frac{hL_3}{k}\right)$$
 (Eq. 145)

2.8 Numerical Methods:

In this section various methods of solving heat conduction problems other than by the classical calculations given previously are considered. Some of the methods are graphical, some computational, and some electrical; some apply to steady-state flow, others to transient heat flow. The principal application is to provide a relatively quick answer to problems, the solution of which by conventional analytic means would be difficult or impossible.

2.8.1 Conformal Mapping: This is usually considered as a graphical method for the solution of two-dimensional steady-state problems where the boundary shapes preclude the use of an analytic solution. The method is based upon the characteristics of the steady-state (Laplace) heat conduction equation

$$\frac{\partial^2 t}{\partial x^2} + \frac{\partial^2 t}{\partial y^2} = 0$$
 (Eq. 146)

which allows for a system of isotherms and lines of constant heat flow that are orthogonal. The procedure used is to construct the boundaries of the system under analysis and then to sketch in by trial and error a system of isotherms and lines of constant heat flux so that they intersect everywhere at right angles to form little quadrilaterals that approximate squares as closely as possible. An example of this is heat conduction in a corner whose inner surface temperature is t₁ and whose outer surface temperature is t₂; refer to Figure 37.

The five lines roughly parallel to these surfaces (except where they bend at the corner) are isotherms that divide the temperature difference t_1 - t_2 into six equal values of Δt each. The lines of constant heat flux, which run at right angles to these isotherms, each contain equal quantities of heat flow between them of amount

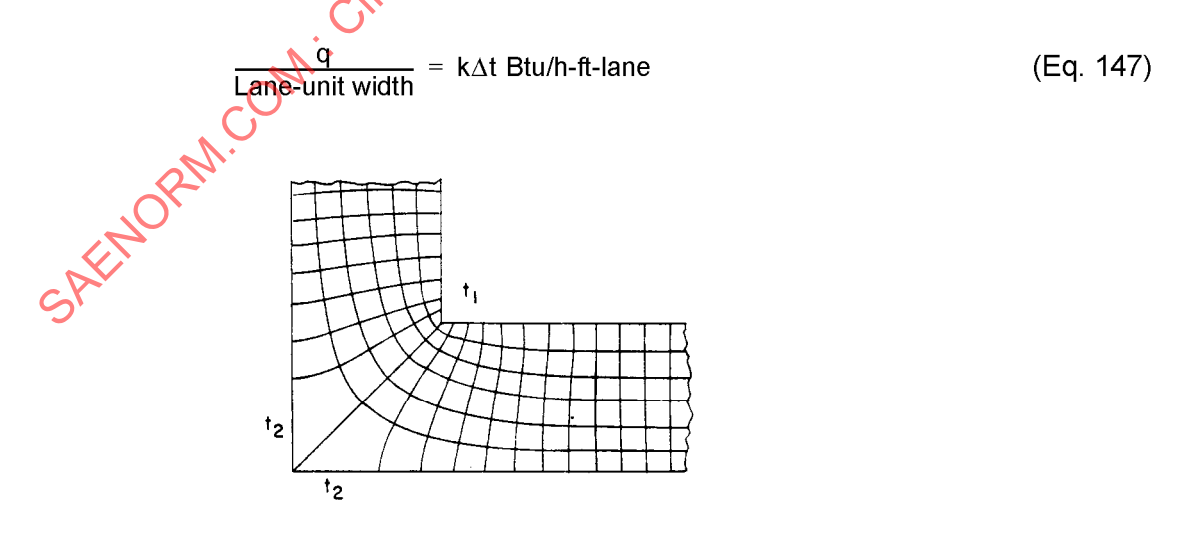


FIGURE 37 - Conformal Mappping

2.8.1 (Continued):

An accurate determination of the heat flow and temperature distribution by this graphical technique is very slow and tedious. It may be speeded up considerably if recourse may be had to an electrolytic tank or electrically conductive paper where bus bars of potential E_1 and E_2 simulate the temperature potentials and the insulated tank walls simulate insulated thermal boundaries. The isotherms (equipotentials) may be then constructed directly by probing with a voltmeter or bridge circuit, and if desired, the lines of constant heat flux may be constructed by reversing the bus bars with the insulated boundaries.

Analytic conformal mapping by coordinate transformations will provide exact solutions for regular geometric situations. Reference 1 discusses this technique in detail.

2.8.2 Relaxation: This numerical technique is applicable to steady-state heat transfer problems in one, two, or three dimensions. The method is essentially a finite difference technique, lumping the conduction into resistors between node points and simultaneously working toward a heat balance for all node points. The method is best illustrated by the sample problem given in Figure 38.

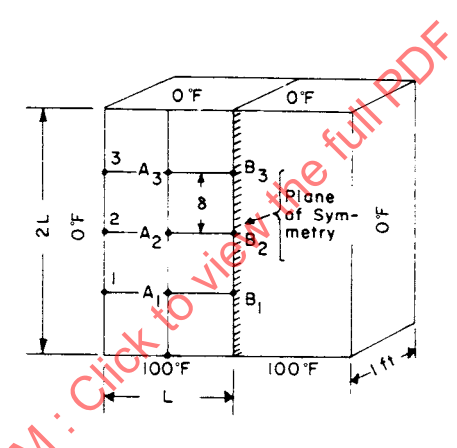


FIGURE 38 - Steady Heat Transfer Into One, Two, or Three Dimensions

Assume a brick of length and width equal to 2L and thickness of 1 ft, one side of which is at temperature 100 °F and whose other sides are at 0 °F. The problem is to find the temperatures at A_1 , A_2 , A_3 , and B_4 , B_2 , and B_3 , points on a square mesh of side $\delta = L/2$. It is noted that for the A nodes, heat is being transferred into each one from four adjacent nodes, while for the B nodes, heat is being transferred into each one from three adjacent nodes (due to symmetry in the L direction). Thus,

$$\Sigma q_{A2} = \frac{k(\delta \cdot 1)}{\delta} \left[(t_{A1} - t_{A2}) + (t_2 - t_{A2}) + (t_{B2} - t_{A2}) + (t_{A3} - t_{A2}) \right] \tag{Eq. 148}$$

2.8.2 (Continued):

or

$$Q'_{A2} = \frac{\Sigma q_{A2}}{k} = t_{A1} + t_2 + t_{B2} + t_{A3} - 4t_{A2}$$
 (Eq. 149)

and

$$\Sigma q_{B2} = k \frac{(\delta \cdot 1)}{\delta} \left[(t_{A2} - t_{B2}) + \frac{1}{2} (t_{B1} - t_{B2}) + \frac{1}{2} (t_{B3} - t_{B2}) \right]$$
 (Eq. 150)

or

$$Q'_{B2} = \frac{\Sigma q_{B2}}{k} = t_{A2} + \frac{t_{B1}}{2} + \frac{t_{B3}}{2} - 2t_{B2}$$
 (Eq. 151)

From this, it is seen that a 1 °F change in t_{A2} changes Q'_{A2} by -4 units and Q'_{A1} , Q'_{A3} , or Q'_{B2} by +1 unit. Also, a 1 °F change in t_{B2} changes Q'_{B2} by -2 units and Q'_{B1} and Q'_{B3} by +1/2 units and Q'_{A2} by +1 units. Schematically, this may be represented by the sketches of Figures 39 and 40.

For the A points:

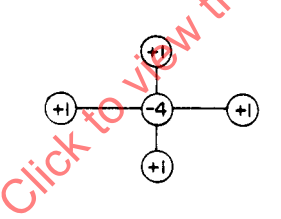


FIGURE 39 - A Nodes

For the B points:



FIGURE 40 - B Nodes

2.8.2 (Continued):

It is the objective of the relaxation method to arrive at a temperature distribution such that all Q's are zero or negligible. A problem is solved by assuming a value of the temperature distribution, calculating the Q's at each node, and then "relaxing" the temperatures at each node (one point at a time) until all Q's vanish. For the same problem, assume the following temperature distribution for the initial guess as given in the accompanying illustration, Figure 41. The calculation sheet is then set up as in Table 2. The circled values of temperature are the final results by relaxation to the nearest 1 °F; a finer mesh would give more accurate results.

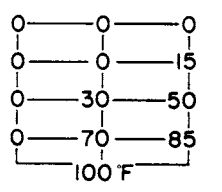


FIGURE 41 - Initial Guess of Temperature Distribution

TABLE 2 - Calculation Sheet

Step	A ₁		A ₂		A ₃ Ø		В	B 1		B 2		B 3	
	Q'	t	Q'	t	Q'	11.	Q'	t	Q′	t	Q'	t	
1. Guess temperature	-65	70	0	30	+ 45	0	-25	85	- 20	50	-5	15	
2. Relax t _{A1}	+15	50	-20		110		- 45						
3. Relax t _{B1}	-10				<u> </u>		+ 5	60	-32.5				
4. Relax t ₈₂			- 40		,		- 5		+7.5	30	-15		
5. Relax t _{A2}	- 22		+8	. 18	+33				-4.5				
6. Relax t _{A1}	+ 18	40	-2 🦰				- 15						
7. Relax t _{B1}	+8)			+5	50	- 9.5				
8. Reiax t ₈₂			+ 10				+1		+6.5	22	- 19		
9. Relax t ₈₃		- /	U.		+23				+1.5		+1	5	
10. Relax t _{A1}	0	(42)) -8				+3						
11. Relax t _{A2}	-3	$^{\prime}$	+4	15	+20				1.5				
12. Relax t _{A3}		M.	+9		0	5					+6		
13. Relax t _{A2}	-1_	77.	+1	17	+2				+0.5			_	
14. Relax t ₈₃	, O)				+5	_			+ 2		0	(8)	
15. Relax t _{A3}	M		+2		+1	(6)				_	1	_	
16. Relax t ₈₂			+3			_	+2.5	_	0	23	+1.5		
17. Relax t ₈₁	0			_			0.5	(51)	+0.5	•			
18. Relax t _{A2}	7 1		-1	(18)	2			_	+1.5				

2.8.3 Schmidt Plot: This is a graphical procedure for the analysis of transient heat flow problems in one dimension with boundary temperatures that may be time dependent. The method also works with no additional difficulty for a composite construction and with any arbitrary initial temperature distribution. The method is based upon a finite difference solution to the heat conduction equation, where the material is divided into n layers Δx thick. There is a unique relationship between the time interval $\Delta \tau$, successive steps, and layer thickness Δx , which is satisfied by

$$\frac{2\alpha\Delta\tau}{(\Delta\mathbf{x})^2} = 1 \tag{Eq. 152}$$

For this condition, the temperature at any plane I at time τ is the arithmetic mean of the temperatures in the planes on each side of it that prevailed $\Delta \tau$ previously. An example of this method is (see Figure 42).

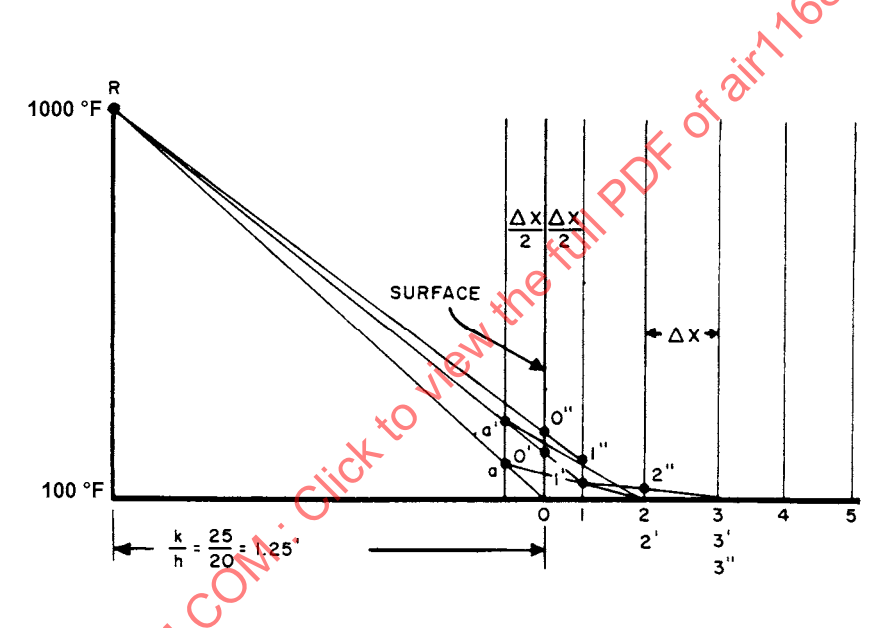


FIGURE 42 - Schmidt Plot

A steel slab 2 ft thick of initial temperature 100 °F is suddenly placed in a furnace with a temperature of 1000 °F. The heat transfer coefficient on the surface is 20 Btu/h-ft²-°F; the thermal conductivity of the slab is 25 Btu/h-ft-°F, and the thermal diffusivity is 0.5 ft²/h. Assume that $\Delta x = 0.2$ ft; then

$$\Delta \tau = \frac{(\Delta x)^2}{2\alpha} = \frac{(0.2)^2}{2(0.5)} = 0.04 \text{ h}$$
 (Eq. 153)

2.8.3 (Continued):

Subsequent steps are

- a. Mark off some vertical lines corresponding to $\Delta x = 0.2$ ft, starting at $\frac{\Delta x}{2}$ from the surface. These are points 1, 2, 3, 4, 5.
- b. To account for the heat transfer coefficient, mark off a distance equal to k/h away from the surface of the slab. Also mark off a distance $\Delta x/2 = 0.1$ ft away from the surface of the slab.
- c. Mark off point R at a vertical ordinate of 1000 °F at k/h = 1.25 ft.
- d. Connect point R with point 0 corresponding to 100 °F at the surface of the slab, and locate Draw the straight lines 0'1' and 1'2' (2' coincides with 2).

 Connect a' with 2' to locate 1".

 Connect 1' with 3' to locate 1. point a in a plane $\Delta x/2$ outside the surface.
- e. Connect point a and point 2 to locate 1'.

- h. Connect a' with 2' to locate 1".
- Connect R and 1" to locate 0".
- k. Draw in the temperature curve 0" 1"2" 3", etc.
- I. At the plane corresponding to x = 1 ft, symmetry exists, so that the temperatures at 6 are the same as those at 5; straight horizontal lines are used to connect them.

Temperature curves are shown in Table 3

TABLE3 - Location of Transient Temperature Points for Schmidt Plot

<u>τ, hr</u>	Curve					
0	012345					
0.04	0'1'.2'3'4'5'					
80.0	0"1"2"3"4"5"					
0.12	0′′′1′′′2′′′3′′′4′′′5′′′					
0.16	0′′′′1′′′′2′′′′3′′′′4′′′′5′′′′					

2.8.4 Resistance - Capacitance Networks: This is a numerical technique that solves the transient heat conduction equation (in one, two or three dimensions) by a finite difference procedure of "lumping" the system under analysis into discrete nodes, which are interconnected by thermal resistors and which also have capacitors to represent thermal storage. This technique is usually carried out on computers, and either passive analog or high-speed, large-capacity digital computers may be used. Conceptually, the problem is solved by analogy to an equivalent electrical network, since the basic equations are the same.

$$q = mc \frac{dt}{d\tau}$$
 (storage) (Eq. 154)

$$i = C \frac{dE}{d\tau}$$
 (Eq. 155)

$$q = \frac{-kA}{\Delta x} \Delta t$$
 (heat or current flow) (Eq. 156)

$$i = \frac{\Delta E}{R}$$
 (Eq. 157)

When solved on an analog computer, a suitable network of resistors and capacitors is set up with scale factors between volts and degrees, amps and Btu/h, ohms and h-°F/Btu, farads and Btu/°F, and machine time and real time. In addition to the network itself, there must be appropriate function generators to represent the boundary conditions (which are often time variant) and a means of recording the output as a function of time. When solved on a digital computer, the problem is maintained in the proper thermal units and it is not necessary to consider any scaling.

The network method is the only practical solution to complex heat transfer problems, and the accuracy of the result is limited only by the accuracy of the assumptions that led to the establishment of the network values and boundary conditions. Thus this method shifts the skill requirements in problem solving from the mathematician to the engineer, who must realistically define the paths of heat flow and the physical properties of the materials and film coefficients in the problem.

With the proper computing equipment and circuit elements, problems with radiation, change of phase, and fluid flow may be solved along with the usual convection, conduction, and storage elements. Since computer equipment is required and only complex problems involving a considerable expenditure of engineering time would be solved by this method, a more thorough review of the technique than is possible within the scope of this manual is recommended.

3. CONVECTION:

Convection is the form of heat transfer that occurs between a body and a fluid in relative motion. The process is classified as:

- a. Free convection, when the relative motion is caused by a density variation within the fluid.
- b. Forced convection, when the motion is caused by external means, such as a fan or the movement of a wing through air.

Although studied as a separate form of heat transfer, convection includes the processes of conduction and mass transfer, and is integrally involved with fluid mechanics.

3.1 Heat Transfer Coefficient:

Convective heat transfer theories for continuum flow consider the effects of a boundary layer next to the surface through which the fluid velocity decreases from the free stream velocity at the outer edge to zero adjacent to the surface. With this zero velocity condition, heat can be transferred between the fluid and the body only by conduction. This may be represented by Fourier's heat conduction law

$$\frac{\mathbf{q}}{\mathbf{A}} = -\left(\mathbf{k}_{\mathsf{f}} \frac{\partial \mathbf{t}}{\partial \mathbf{y}}\right)_{\mathsf{y}} \tag{Eq. 158}$$

where:

k_f = Conductivity of the fluid

 $-\partial t/\partial y$ = Negative fluid temperature gradient, evaluated at the surface

This temperature gradient is difficult to evaluate, and the convection process is commonly represented by

$$\frac{\mathbf{q}}{\Delta} = \mathbf{h}\Delta \mathbf{t}$$
 (Eq. 159)

(Newton's law of cooling) where h is the heat transfer coefficient and Δt represents the temperature difference between the fluid and the surface.

3.2 **Dimensionless Parameters:**

The correlation of empirical data and the construction of formulas for convective heat transfer are made easier by the use of a number of dimensionless ratios:

For V = ft/s and $\mu = lb/ft-s$:

Reynolds number =
$$N_{Re} = \frac{\rho g V x}{u}$$
 (Eq. 160)

Nusselt number =
$$N_{Nu} = \frac{hx}{k}$$
 (Eq. 161)

Stanton number =
$$N_{St} = \frac{h}{\rho g V c_p}$$
 (Eq. 162)

For V = ft/s,
$$N_{St} = \frac{h}{3600\rho gVc_p}$$
 (Eq. 163)

Prandtl number =
$$N_{Pr} = \frac{\mu c_p}{k}$$
 (Eq. 164)

Nusselt number =
$$N_{Nu} = \frac{hx}{k}$$
 (Eq. 161)

For V = ft/h:

Stanton number = $N_{St} = \frac{h}{\rho g V c_p}$ (Eq. 162)

For V = ft/s, $N_{St} = \frac{h}{3600 \rho g V c_p}$ (Eq. 163)

Prandtl number = $N_{Pr} = \frac{\mu c_p}{k}$ (Eq. 164)

Grashof number = $N_{Gr} = \frac{\Delta t x^3 (\rho g)^2 g \beta}{\mu^2}$ (Eq. 165)

Mach number = $M = \frac{V}{a_0}$ (Eq. 166)

where a_0 = local speed of sound

Graetz number = $N_{Gz} = \frac{W c_p}{kx}$ (Eq. 167)

Euler number = $N_{Eu} = \frac{Q \Delta p}{\rho g V^2}$ (Eq. 168)

Schmidt number = $N_{Sc} = \frac{\mu}{\rho g D}$ (Eq. 169)

NOTE: The reader is cautioned to prove to himself that the units he uses makes these equations

Mach number =
$$M = \frac{V}{a_0}$$
 (Eq. 166)

Graetz number =
$$N_{Gz} = \frac{Wc_p}{kx}$$
 (Eq. 167)

Euler number =
$$N_{Eu} = \frac{g\Delta p}{\rho g V^2}$$
 (Eq. 168)

Schmidt number
$$\neq N_{Sc} = \frac{\mu}{\rho gD}$$
 (Eq. 169)

NOTE: The reader is cautioned to prove to himself that the units he uses makes these equations truly dimensionless.

3.2 (Continued):

where D = self-diffusion coefficient

Lewis number =
$$N_{Le} = \frac{N_{Sc}}{N_{Pr}} = \frac{\alpha}{D}$$
 (Eq. 170)

where α = thermal diffusivity

Knudsen number =
$$N_{Kn} = \frac{\lambda_m}{x}$$
 (Eq. 171)

where λ_{m} = Molecular mean free path

A subscript on the dimensionless parameter indicates the characteristic dimension used and/or the condition at which the properties are evaluated.

3.3 Basic Boundary Layer Concepts:

When a real fluid and a body are in motion with respect to each other, viscous forces in the fluid tend to retard the flowing particles near the body surface. This results in the development of a region called the "boundary layer", extending outward from the surface where the relative velocity is zero to the point where the velocity is the same as the free stream velocity. The viscous shearing stresses cause it to thicken as it progresses back from the leading edge. Figure 43 illustrates the development of the boundary layer along a flat surface parallel to the flow direction.

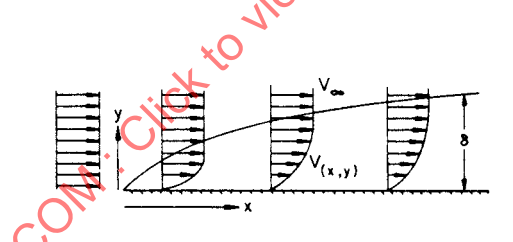


FIGURE 43 - Boundary Layer Along a Flat Surface Parallel to Direction of Flow

Initially, as is shown in Figure 43, the streamlines are laminar (that is, are parallel to each other). At some distance back from the leading edge, because of flow instability or the influence of some external disturbance (such as surface roughness), the flow may become turbulent.

3.3 (Continued):

In the turbulent boundary layer, no parallel streamlines are present; rather, eddies are formed and the streamlines become well mixed. The turbulent boundary layer, as shown in Figure 44, is considered to be made up of three regions:

- a. A laminar sublayer, in which viscous forces predominate.
- b. A buffer region, in which both viscous and turbulent forces exist.
- c. A completely turbulent region.

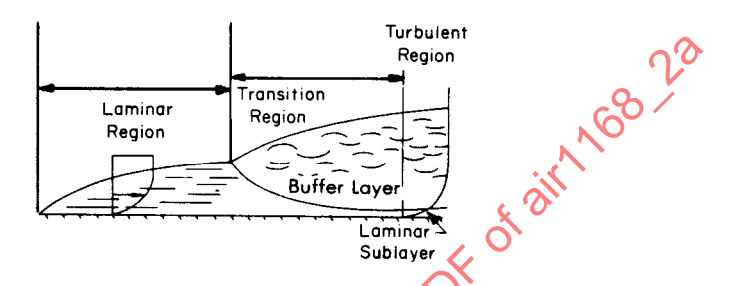


FIGURE 44 - Regions of Turbulent Boundary Layers

Because of the eddying motion within the turbulent region, heat is transferred more rapidly than with a laminar boundary layer. Figure 44 illustrates the laminar and turbulent velocity profiles, which may be approximated by

$$\frac{V}{V_{\infty}} = a + b\left(\frac{y}{\delta}\right) + c\left(\frac{y}{\delta}\right)^2 + d\left(\frac{y}{\delta}\right)^3$$
 (Eq. 172)

for laminar flow, where a, b, c and d are constants, and

$$\frac{V}{V_{c}} = \left(\frac{y}{\delta}\right)^{1/7}$$
 (Eq. 173)

for turbulent flow in the portion of the boundary layer outside the buffer region.

The change from aminar to turbulent flow is seldom abrupt, but usually occurs gradually in an area called the transition region. For flow along a free surface, the boundary layer will continue to increase in thickness until it reaches the end of the body. However, when its development is restricted (as in the case in channel flow) boundary layers build up from opposite sides of the channel, and eventually meet some distance back from the entrance. This is shown in Figure 45.

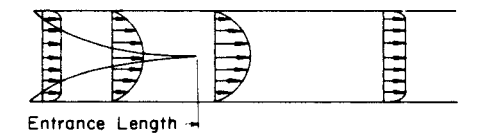


FIGURE 45 - Transition Region of Laminar to Turbulent Flow

3.3.1 Boundary Layer Thickness: The boundary layer thickness, δ , is the distance from the wall outward to the point where the velocity is that of the undisturbed stream. Since the velocity approaches free stream velocity asymptotically, δ is often taken as the distance where the velocity is 99% of that of the free stream.

Other definitions of the boundary layer thickness in common use are: $\delta^* = D$ splacement thickness; this is the amount by which the streamlines external to the boundary layer are shifted outward because of the formation of the boundary layer. The defining equation is

$$\delta^* = \int_0^\infty \left(I - \frac{\rho V}{\rho_\infty V_\infty} \right) dy \tag{Eq. 174}$$

 θ = Momentum thickness; this is a measure of the loss of momentum in the boundary layer. It is defined as

$$\theta = \int_{0}^{\infty} \left(\frac{\rho V}{\rho_{\infty} V_{\infty}} \left\{ \sqrt{\frac{V}{V_{\infty}}} \right\} \right) dy$$
 (Eq. 175)

 δ_t = Thermal boundary layer thickness this is given by

$$\int_{0}^{\infty} \frac{\rho V}{\rho_{\infty} V_{\infty}} \left(I - \frac{T}{T_{\infty}} \right) dy$$
(Eq. 176)

The "thermal boundary layer" is the distance in which the fluid temperature changes from the temperature immediately adjacent to the surface to that of the undisturbed flow. The thermal and velocity boundary layers generally do not have the same profile or thickness.

Free Convection: 3.4

Mechanism: When a body is placed in a fluid at a temperature different from that of the body, heat is transferred by conduction between the body and the fluid. This gives rise to density differences, and the heated portions of the fluid tend to rise and be replaced by colder fluid. Natural convection is therefore due to buoyancy (gravitational) forces. Natural convection can also be caused by other forces, such as centrifugal and Coriolis forces.

Correlations of heat transfer by free convection usually take the form:

$$N_{Nu} = C(N_{Gr}N_{Pr})^{n}$$
 (Eq. 177)

where:

C = Empirical constant

The product of Grashof and Prandtl numbers is

$$N_{Nu} = C(N_{Gr}N_{Pr})^n \tag{Eq. 177}$$
 ont
$$N_{Gr}N_{Pr} = \frac{\Delta t L^3(\rho g)^2 g\beta c_p}{\mu k} \tag{Eq. 178}$$
 erence, °F nension, ft cumetric expansion = 1/T, °F-1 (valid only for gases) vity, Btu/s-ft-°F

where:

 Δt = Temperature difference, °F

L = Characteristic dimension, ft

 β = Coefficient of volumetric expansion = 1/T, °F⁻¹ (valid only for gases)

k = Thermal conductivity, Btu/s-ft-°F

μ = Absolute viscosity, lb/ft-s

The factor

$$Y = \frac{(\rho g)^2 g \beta c_p}{\mu k}$$
 (Eq. 179)

is plotted as a function of temperature for air at atmospheric pressure in Figure 46.

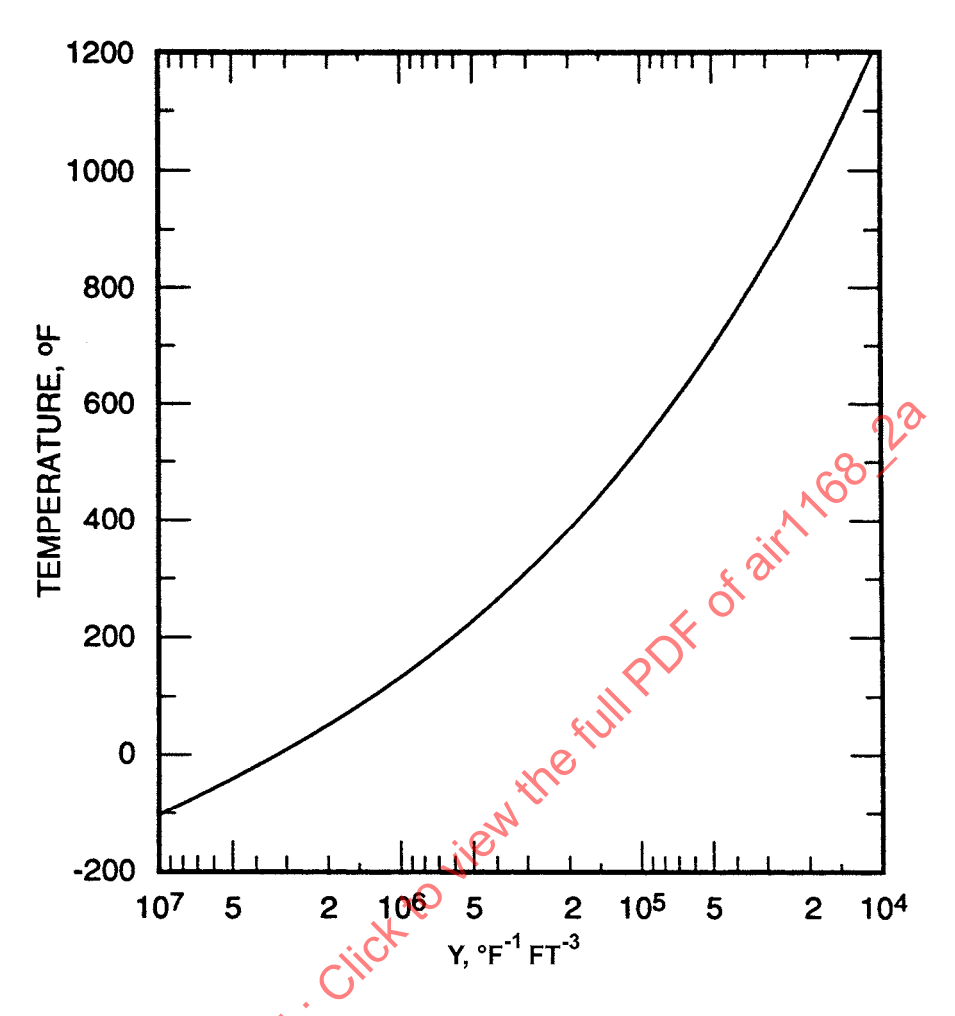


FIGURE 46 - Free Convection Heat Transfer Parameter $Y = (\rho g)^2 g \beta c_p / \mu k$

3.4.2 Free Convection in Open Spaces: The general equations and the simplified equations for air are given below for five different flow geometries.

CASE 1. Vertical Plates and Cylinders - See Figure 47.



FIGURE 47 - Sketch of a Vertical Plate or Cylinder

3.4.2 (Continued):

General equations are:

$$N_{Nu,av} = \frac{h_{av}x}{k} = 0.59 (N_{Gr}N_{Pr})^{1/4}$$
 (Eq. 180)

for
$$10^3 < N_{Gr}N_{Pr} < 10^9$$
 (Eq. 181)

 $N_{Nu,av} = \frac{h_{av}x}{k} = 0.13 (N_{Gr}N_{Pr})^{1/3}$ and (Eq. 182)

for
$$10^9 < N_{Gr}N_{Pr} < 10^{12}$$
 (Eq. 183)

where the characteristic dimension L to be used in the N_{Gr}N_{Pr} equation (Equation 178) is x

Simplified equations for air are:

$$h_{av} = 0.29 \left(\frac{P}{14.7}\right)^{1/2} \left(\frac{\Delta t}{x}\right)^{1/4}$$
 (Eq. 184)

are:
$$h_{av} = 0.29 \left(\frac{P}{14.7}\right)^{1/2} \left(\frac{\Delta t}{x}\right)^{1/4} \qquad (Eq. 184)$$

$$h_{av} = 0.19 \left(\frac{P}{14.7}\right)^{2/3} (\Delta t)^{1/3} \qquad (Eq. 185)$$
 or air, P is the fluid static pressure in psia, Δt is the temperature

In the simplified equations for air, P is the fluid static pressure in psia, Δt is the temperature difference between fluid and surface, and x, D are in feet.

CASE 2. Horizontal Cylinders - See Figure 48.



FIGURE 48 - Sketch of a Horizontal Cylinder

3.4.2 (Continued):

General equations are:

$$N_{Nu,av} = \frac{h_{av}D}{k} = 0.53 (N_{Gr}N_{Pr})^{1/4}$$
 (Eq. 186)

for
$$10^3 < N_{Gr}N_{Pr} < 10^9$$
 (Eq. 187)

 $N_{Nu,av} = \frac{h_{av}D}{k} = 0.126 (N_{Gr}N_{Pr})^{1/3}$ and (Eq. 188)

for
$$10^9 < N_{Gr}N_{Pr} < 10^{12}$$
 (Eq. 189)

where the characteristic dimension is D

Simplified equations for air are:

nension is D

are:
$$h_{av} = 0.27 \left(\frac{P}{14.7}\right)^{1/2} \left(\frac{\Delta t}{D}\right)^{1/4} \qquad (Eq. 190)$$

$$h_{av} = 0.18 \left(\frac{P}{14.7}\right)^{2/3} (\Delta t)^{1/3} \qquad (Eq. 191)$$
Plates (Hot Face Up or Cooled Face Down) - See Figure 49.

$$h_{av} = 0.18 \left(\frac{P}{14.7}\right)^{2/3} (\Delta t)^{1/3}$$
 (Eq. 191)

CASE 3. Horizontal Square Plates (Hot Face Up of Cooled Face Down) - See Figure 49.



FIGURE 49 - Horizontal Square Plate (Hot Face Up or Cooled Face Down)

General equations are:

$$N_{Nu,av} = \frac{h_{av}x}{k} = 0.54 (N_{Gr}N_{Pr})^{1/4}$$
 (Eq. 192)

SAE AIR1168/2A Page 71 of 194

3.4.2 (Continued):

for
$$10^5 < N_{Gr}N_{Pr} < 2 \times 10^7$$
 (Eq. 193)

and
$$N_{Nu,av} = \frac{h_{av}x}{k} = 0.14 (N_{Gr}N_{Pr})^{1/3}$$
 (Eq. 194)

for
$$2 \times 10^7 < N_{Gr}N_{Pr} < 3 \times 10^{10}$$
 (Eq. 195)

where the characteristic dimension is x

Simplified equations for air are:

$$h_{av} = 0.27 \left(\frac{P}{14.7}\right)^{1/2} \left(\frac{\Delta t}{x}\right)^{1/4}$$
 (Eq. 196)

$$h_{av} = 0.22 \left(\frac{P}{14.7}\right)^{2/3} (\Delta t)^{1/3}$$
 (Eq. 197)

CASE 4. Horizontal Square Plates (Hot Face Down or Cooled Face Up) - See Figure 50.



FIGURE 50 - Horizontal Square Plate (Hot Face Down or Cooled Face Up)

The general equation is:

$$N_{Nu,av} = \frac{h_{av}x}{k} = 0.27 (N_{Gr}N_{Pr})^{1/4}$$
 (Eq. 198)

for
$$3 \times 10^5 < N_{Gr} N_{Pr} < 3 \times 10^{10}$$
 (Eq. 199)

where the characteristic dimension is x

3.4.2 (Continued):

The simplified equation for air is:

$$h_{av} = 0.12 \left(\frac{P}{14.7}\right)^{1/2} \left(\frac{\Delta t}{x}\right)^{1/4}$$
 (Eq. 200)

CASE 5. Sphere - See Figure 51.



FIGURE 51 - Sphere

The general equation is:

$$N_{Nu,av} = \frac{h_{av}D}{k} = 0.51 (N_{Gr}N_{Pr})^{1/4}$$
 (Eq. 201)

for
$$10^3 < N_{Gr}N_{Pr} < 10^7$$
 (Eq. 202)

where the characteristic dimension is D
The simplified equation for air is:

$$G_{av} = 0.487 \left(\frac{P}{14.7}\right)^{1/2} \left(\frac{\Delta t}{D}\right)^{1/4}$$
 (Eq. 203)

Free Convection in Enclosed Spaces: The equations for enclosed spaces are similar to those for 3.4.3 open spaces except that Δt is the difference in temperature between the two surfaces, h' is the average free convection heat transfer coefficient based on the temperature difference between the two surfaces, and the net convective heat transfer is given by

$$q_c = h'A\Delta t$$
 (Reference 3) (Eq. 204)

Radiation occurs between the two surfaces; in this section the effect of radiation is not included.

3.4.3 (Continued):

If the clearance, δ , between the plates is very small, free convection is suppressed and heat is transferred by conduction only. The ratio of actual heat transferred to that transferred by conduction only is

$$\frac{q_c}{q_k} = \frac{h'\delta}{k} = N'_{Nu}$$
 (Eq. 205)

The general equations and limits are given below for three different flow geometries.

CASE 1. Vertical Parallel Plates - See Figure 52.



FIGURE 52 - Vertical Parallel Plate

$$N_{Nu} = \frac{h'\delta}{k} = \frac{0.2}{(\lambda_0)^{1/9}} (N_{Gr}N_{Pr})^{1/4}$$
 (Eq. 206)

for
$$2 \times 10^4 < N_{Gr} < 2.1 \times 10^5$$

(Eq. 209)

and

$$N_{Nu} = \frac{h'\delta}{k} = \frac{0.071}{(1/\delta)^{1/9}} (N_{Gr} N_{Pr})^{1/3}$$
 (Eq. 208)

for 2.1 x
$$10^5 < N_{Gr} < 1.1 \times 10^7$$

where the characteristic dimension is δ

CASE 2. Horizontal Parallel Plates (Heat Flow Upward) - See Figure 53.



FIGURE 53 - Horizontal Parallel Plates

3.4.3 (Continued):

$$N_{Nu} = \frac{h'\delta}{k} = 0.21 (N_{Gr}N_{Pr})^{1/4}$$
 (Eq. 210)

for
$$10^4 < N_{Gr} < 3.2 \times 10^5$$
 (Eq. 211)

$$N_{Nu} = \frac{h'\delta}{k} = 0.075 (N_{Gr}N_{Pr})^{1/3}$$
 (Eq. 212)

for
$$3.2 \times 10^5 < N_{Gr} < 10^7$$
 (Eq. 213)

where the characteristic dimension is δ

CASE 3. Horizontal Annular Enclosed Spaces - See Figure 54.

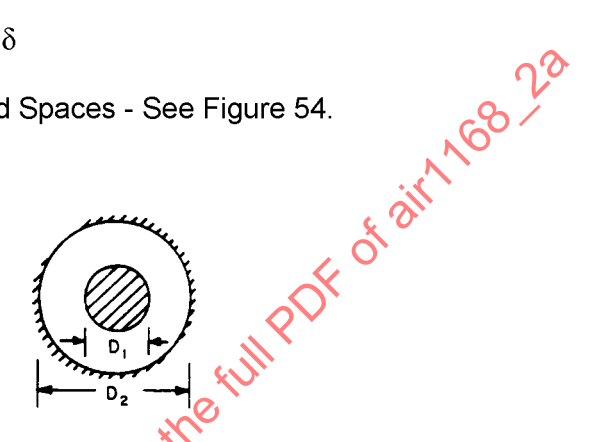


FIGURE 54 - Horizontal Annular Enclosed Space

$$h' = D_1 \ln(D_2/D_1)$$
 (Eq. 214)

(Experimental data for $1.2 < D_2/D_1 < 3$). Obtain N'_{Nu} from the relation given in Equations 206 and 208 for vertical parallel plates. (Editor's Note: No information can be found in McAdams (Reference 6) or other heat transfer references about what characteristic dimension to use in the $N_{Gr}N_{Pr}$ Equations 206 and 208 and Equation 178. My estimate is $(D_2-D_1)/2$.)

$$q = h'A_1\Delta t (Eq. 215)$$

Figure 55 shows the effect of plate separation distance on the heat transfer coefficient h'.

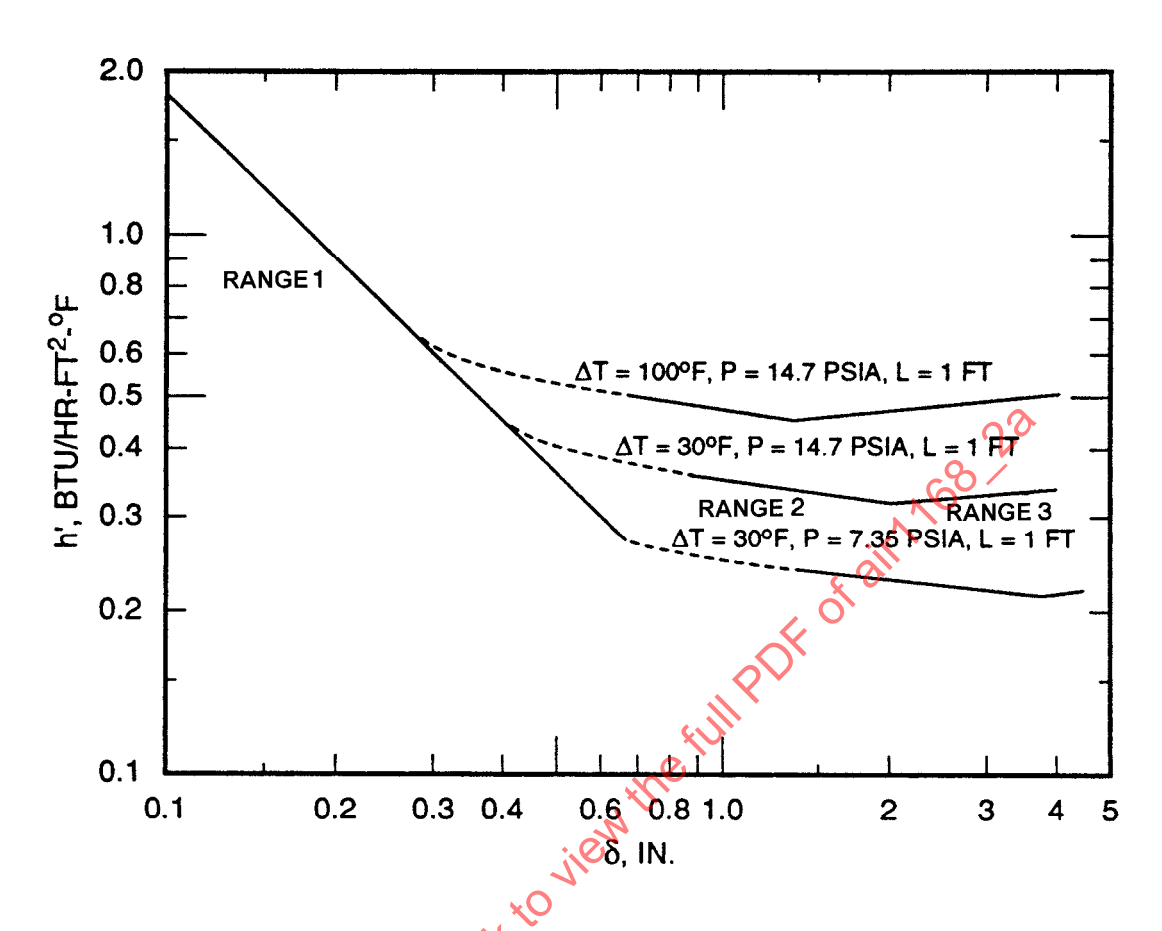


FIGURE 55 - Free Convection in Enclosed Space (Air at 70 °F)
Range 1 - h' = k/
$$\delta$$
. Range 2 - h' =
$$\frac{(k/\delta)(0.2)(N_{Gr}N_{Pr})^{1/4}}{(L/\delta)^{1/9}}$$
. Range 3 - h' =
$$\frac{(k/\delta)(0.071)(N_{Gr}N_{Pr})^{1/3}}{(L/\delta)^{1/9}}$$

Forced Convection in Incompressible Flow: 3.5

The heat transfer is expressed by

$$q = hA(t_f - t_w)$$
 (Eq. 216)

The heat transfer coefficient is often expressed nondimensionally as

$$N_{Nu} = \frac{hx}{k} = f(N_{Re}, N_{Pr})$$
 (Eq. 217)

$$N_{St} = \frac{h}{\rho g V c_p} = f(N_{Re}, N_{Pr})$$
 (Eq. 218)

The average heat transfer coefficient, hav, is related to the local value by

$$h_{av} = \frac{1}{x} \int_{o}^{x} h_{x} d_{x}$$
 (Eq. 219)

Unless otherwise noted, fluid properties are to be evaluated at the arithmetic mean between the wall and freestream temperatures:

$$t = \frac{t_w + t_f}{2}$$
 (Eq. 220)

The relationship between local heat transfer and local skin friction is

$$N_{St} = \frac{c_f}{2N_{Pr}^{2/3}}$$
 (Colburn's equation) (Eq. 221)

where:

c_f = Skin friction coefficient

The skin friction coefficient is related to the shearing stress at the wall, $\tau_{\rm W}$ through the formulas

$$c_f = \frac{T_W}{(Eq. 222)}$$

3.5.1 Laminar and Turbulent Flow: General cases for both laminar and turbulent flows with constant wall temperature are explained below.

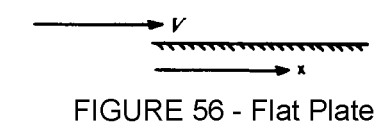
NOTE: Symbols for simplified equations for air in 3.5 have the following units:

P =
$$lb/ft^2$$

V = ft/s
x, X, D, b, y = ft
h = $Btu/h-ft^2-°F$
T = $°R$
w = lb/h
G = $lb/h-ft^2$

Laminar Flow: Generalized equations and simplified equations for air are given for six different cases of flow geometry.

CASE 1. Flat Plate - See Figure 56.



The general equations are:

$$N_{Nu,x} = \frac{h_x x}{k} = 0.332 (N_{Re,x})^{1/2} (N_{Pr})^{1/3}$$
 (Eq. 224)

$$N_{Nu,x} = \frac{h_x x}{k} = 0.332 (N_{Re,x})^{1/2} (N_{Pr})^{1/3}$$

$$N_{St,x} = \frac{h_x}{3600 \rho gVc_p} = \frac{0.332}{(N_{Re,x})^{1/2} (N_{Pr})^{2/3}}$$
(Eq. 224)

ion for air is:

The simplified equation for air is:

s:

$$h_{x} = 0.0077 \left(\frac{PV}{x}\right)^{1/2}$$
(Eq. 226)

CASE 2. Cylinder With External Flow Parallel to Axis (N_{Re.x} < 500,000) - See Figure 57.

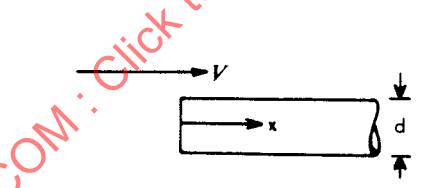


FIGURE 57 - Cylinder With External Flow Parallel to Axis

The general equations are:

$$c_f = \frac{0.664}{(N_{Re})^{1/2}}$$
 (See Figure 58) (Eq. 227)

$$N_{Nu,x} = 0.332 (N_{Re,x})^{1/2} (N_{Pr})^{1/3}$$
 (Eq. 228)

Verified experimentally by Jakob and Dow, Reference 20:

$$h_{av} = 2h_x \tag{Eq. 229}$$

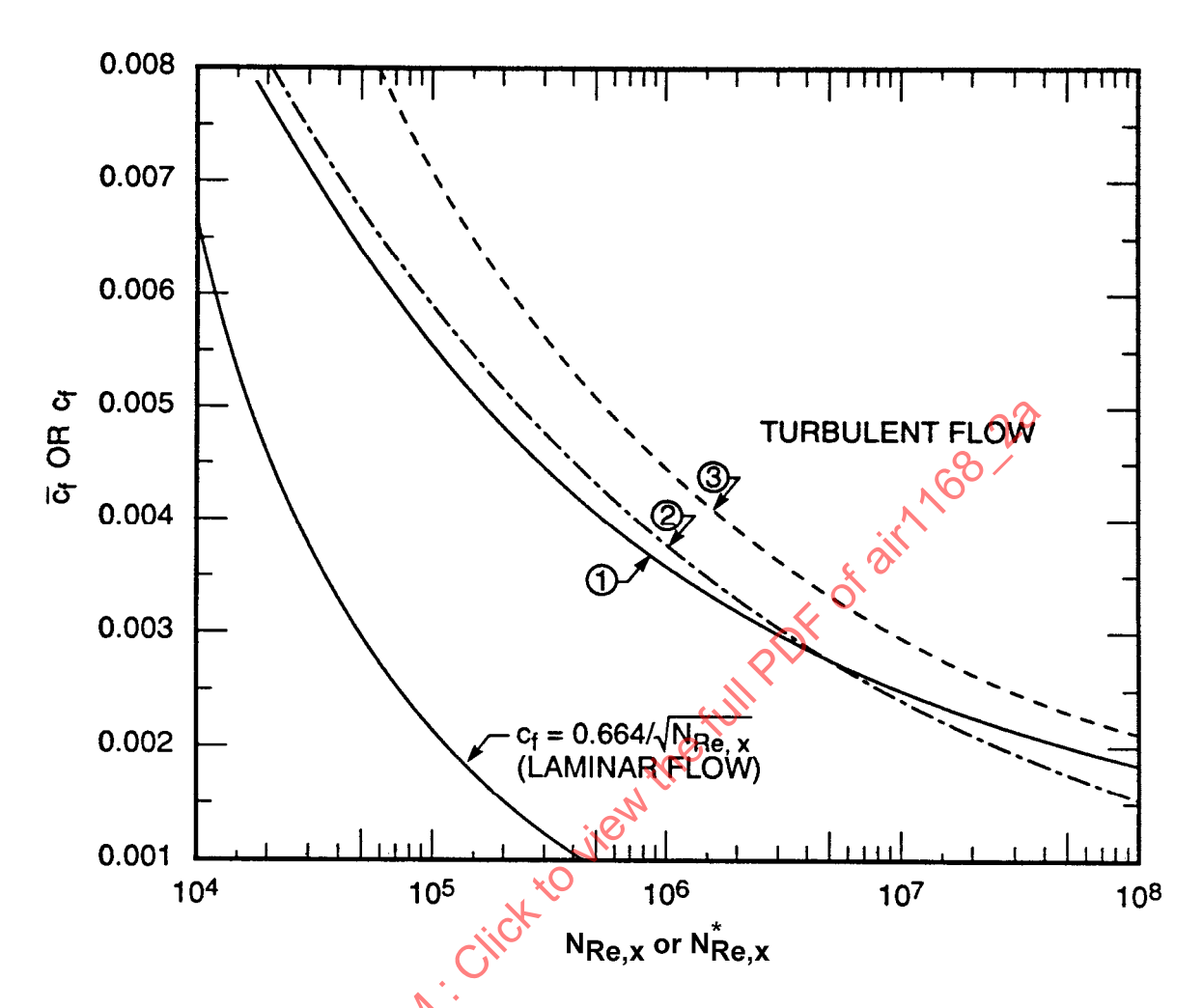


FIGURE 58 - Duct Flow Skin Friction Coefficient Versus Reynolds Number at Edge of Boundary Layer (1) $c_f = 0.557 \bar{c}_f/(0.557 + 2\sqrt{\bar{c}}_f)$, (2) $c_f = 0.0592/N_{Re,x}^{0.2}$, (3) $\sqrt{\bar{c}}_f = 0.252/log_{10} (N_{Re,x} \bar{c}_f)$

3.5.1.1 (Continued):

CASE 3. Cylinder With External Flow Normal to Axis (1000 < $N_{Re,D}$ < 50,000) - See Figure 59.

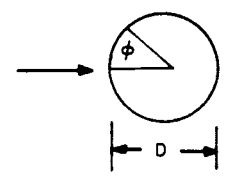


FIGURE 59 - Cylinder With External Flow Normal to Axis

The general equations are:

$$N_{Nu,\phi} = \frac{h_{\phi}D}{k} = 1.14(N_{Re,D})^{1/2} (N_{Pr})^{0.4} \left[1 - \left(\frac{\phi}{90}\right)^3\right], 0 < \phi \approx 80^{\circ}$$
 (Eq. 230)

$$N_{Nu,av} = \frac{h_{av}D}{k} = 0.26(N_{Re,D})^{0.6}(N_{Pr})^{0.3}$$
 (over the entire cylinder) (Eq. 231)

The simplified equations for air are:

$$h_{\phi} = 0.0266 \left(\frac{PV}{D}\right)^{0.5} \left[1 - \left(\frac{\phi}{90}\right)^{3}\right]$$
 (Eq. 232)

for air are:
$$h_{\phi} = 0.0266 \left(\frac{\text{PV}}{\text{D}}\right)^{0.5} \left[1 - \left(\frac{\phi}{90}\right)^{3}\right] \tag{Eq. 232}$$

$$h_{\text{av}} = \frac{0.0194}{\text{T}^{0.17}} \frac{(\text{PV})^{0.6}}{\text{D}^{0.4}} \tag{Eq. 233}$$
 With Parabolic Velocity Distribution - See Figure 60.

CASE 4. Round Tubes With Parabolic Velocity Distribution - See Figure 60.



FIGURE 60 - Round Tube With Parabolic Velocity Distribution

The general equation is:

$$N_{Nu,x} = \frac{h_x D}{k} 1.16 \left(31 + \frac{w c_p}{kx}\right)^{1/3}$$
 (Eq. 234)

3.5.1.1 (Continued):

The simplified equation for air is:

$$h_{x} = 3.65 \frac{k}{D} \left(1 + 0.38 \frac{w}{x} \right)^{1/3}$$
 (Eq. 235)

CASE 5. Rectangular Tubes With Parabolic Velocity Distribution - See Figure 61.

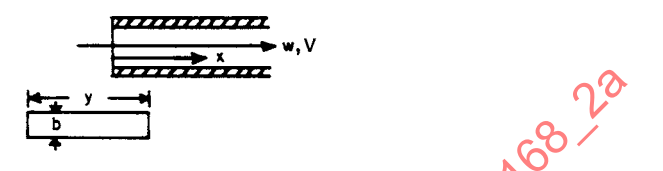


FIGURE 61 - Rectangular Tube With Parabolic Velocity Distribution

The general equation is:

$$N_{\text{Nu,b}} = \frac{h_{\text{x}}b}{k} \, 0.98 \, \left(59 + \frac{wc_{\text{p}}b}{kxy}\right)^{1/3} \tag{Eq. 236}$$
 for air is:
$$h_{\text{x}} = 3.80 \, \frac{k}{b} \, \left(1 + 0.20 \, \frac{wb}{xy}\right)^{1/3} \tag{Eq. 237}$$

$$N_{\text{Re,D}} < 150,000) \, - \, \text{See Figure 62}.$$

The simplified equation for air is:

$$h_x = 3.80 \frac{k}{b} \left(1 + 0.20 \frac{wb}{xy}\right)^{1/3}$$
 (Eq. 237)

CASE 6. Sphere (20 < $N_{Re,D}$ < 150,600) - See Figure 62.

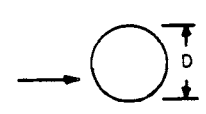


FIGURE 62 - Sphere

The equation for air is:

$$N_{Nu,D} = \frac{hD}{k} = 0.33 (N_{Re,D})^{0.6}$$
 (Eq. 238)

3.5.1.2 Turbulent Flow: Generalized equations and simplified equations for air are given for four different flow geometries. The equations are valid over the Prandtl No. range of 0.5 to 10.

CASE 1. Flat Plate - See Figure 63.

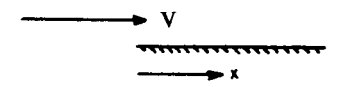


FIGURE 63 - Flat Plate

The general equation is:

$$N_{St,x} = \frac{0.0296}{(N_{Re,x})^{0.2}(N_{Pr})^{2/3}} = \frac{h_x}{3600 \ \rho g V c_p}$$
 (Eq. 239)

The simplified equation for air is:

$$h_{x} = \frac{0.0212}{T^{0.5}} \frac{(PV)^{0.8}}{x^{0.2}}$$
 (Eq. 240)

for $N_{Re,x} < 10^7$

CASE 2. Cylinders With External Flow Parallel to Axis - See Figure 64.

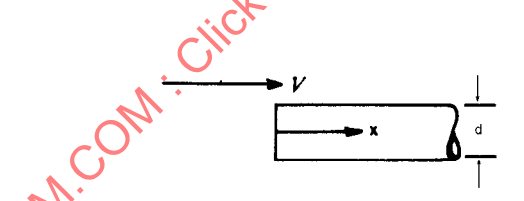


FIGURE 64 - Cylinder With External Flow Parallel to Axis

3.5.1.2 (Continued):

The general equations are:

$$N_{St,x} = 0.0243 (N_{Re,x})^{0.8} (N_{Pr})^{0.4}$$
 (Eq. 241)

$$c_f = \frac{0.0592}{(N_{Re,x})^{0.2}}$$
 (See Figure 58, line 2) (Eq. 242)

$$h_{av} = 1.25 h_x$$
 (Eq. 243)

for $N_{Re.x} > 10^7$

The simplified equation for air is:

$$N_{St} = 0.020 (N_{Re})^{0.8} (N_{Pr})^{0.4}$$
 (Eq. 244)

CASE 3. Duct (Channel) With Flow Near Entrance - See Figure 65

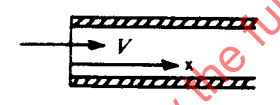


FIGURE 65 - Duct (Channel) With Flow Near Entrance

In this case $0 < x \le 4.4 D_H$ where D_H is the hydraulic diameter.

General equations:

$$\sqrt{\bar{c}_f} \in \frac{0.252}{\log_{10}(N_{Re,x}\bar{c}_f)}$$
 (See Figure 58, line 3) (Eq. 245)

$$c_{f} = \frac{0.557\bar{c}_{f}}{0.557 + 2\sqrt{\bar{c}_{f}}} \text{ (See Figure 58, line 1)}$$

$$N_{St,x} = \frac{h_{x}}{3600g\rho Vc_{p}} = \frac{c_{f}}{2(N_{Pr})^{2/3}}$$
(Eq. 247)

$$N_{St,x} = \frac{h_x}{3600g\rho Vc_p} = \frac{c_f}{2(N_{Pr})^{2/3}}$$
 (Eq. 247)

$$N_{St,av} = \frac{h_{av}}{3600g\rho Vc_p} = \frac{c_f}{2(N_{Pr})^{2/3}}$$
 (Eq. 248)

(Iterative solution required).

3.5.1.2 (Continued):

CASE 4. Channel Flow, Fully Developed - See Figure 66. In this case, 4.4 D_H < x; N_{Re,D_H} > 2200.

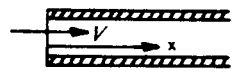


FIGURE 66 - Channel Flow, Fully Developed

General equations:

$$N_{St,av} = \frac{h_{av}}{3600g\rho Vc_p} = \frac{0.0225}{(N_{Re,Du})^{0.2}(N_{Pr})^{2/3}}$$
 (Eq. 249)

$$N_{\text{Nu,av}} = \frac{h_{\text{av}}D_{\text{H}}}{k} = 0.0225 \ (N_{\text{Re},D_{\text{H}}})^{0.8} (N_{\text{Pr}})^{1/3}$$
 (Eq. 250)

$$h_{av} = h_x \left(1 + 1.1 \frac{D_H}{x} \right)$$
 (Eq. 251)

Simplified equations for air:

$$h_{av} \approx 5.4 \times 10^{-4} \text{ T}^{0.3} \frac{\text{G}^{0.8}}{\text{D}_{H}^{0.2}}$$
 (Eq. 252)

ral equations:
$$N_{St,av} = \frac{h_{av}}{3600g\rho Vc_p} = \frac{0.0225}{(N_{Re,D_H})^{0.2}(N_{Pr})^{2/3}} \qquad (Eq. 249)$$

$$N_{Nu,av} = \frac{h_{av}D_H}{k} = 0.0225 \ (N_{Re,D_H})^{0.8} (N_{Pr})^{1/3} \qquad (Eq. 250)$$

$$h_{av} = h_x \left(1 + 1.1 \frac{D_H}{x}\right) \qquad (Eq. 251)$$
iffied equations for air:
$$h_{av} \cong 5.4 \times 10^{-4} \ T^{0.3} \ \frac{G^{0.8}}{D_H^{0.2}} \qquad (Eq. 252)$$

$$\cong \frac{0.0157}{T^{0.5}} \frac{(PV)^{0.8}}{D_H^{0.2}} \qquad (Eq. 253)$$

3.5.2 Airfoils: The Equivalent Wedge in Subsonic Flow: The laminar heat transfer coefficient at any point on a cylinder of arbitrary cross section such as an airfoil can be taken to be the same as that on a wedge at the same distance from the stagnation point, provided the stream velocity and its gradient are the same on both wedge and cylinder at the given location. The velocity on a wedge is

$$v = ax^{N_{Eu}}$$
 (Eq. 254)

where:

 N_{Eu} = Euler number

$$N_{Eu,l} = \frac{x^*}{v^*} \left(\frac{dv^*}{dx^*} \right)$$
 (Eq. 255)

$$N_{Eu}$$
 = Euler number a = Constant

To obtain h it is necessary to compute the local Euler number, defined as $N_{Eu,l} = \frac{x^*}{v^*} \left(\frac{dv^*}{dx^*} \right)$ (Eq. 255)

Then h is obtained from $N_{Nu} = \frac{hC}{k} = F\sqrt{N_{Re,C}} \sqrt{\frac{v^*}{x^*}}$ (Eq. 256) where:

where:

$$x^* = \frac{x}{C}$$
 = Distance from stagnation point/Airfoil chord length, dimensionless (Eq. 257)

$$v^* = \frac{V}{V}$$
 = Local surface velocity/Freestream velocity, dimensionless (Eq. 258)

$$\frac{dv^*}{dx^*}$$
 = Local slope of velocity gradient, dimensionless (Eq. 259)

$$N_{Re,C}$$
 = Freestream Reynolds number based on the length C (Eq. 261)

F is obtained from Figure 67 as a function of N_{Full}.

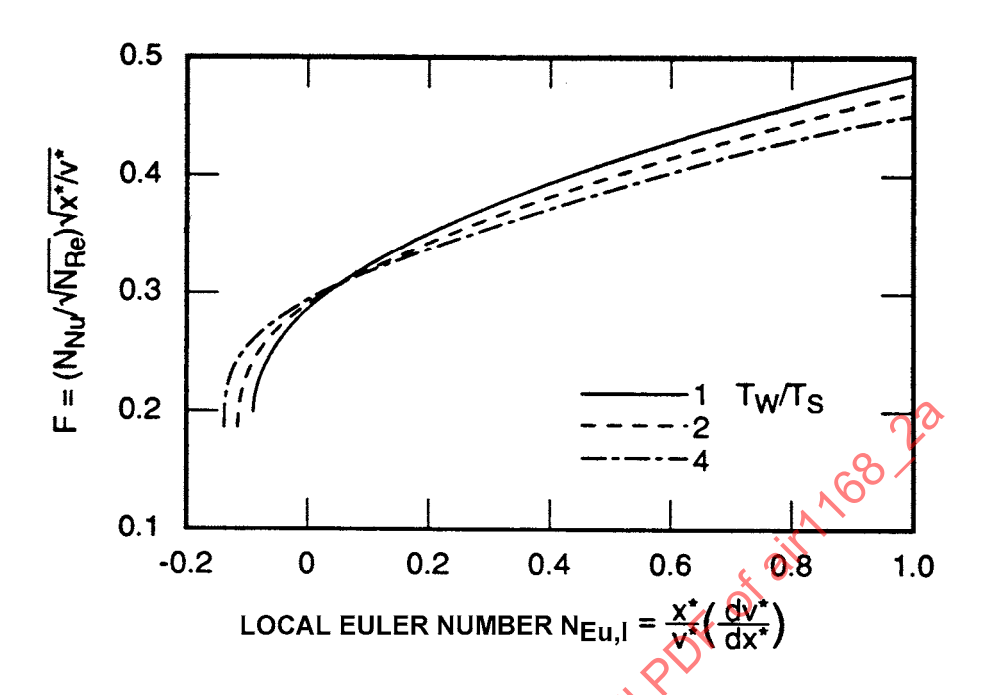


FIGURE 67 - Laminar Heat Transfer on a Wedge (Subsonic Flow)

3.5.3 Transition and Effective Turbulent Origin: No definite predictions of transition location can be made; the location is a function of Reynolds number, Mach number, wall-to-freestream temperature ratio, pressure gradient, surface roughness, approach conditions, and time.

Commonly used estimates for transition Reynolds numbers are given in Table 4.

TABLE 4 - Estimates for Transition Reynolds Numbers

Situation	Reynolds Number Based On	Transition Reynolds Number
Flat Plate, Subsonic	X	100,000-500,000
Flat Plate, Supersonic	×	500,000-2,000,000
Cylinder Subsonic Flow Normal to Axis	D	50,000
Channel Flow	D or D _H	2,000-3,000

The calculation of local turbulent heat transfer on a flat plate must consider an effective turbulent length less than the actual distance from the leading edge, if the flow at the leading edge is laminar. This is because the turbulent boundary layer does not originate at the leading edge. Figure 68 illustrates this, where x is the actual distance from the leading edge to the point under consideration; x_{eff} is the effective turbulent length, measured from the "effective origin" of the turbulent boundary layer; and x_{i} is the distance from the leading edge to the transition point.

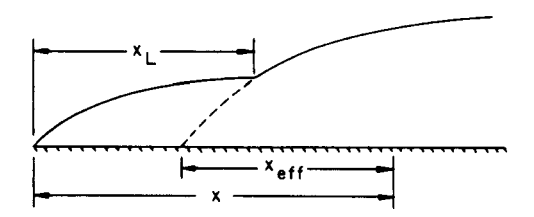


FIGURE 68 - Effective Turbulent Length as a Function of Turbulent Heat Transfer

3.5.3 (Continued):

Assuming that turbulent and laminar momentum thicknesses are equal at the transition point,

$$x_{eff} = x - x_{L} \left(1 - \frac{20.5}{(N_{Re.L})^{0.375}} \right)$$
 (Eq. 262)

$$N_{\text{Re,eff}} = N_{\text{Re,x}} \left(\frac{x_{\text{eff}}}{x} \right)$$

$$= N_{\text{Re,x}} \cdot \left(1 - \frac{x_{\text{L}}}{x} \left(1 - \frac{20.5}{N_{\text{Re,L}}} \right)^{0.375} \right)$$
(Eq. 263)

where:

N_{Re,L} = Transition Reynolds number

3.5.4 Nonisothermal Walls: The equations and methods listed previously have been derived for the case of constant wall temperature. In many situations this condition is not satisfied.

The following method for calculating the effect on heat transfer rate is suggested in Reference 15 for a constant property fluid and negligible pressure gradient.

For the local heat transfer rate:

$$q(x) = \int_0^x h(x,\xi) \frac{dt_w}{d\xi} d\xi + \sum h(x,\xi_i) [t_w(\xi_i^+) - t_w(\xi_i^-)]$$
 (Eq. 264)

where the summation expressed by the second term accounts for any discontinuities in the wall temperature; $t_w(\xi_i^+)$ and $t_w(\xi_i^-)$ are the wall temperatures immediately downstream and upstream, respectively, of the discontinuity; x and ξ are the distances from the origin of the laminar or turbulent boundary layer to the point in question and to any discontinuity in the wall temperature, respectively.

3.5.4 (Continued):

The term $h(x,\xi)$ may be expressed for laminar flow as

$$h(x,\xi) = 0.332 \frac{k}{x} (N_{Pr})^{1/3} (N_{Re,x})^{1/2} \cdot \left[1 - \left(\frac{\xi}{x}\right)^{3/4}\right]^{-1/3}$$
 (Eq. 265)

and for turbulent flow as

$$h(x,\xi) = 0.0296 \frac{k}{x} (N_{Re,x})^{0.8} (N_{Pr})^{1/3} \cdot \left[1 - \left(\frac{\xi}{x}\right)^{39/40}\right]^{-7/39}$$
 (Eq. 266)

The total heat transfer, q(x), from the origin of the boundary layer to the point x max be obtained by integrating the local heat transfer rates to the point

$$q(x) = b \int_0^x q(x) dx$$
 (Eq. 267)

where:

b = Width of the plate

For the case where the only discontinuity occurs at the leading edge (that is, the leading edge surface temperature is different from the recovery temperature), the following results are obtained.

For laminar flow:

r flow:
$$q(x) = 0.644 \text{ bk } N_{Re,x}^{1/2} N_{Pr}^{1/3} \left\{ (t_{w0} - t_{aw}) + \int_{0}^{x} \left[1 - \left(\frac{\xi}{x}\right)^{3/4} \right]^{2/3} \cdot \frac{dt_{w}}{d\xi} d\xi \right\}$$
 (Eq. 268)

For turbulent flow:

$$q(x) = 0.0870 \text{ bk } N_{Pr}^{1/3} N_{Re,x}^{0.8} \cdot \left\{ (t_{w0} - t_{aw}) + \int_{0}^{x} \left[1 - \left(\frac{\xi}{x}\right)^{39/40} \right]^{32/39} \cdot \frac{dt_{w}}{d\xi} d\xi \right\}$$
 (Eq. 269)

where:

 t_{w0} and t_{aw} = Wall temperature at the leading edge and the recovery temperature, respectively

Reference 15 extends the development of the nonisothermal wall for several special cases.

3.6 Forced Convection in Compressible Flow:

At freestream velocities less than the speed of sound, the effect of compressibility on heat transfer is not large. At supersonic and hypersonic speeds, the effects of compressibility and real-gas effects seriously alter the heat transfer and skin friction from that calculated by subsonic relations.

At very high temperatures, where real-gas effects become important ($M \ge 5$), the enthalpy gradient is a better criterion of the energy potential than is the temperature gradient, and this fact should be accounted for in calculations.

This section will present relationships derived particularly for air as a real, compressible fluid.

3.6.1 Definitions: The total (stagnation) enthalpy and temperature are the enthalpy and temperature, respectively, that the fluid would reach if adiabatically brought to rest.

$$i_{T} = i_{S} + \frac{V^{2}}{2gJ}$$

$$T_{T} = T_{S} + \frac{V^{2}}{2gJc_{p}} = T_{s} \left(1 + \frac{\gamma - 1}{2} M^{2}\right) \text{ (for a perfect gas)}$$
(Eq. 270)

where the subscripts

T = Total (stagnation) conditions

S = Static conditions

Unless otherwise noted, the units used in this section are °R for temperature and Btu/lb for enthalpy.

The adiabatic wall (recovery) enthalpy and temperature are the enthalpy or temperature, respectively, that the surface in a moving fluid would reach if the surface had zero heat transfer to or away from it.

The recovery factor ris defined as

$$r = \frac{i_{aw} - i_{S}}{i_{T} - i_{S}}$$
 or $r = \frac{T_{aw} - T_{S}}{T_{T} - T_{S}}$ (Eq. 271)

where the subscripts

aw = Adiabatic wall

T = Total condition

S = Static condition

3.6.1 (Continued):

For flat plates, r is a function of Prandtl number:

$$r = \sqrt{N_{Pr}}$$
 for laminar flow (~0.85 for air) (Eq. 272)

$$r = \sqrt[3]{N_{Pr}}$$
 for turbulent flow (~0.89 for air) (Eq. 273)

Adiabatic wall enthalpy and temperature are calculated from

$$i_{aw} = i_S + \frac{rV^2}{2gJ}$$
 (Eq. 274)

$$i_{aw} = i_S + \frac{rV^2}{2gJ}$$

$$T_{aw} = T_S + \frac{rV^2}{2gJc_p} = T_S \left(1 + \frac{\gamma - 1}{2} rM^2\right) \text{ (for a perfect gas)}$$

$$\text{(Eq. 274)}$$

$$\text{(Eq. 275)}$$

$$\text{(s not adiabatic, the heat transfer is}$$

$$q = hA(T_{aw} - T_w)$$

$$\text{(Eq. 276)}$$

When the wall is not adiabatic, the heat transfer is

$$q = hA(T_{aw} - T_{w})$$
 (Eq. 276)

or

$$q = h_i A(i_{aw} - i_w)$$
 (see Equation 281) (Eq. 277)

Evaluation of Fluid Properties: When air flows at very high speed, large variations in temperature 3.6.2 may occur through the boundary layer, and the choice of a temperature at which to evaluate the air properties becomes somewhat more difficult than in the case of incompressible flow. Typical boundary layer temperature profiles are illustrated in Figure 69.

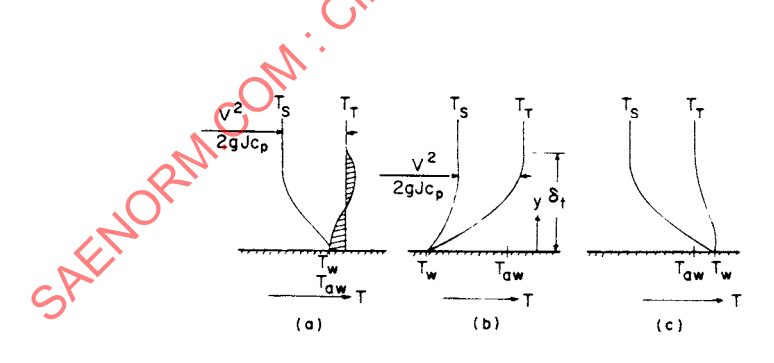


FIGURE 69 - Typical Boundary Layer Temperature Profiles (a) Adiabatic Wall, (b) Cooled Wall, (c) Heated Wall

3.6.2 (Continued):

The method shown here for evaluating fluid properties will be the "reference temperature" method. In using this method, all fluid properties are to be evaluated using the reference temperature T*. Quantities evaluated at this temperature are denoted by the superscript *.

$$T^* = 0.5(T_w + T_\delta) + 0.22(T_{aw} + T_\delta)$$
 (Eq. 278)

At hypersonic velocities, the reference enthalpy should be used:

$$i^* = 0.5(i_w + i_s) + 0.22(i_{aw} + i_s)$$
 (Eq. 279)

where the subscripts

w = Wall conditions

aw = Adiabatic wall conditions

 δ = Conditions outside the boundary layer

The reference temperature is the temperature corresponding to the reference enthalpy.

These equations may be simplified to:

$$i^* = 0.5(i_w + i_\delta) + 0.22\frac{v^2}{2gJ}$$
 (Eq. 280)

For a perfect gas the preceding equation may be written as

$$T^* = 0.5(T_W + T_{\delta}) + 0.044 \text{rM}_{\delta}^2 T_{\delta}$$
 (Eq. 281)

or

$$\frac{T^*}{T_{\delta}} = 0.5 \left(\frac{T_{W}}{T_{\delta}} + 1\right) + 0.044 \text{rM}_{\delta}^{2}$$
 (Eq. 282)

Figure 70 presents T_{δ}/T_{δ} versus T_{w}/T_{δ} and M_{δ} for air, assuming $r_{lam} = 0.85 \quad \text{and} \quad r_{turb} = 0.89$

$$r_{lam} = 0.85$$
 and $r_{turb} = 0.89$ (Eq. 283)

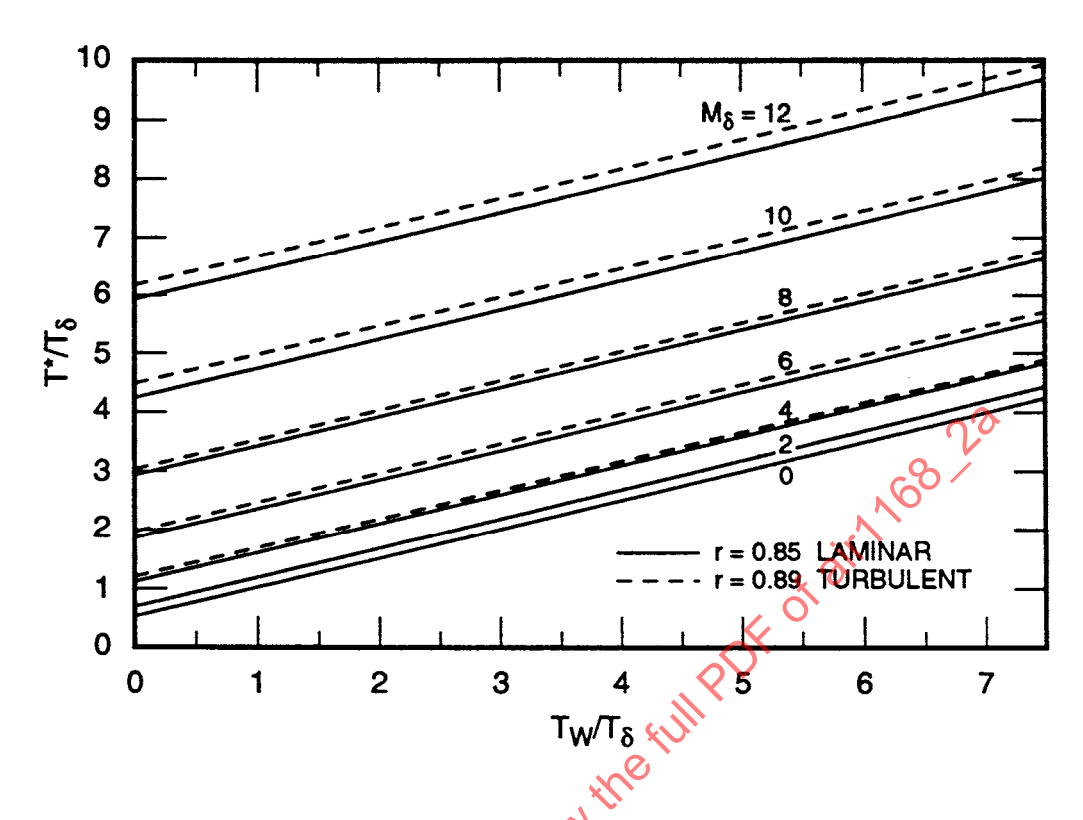


FIGURE 70 - High Speed Flow Reference Temperature

3.6.2 (Continued):

The formulas for heat transfer become

$$q = h*A (T_{aw} - T_{w})$$
 (Eq. 284)

or

$$q = h_i^* A (i_{aw} - i_w)$$
 (Eq. 285)

$$h^* = N_{St}^*(\rho g)^* V c_p^*$$
 (Eq. 286)
$$h_i^* = N_{St}^*(\rho g)^* V$$

where the subscript i denotes quantities based on the enthalpy gradient. The relationship between \mathbf{h}_{i} and \mathbf{h} is

$$h_i = h \frac{T_{aw} - T_w}{i_{aw} - i_w}$$
 (Eq. 287)

3.6.3 Flow Over Flat Plates: Heat transfer and skin friction coefficients for compressible flow are found by the methods shown in 3.5 except that fluid properties are evaluated at the reference temperature T*, discussed in 3.6.2.

For laminar flow, the skin friction coefficient is

$$c_f^* = \frac{0.664}{\sqrt{N_{Re}^*}} = \frac{0.664}{\sqrt{(\rho g)^* V x / \mu^*}}$$
 (Eq. 288)

and the heat transfer coefficient is

$$h^* = 3600 N_{St}^* (\rho g)^* V c_p^* = 3600 (\rho g)^* V \cdot \left(\frac{c_f^*}{(2N_{Pr}^*)^{2/3}} \right) c_p^*$$

$$g)^* = P/RT^* \text{ (the perfect gas law) and}$$

$$c_p^* = \sqrt{T_p^*} c_p^{1.5}$$
(Eq. 289)

Assuming that $(\rho g)^* = P/RT^*$ (the perfect gas law) and

$$\mu^* = 2.27 \times 10^{-8} g \frac{(T^*)^{1.5}}{T^* + 200}$$
 (the Sutherland equation) (Eq. 290)

then

$$h^* = \frac{0.144c_p^*}{(N_{Pr})^{2/3}} \sqrt{\frac{P_x V_v}{T^* + 200}}$$
 (Eq. 291)

$$h_i^* = \frac{h^*}{c_p^*}$$
 (Eq. 292)

For turbulent flow, with $N_{Re,X} > 10^7$, the skin friction coefficient is

$$C_{\text{Re}}^{\frac{1}{2}} = 0.00778 \left(\frac{1}{\text{PVx}}\right)^{0.2} \cdot \left(\frac{T^{*2.5}}{T^{*} + 200}\right)^{0.2}$$
 (Eq. 293)

3.6.3 (Continued):

and the heat transfer coefficient is

$$h^* = 41.7c_f^* \left(\frac{PV}{T^*}\right) c_p^*$$
 (Eq. 294)

$$h_i^* = \frac{h^*}{c_p^*} \left(\frac{40.5}{41.7} \right)$$
 (Eq. 295)

For $N_{Re.x} > 10^7$,

$$\sqrt{\overline{c}_f} = \frac{0.242}{\log_{10}(N_{Re}^* \overline{c_f})}$$
 (iterative solution required) (Eq. 296)

$$\sqrt{\overline{c}_f} = \frac{0.242}{\log_{10}(N_{Re}^*\overline{c}_f)} \text{ (iterative solution required)} \tag{Eq. 296}$$

$$c_f^* = \frac{0.557\overline{c}_f}{0.557 + 2\sqrt{\overline{c}_f}} \text{ (see Figure 58, Equation 1)} \tag{Eq. 297}$$

$$c_f^* \text{ and } \overline{c}_f \text{ as a function of } N_{Re,x}^*.$$
in Supersonic Flow: For flow over a wedge with an attached shock at the viscid flow properties are the same at any point behind the shock. Therefore,

Figure 58 presents c_f^\star and $\overline{c}_f^{}$ as a function of $N_{\text{Re},x}^\star$.

Wedges and Cones in Supersonic Flow: For flow overawedge with an attached shock at the 3.6.4 leading edge, the inviscid flow properties are the same at any point behind the shock. Therefore, the flat plate equations given in 3.6.3 apply. The flow properties (δ conditions) to be used are those following the oblique shock at the leading edge?

The supersonic flow over a cone with an attached shock is three-dimensional; however, the inviscid flow properties are the same along the cone surface at any point behind the shock. Therefore, the flat plate equations of 3.6.3 apply when multiplied by the following ratios:

Laminar flow:

$$h_{cone} = \sqrt{3} h_{plate}$$
 (Eq. 298)

$$c_{f \text{ cone}} = \sqrt{3} c_{f \text{ plate}}$$
 (Eq. 299)

the flat plate equations of 3.6.5 apply when multiplied by the following ratios.

$$h_{cone} = \sqrt{3} \ h_{plate} \qquad (Eq. 298)$$

$$c_{f \ cone} = \sqrt{3} \ c_{f \ plate} \qquad (Eq. 299)$$

$$h_{av \ cone} = \frac{2}{\sqrt{3}} \ h_{av \ plate} \qquad (Eq. 300)$$

3.6.4 (Continued):

Turbulent flow:

$$h_{cone} = 1.15 h_{plate}$$
 (Eq. 301)

$$c_{f cone} = 1.15 c_{f plate}$$
 (Eq. 302)

$$h_{av cone} = 1.022 h_{av plate}$$
 (Eq. 303)

Blunt Body Heat Transfer: At the stagnation point of a sphere (M > 2.0), 3.6.5

$$q = \frac{113.7}{(N_{Pr',2})^{0.6}} \left(\frac{g\rho_{w}\mu_{w}}{g\rho_{2}\mu_{2}}\right)^{0.1} \cdot \sqrt{\frac{g\rho_{2}\mu_{2}}{R_{N}}} \frac{\sqrt{2(P_{2}-P_{1})}}{g\rho_{2}}$$

$$\times \left(1 + \frac{(N_{Le}^{0.52}-1) i_{D}}{i_{2} + (V_{2}^{2}/2g)}\right) \cdot \left(i_{2} + \frac{V_{2}^{2}}{2g} - i_{w}\right) \tag{Eq. 304}$$

where:

q = Heat flux, Btu/h-ft²

 $N_{Pr',2}$ = Prandtl number = 0.71 for air

 $R_N = Radius of sphere, ft$

 $N_{l,e}$ = Lewis number $\cong 1.4$

i_D = Dissociation enthalpy

The dissociation enthalpy i_{D} may be calculated as follows:

$$i_D = 5.13 \times 10^6 (f_2^{-1})$$
 (Eq. 305)

For
$$1.0 < f_2 < 1.2$$
,
$$i_D = 5.13 \times 10^6 (f_2^{-1})$$
 (Eq. 305)
$$i_D = 11.28 \times 10^6 (f_2^{-1.2}) + 1.03 \times 10^6$$
 (Eq. 306)

For $2.0 < f_2$

$$i_D = 15.15 \times 10^6 (f_2^{-2}) + 10.06 \times 10^6 (f_2^{-2})$$
 (Eq. 307)

3.6.5 (Continued):

where:

 f_2 = Compressibility factor

$$P = \rho g f R T$$
 (Eq. 308)

and subscripts

1 = Free stream

2 = Following normal shock

w = Wall or surface

NOTE: The units of enthalpy in this case are ft-lb/lb.

lf

$$i_w << i_2 + (V_2^2/2g),$$
 (Eq. 309)

this case are ft-lb/lb.
$$i_{\rm w} << i_2 + (V_2^2/2{\rm g}), \tag{Eq. 309}$$

$$q \cong 52.2 (M_\infty^{3.1}) \sqrt{\frac{P_1}{R_N}} \tag{Eq. 310}$$
 above values are to be multiplied by 0.73.

For the case of a cylinder, the above values are to be multiplied by 0.73.

Surface Equilibrium Temperature: For the situation illustrated in Figure 71,

$$T_{aw} = T_{w} + \frac{\sigma T_{w}^{4}}{h/\epsilon}$$
 (Eq. 311)

where:

 T_{δ} = Static air temperature outside the boundary layer, °R

T_{aw} = Adiabatic wall temperature, °R

T_w = Surface equilibrium temperature, °R

 T_r = Radiation sink temperature, 0 °R in this case

 $q_c = Convective heat transfer to surface, Btu/h-ft^2$

 q_r = Radiation heat transfer from surface

q_x = Arbitrary heat load directed from surface

 ε = Emissivity, dimensionless

 σ = Stefan-Boltzmann constant, 0.173 x 10⁻⁸ Btu/h-ft²- $^{\circ}$ R⁴

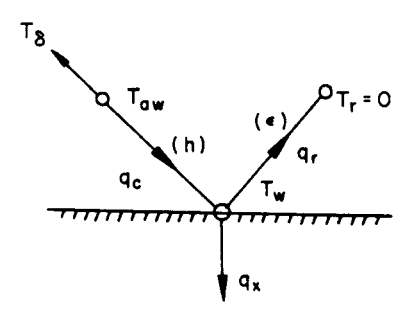


FIGURE 71 - Surface Equilibrium Temperature

3.6.6 (Continued):

Figure 72 presents equilibrium surface temperatures as a function of the quantities (h/ɛ) and (T_{aw} - (q_x/h)).

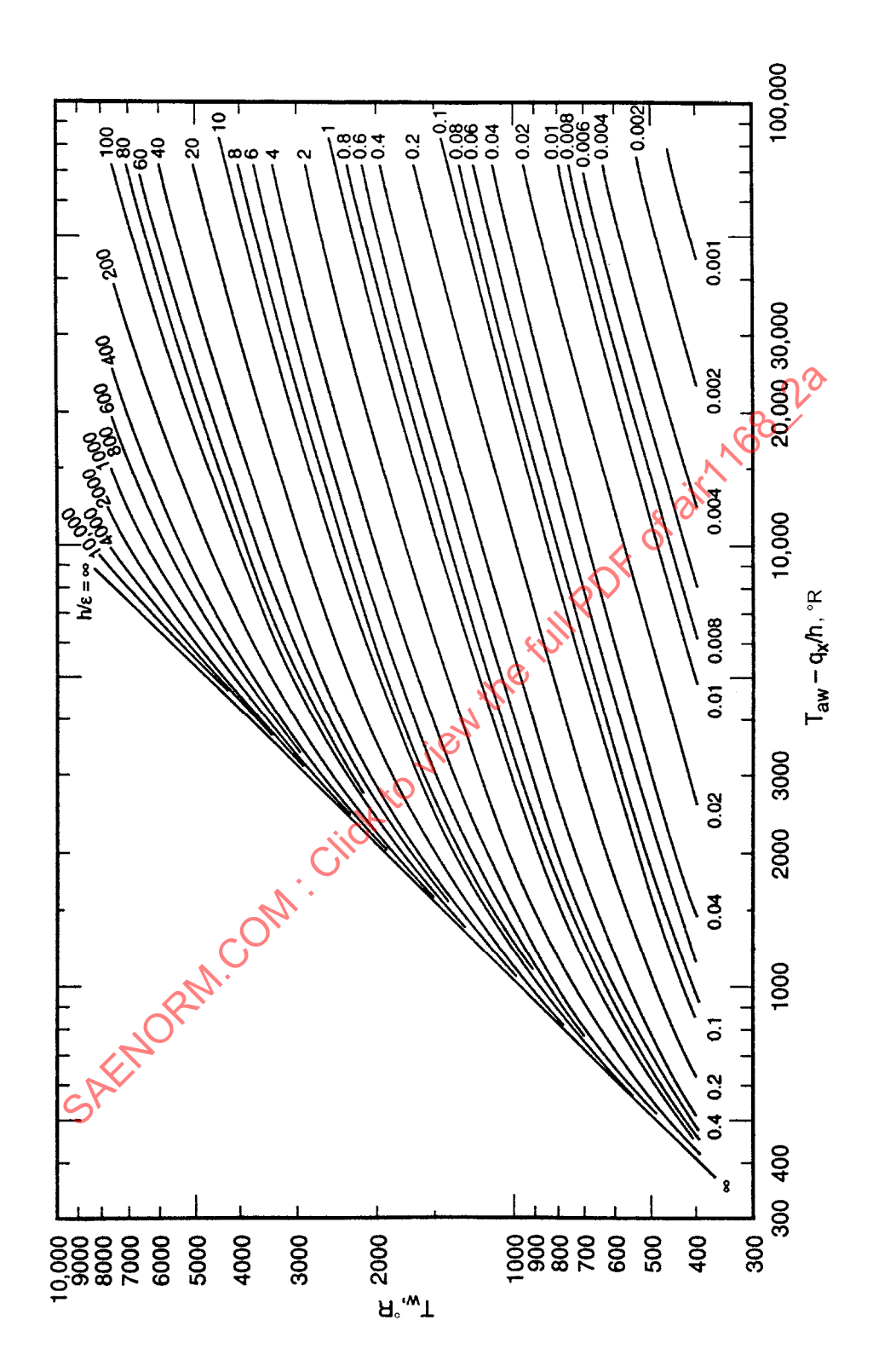


FIGURE 72 - Wall Equilibrium Temperature for Aerodynamic Heating With Arbitrary Heat Load

3.6.6 (Continued):

If q_x is zero, the change in temperature produced by a change in h may be approximated by

$$\begin{split} \frac{dT_{w}}{T_{w}} &= \frac{dh}{h} \frac{T_{aw} - T_{w}}{4T_{aw} - 3T_{w}} \\ &= \frac{dh/h}{4 + [T_{w}/(T_{aw} - T_{w})]} \\ &= \frac{dh}{4h} \frac{1 + 0.2rM^{2} - (T_{w}/T_{\delta})}{1 + 0.2rM^{2} - (3/4)(T_{w}/T_{\delta})} \\ &= \frac{dh/h}{4 + \left\{ (T_{w}/T_{\delta})/[1 + 0.2rM^{2} - (T_{w}/T_{\delta})] \right\}} \end{split} \tag{Eq. 312}$$

These equations provide a quick estimate of the effect on equilibrium temperature of an error in obtaining the heat transfer coefficient.

The stagnation point surface radiation-equilibrium temperature on a sphere with a nose radius of 2 ft and a surface emissivity of 0.9 is shown in Figure 73. This curve may be corrected to represent a cylinder at any sweep angle, nose radius, and surface emissivity by the following equation:

$$T = 1.064 \left(\frac{K\cos\phi}{\epsilon}\right)^{1/4} (T_c)$$
 (Eq. 313)

where:

K = Constant (0.73 for cylinder and 1.0 for sphere)

 ϕ = Sweep angle, degrees for O $\leq \phi \leq 60^{\circ}$

r = Nose radius, ft

 ε = Surface emissivity

T_c = Temperature from curve plus 460 °R (Figure 73)

T = Temperature at desired conditions, °R

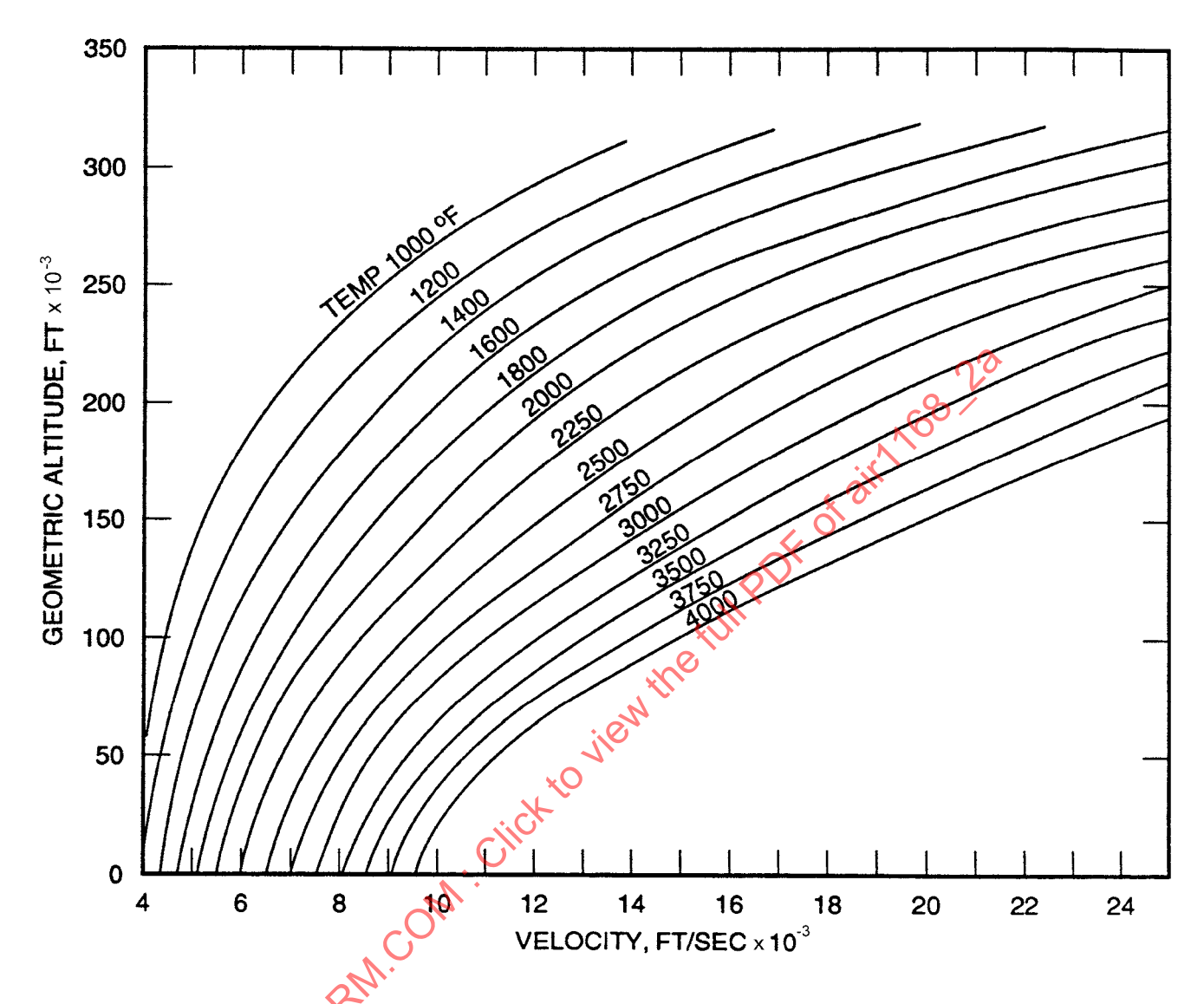


FIGURE 73 - Stagnation Point Radiation Equilibrium Temperature, ϵ = 0.9, r = 2 ft (ARDC 1956 Atmosphere)

3.7 Compact Heat Exchangers:

The emphasis on small, lightweight heat exchanger installations has indicated the need for extended fin surfaces that are more compact than circular tubes. A time saving solution to an extended surface exchanger is in the use of exchanger effectiveness, ε . The characteristics of the extended surface must first be determined by test and plotted as Colburn modulus and friction factor f ordinates versus Reynolds number.

$$\varepsilon_{hot} = \frac{T_{hot fluid in} - T_{hot fluid out}}{T_{hot fluid in} - T_{cold fluid in}}$$
(Eq. 314)

$$\frac{h_{H}A_{H}\eta_{0H} + h_{c}A_{c}\eta_{0C}}{h_{c}A_{c}\eta_{0C} \times h_{H}A_{H}\eta_{0H}} = UA \quad Btu/h-°F$$
 (Eq. 315)

$$\eta_0 = 1 - \eta_F \left(1 - \frac{A_F}{A_T} \right)$$
 overall fin effectiveness (Eq. 316)

where:

$$\frac{A_F}{A_T} = \frac{\text{fin area, ft}^2}{\text{total area, ft}^2}$$
 (Eq. 317)

$$\eta_{F} = \frac{\tanh ml}{ml}$$
 (Eq. 318)

$$mI = \frac{1}{2} \sqrt{\frac{2h}{k\delta}}$$
 (Eq. 319)

for a fin between two plates,

and

$$mL = 1\sqrt{\frac{2h}{k\delta}}$$
 (Eq. 320)

for an extended fin heated at one end only, where δ = fin thickness in feet, and I = fin length in feet.

$$\frac{e_{min}}{c_{max}} = \frac{W_{min}c_p}{W_{max}c_p}$$

$$= \frac{\text{hot or cold fluid capacity rate}}{\text{cold or hot fluid capacity rate}}$$
(Eq. 321)

and

$$\frac{\text{UA}}{\text{c}_{\min}} = \text{NTU (number of transfer units)}$$
 (Eq. 322)

Curves plotting effectiveness versus NTU are shown in Figures 74 through 77. A complete discussion on the use of effectiveness in solving heat transfer equations is contained in Reference 19. For Figures 74 through 77, the following equations are provided.

For Figure 74,

$$\epsilon = \frac{1 - e \exp\left\{-NTU\left[1 - \left(\frac{c_{min}}{c_{max}}\right)\right]\right\}}{1 - \left(\frac{c_{min}}{c_{max}}\right) e \exp\left\{-NTU\left[1 - \left(\frac{c_{min}}{c_{max}}\right)\right]\right\}}$$
 (Eq. 323)

where:

 ε = Side that has c_{min}

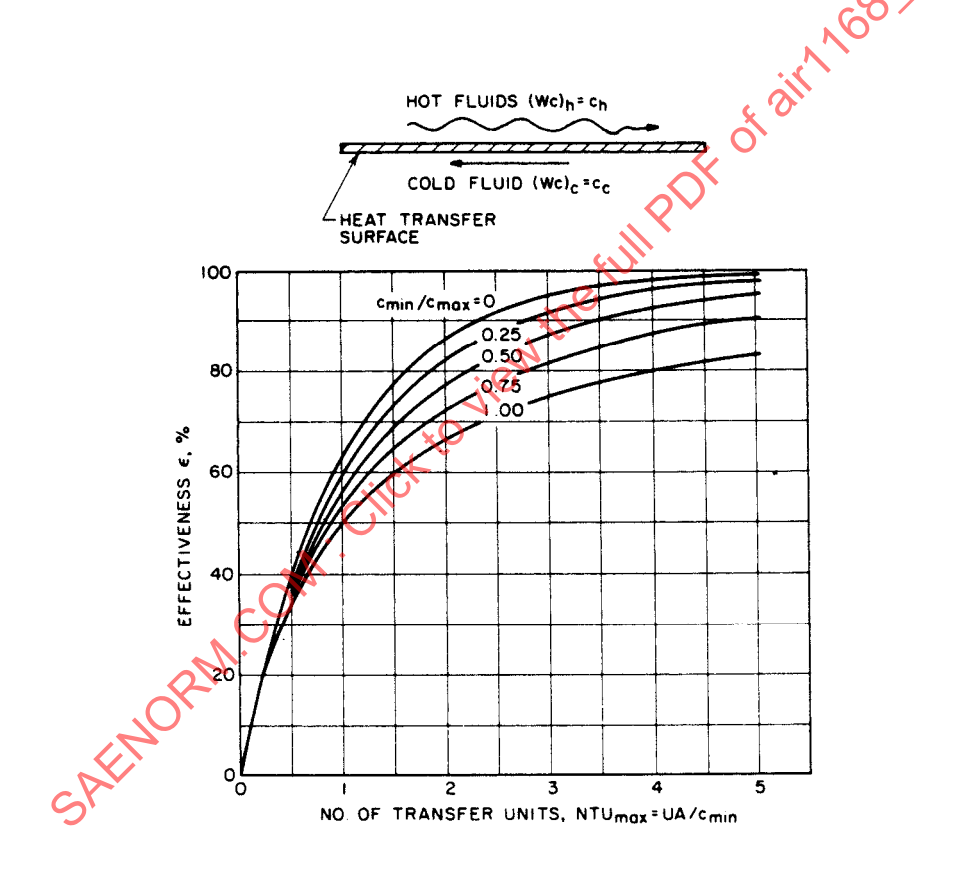


FIGURE 74 - Counterflow Exchanger Performance

For Figure 75, see Reference 19. For Figure 76,

$$\varepsilon = \frac{n\varepsilon_p}{1 + (n-1)\varepsilon_p} \tag{Eq. 324}$$

where:

 $\epsilon_{\rm p}$ = Effectiveness of each pass ϵ = Side with $\rm c_{\rm min}$

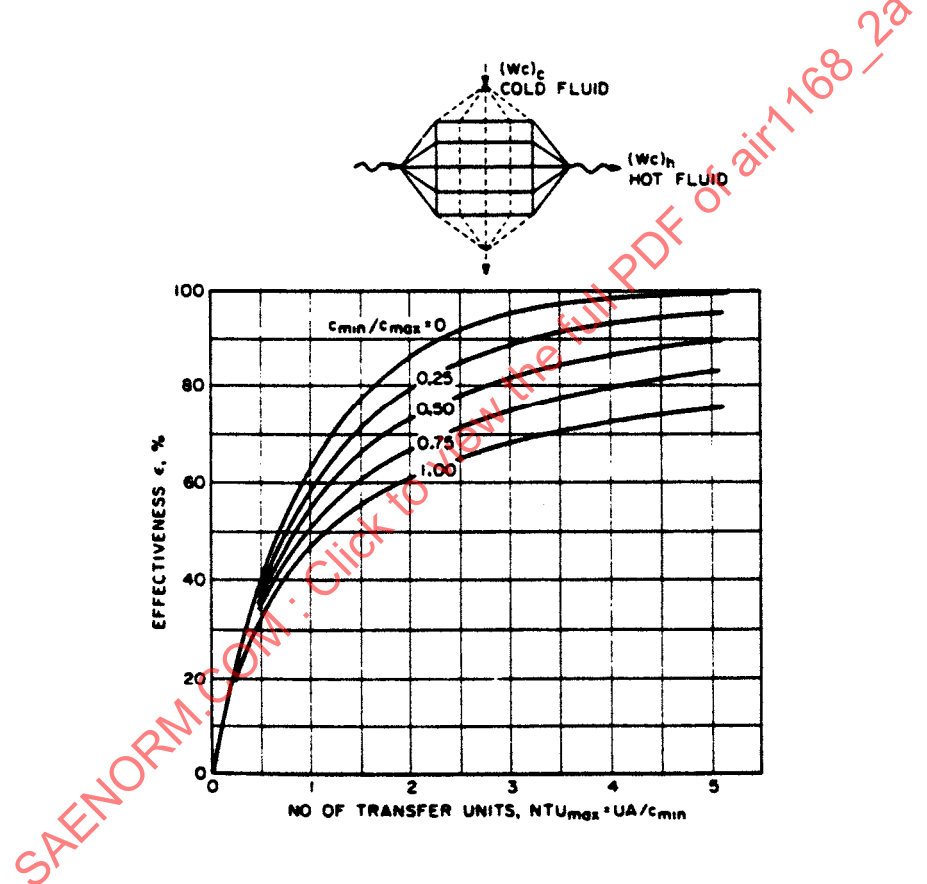


FIGURE 75 - Cross Flow Exchanger With Fluids Unmixed

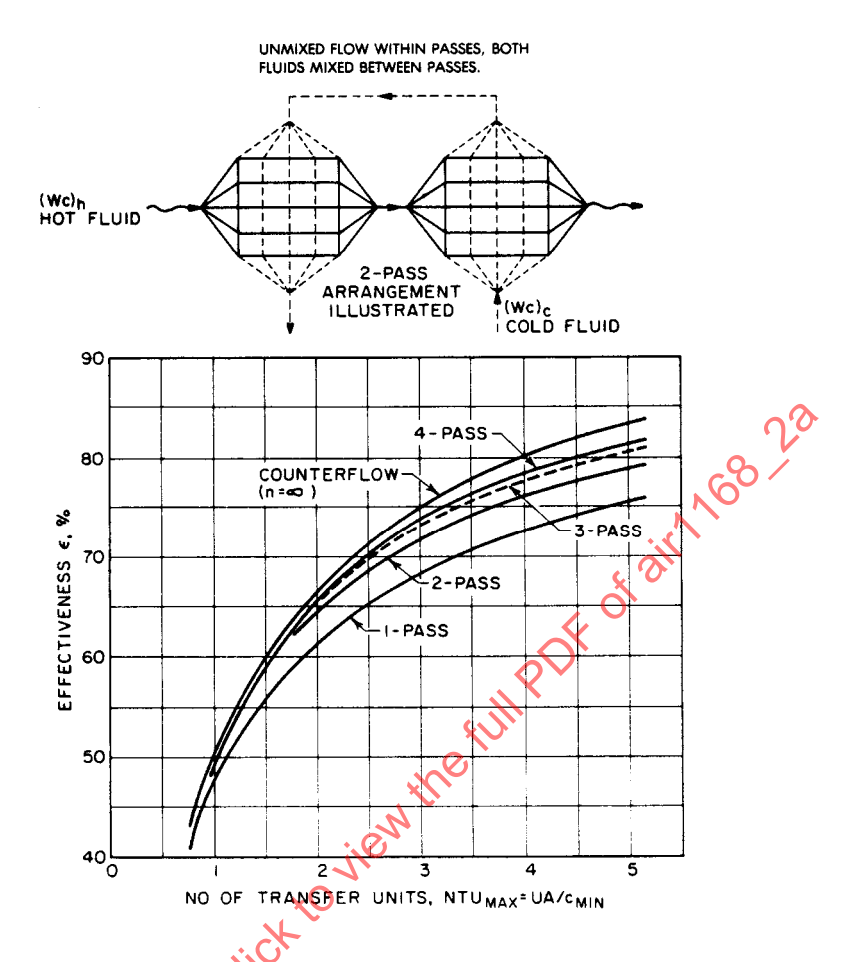


FIGURE 76 - Multipass Cross Counterflow Exchanger; $C_{min}/C_{max} = 1$

For Figure 77,

$$\varepsilon = \frac{2}{1 + \frac{c_{\min}}{c_{\max}} + \sqrt{\frac{c_{\min}}{c_{\max}}^2 \left(\frac{1 + e^{-r}}{1 - e^{-r}}\right)}}$$
 (Eq. 325)

where:

$$r = NTU \sqrt{1 + (c_{min}/c_{max})^2}$$
 (Eq. 326)

$$\varepsilon = \text{Side with } c_{min}$$

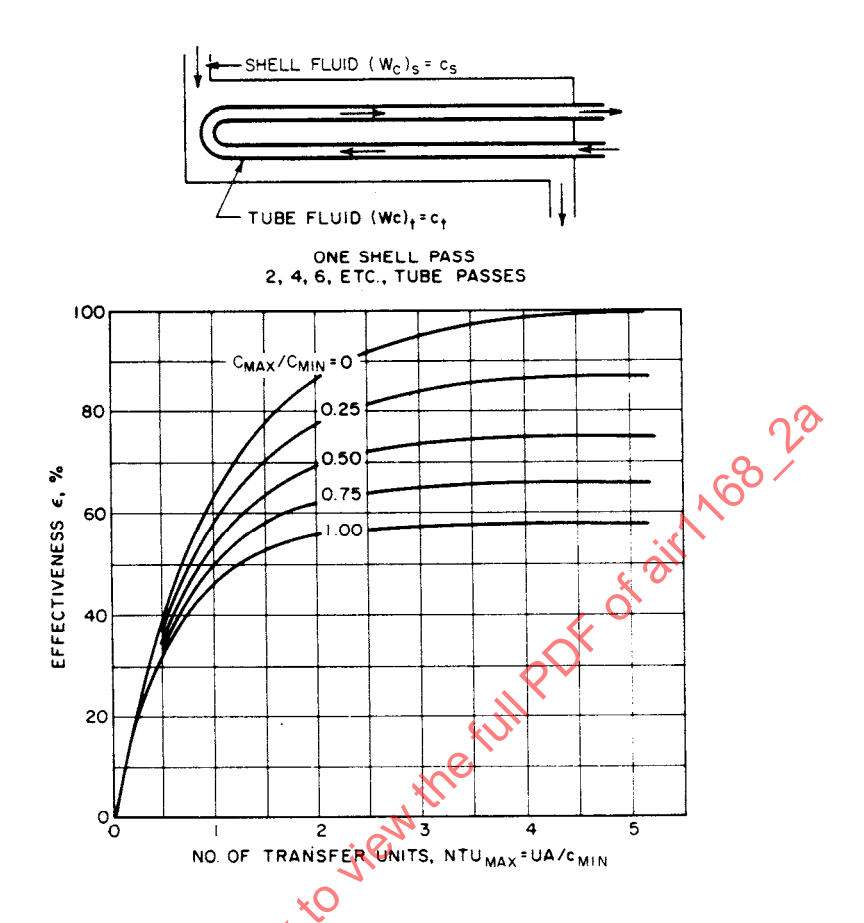


FIGURE 77 - One to Two Parallel Counterflow Exchanger Performance

4. RADIATION:

4.1 Definition:

Thermal radiation consists of a continuous spectrum of electromagnetic waves that are produced by the emitting body and absorbed by the receiving body. At high temperatures the radiation is visible.

Radiation falling on a body is either reflected, absorbed, or transmitted. The sum of the reflected fraction, ρ (reflectivity), the absorbed fraction, α (absorptivity), and transmitted fraction, τ (transmissivity) is equal to 1.

$$\rho + \alpha + \tau = 1 \tag{Eq. 327}$$

A body is

- a. Specular, when it reflects all energy falling on it and reflection is not diffuse; $\rho = 1$, $\alpha = \tau = 0$.
- b. White, when it reflects all energy falling on it and reflection is diffuse; $\rho = 1$, $\alpha = \tau = 0$.
- c. Black, when it absorbs all energy falling on it; $\alpha = 1$, $\rho = \tau = 0$.
- d. Gray, when it reflects the same fraction of energy over all wavelengths.
- e. Colored, when it reflects different fractions of energy in some wavelengths.
- f. Transparent, when it transmits all energy falling on it; $\alpha = 0$, $\tau = 1$, $\rho = 0$.

4.2 Kirchhoff's Law:

A black body emits the maximum possible amount of radiation for a given temperature. Any other body at the same temperature emits less. The ratio of the emission of a nonblack body to that of a black body is loosely termed the emissivity ε . It is important when speaking of emissivity to distinguish the following:

Spectral emissivity = Ratio of emission at a given wavelength

Total emissivity = Ratio of emission over all wavelengths (defined only for a gray body)

Normal emissivity = Ratio of emission in direction normal to surface

Hemispherical emissivity = Ratio of emission overall directions from surface (defined only for a Lambert surface, 4.6)

Frequently, the term emissivity is used to designate the emissive power of a surface at the surface temperature, while the absorptivity refers to the absorptive power of a surface for the characteristic spectrum of a second radiating surface. For example, the solar absorptivity of a surface usually refers to the fraction of the solar spectrum absorbed by the surface at a surface temperature not in equilibrium with the sun. This common usage of emissivity and absorptivity usually implies that the surfaces are gray and obey Lambert's cosine law. Thus, a great deal of care must be exercised in using such emissivity data.

Planck's Law: 4.3

The intensity of radiation, $I_{\lambda bn}$, at wavelength λ and temperature T, is given by

$$I_{\lambda bn} = \frac{2\pi hC^2}{\lambda^5 [e \exp(Ch/K\lambda T) - 1]}$$
 (Eq. 328)

where:

C = Speed of light

h = Planck's constant

K = Boltzmann's constant

 λ = Wavelength, microns (1 micron = 10⁻⁶ m)

T = Temperature, °R

or

Interior instant errors (1 micron =
$$10^{-6}$$
 m)
$$I_{\lambda bn} = \frac{0.37784 \times 10^8}{\lambda^5 [\text{e exp } (25.896/\lambda\text{T}) - 1]}$$
 (Eq. 329) tic intensity of radiation at wavelength λ , Btu/ft²-h- μ -°R⁵

where:

 $I_{\lambda bn} = \text{Monochromatic intensity of radiation at wavelength } \lambda, \text{ Btu/ft}^2\text{-h-}\mu\text{-}^\circ\text{R}^5$ gure 78.

See Figure 78.

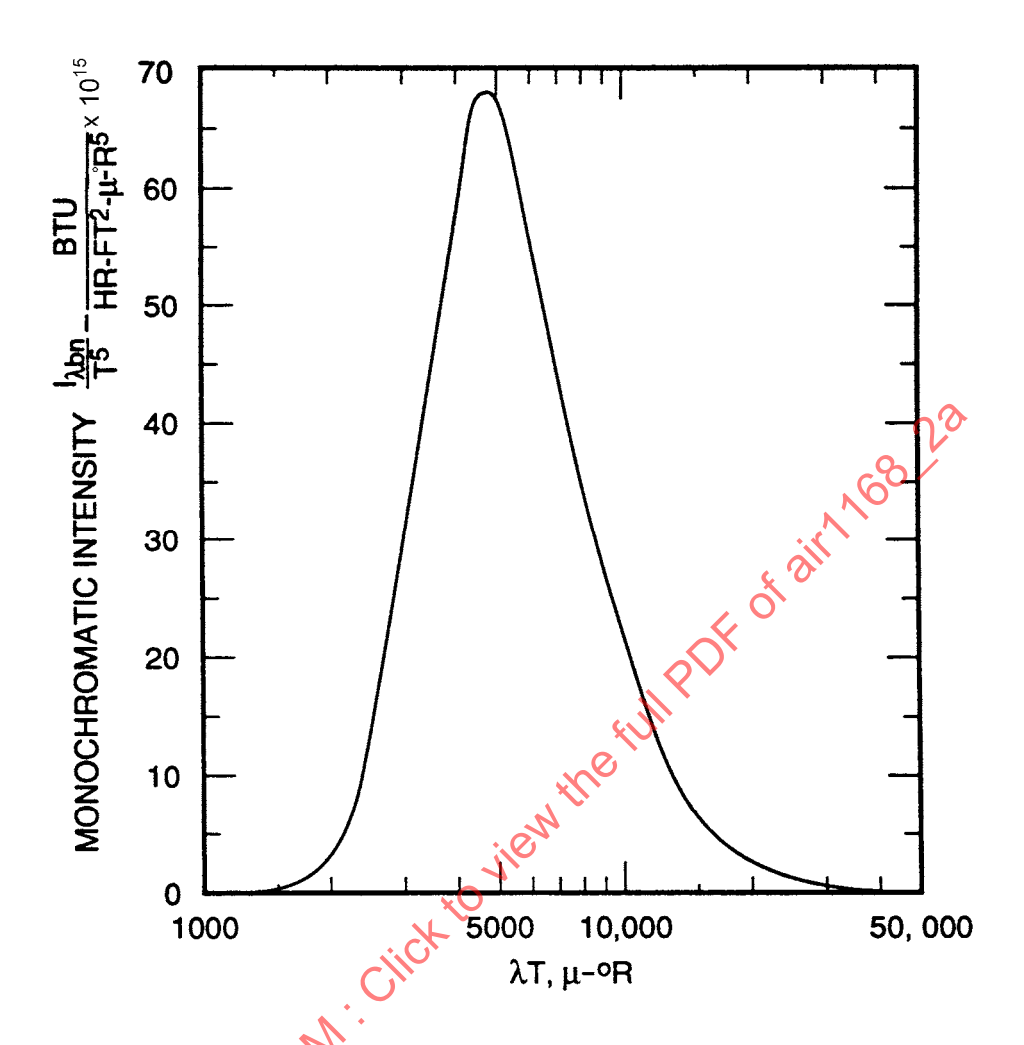


FIGURE 78 - Monochromatic Radiation Intensity of a Black Body in the Direction Normal to the Surface. λ = Wavelength in Microns.

4.4 Stefan-Boltzmann Law:

Integration of Planck's equation over all wavelengths results in the total radiation, I_b, emitted from a black body at temperature T:

$$I_b = \sigma T^4 \tag{Eq. 330}$$

where:

 σ = Stefan-Boltzmann constant = 0.1714 x 10⁻⁸ Btu/h-ft²- $^{\circ}$ R⁴

T = Temperature, °R

4.5 Wien's Displacement Law:

The wavelength of maximum intensity is inversely proportional to the temperature:

$$\lambda_{\text{max}} = \frac{5215}{T}$$
 (Eq. 331)

where:

$$\lambda_{\text{max}}$$
 is in microns, μ T is ${}^{\circ}R$

4.6 Lambert's Cosine Law:

Radiation is emitted from an elemental surface with a directional intensity I which varies as the cosine of the angle from the normal to the surface, φ:

$$I_{\phi} = I_{n} \cos \phi \tag{Eq. 332}$$

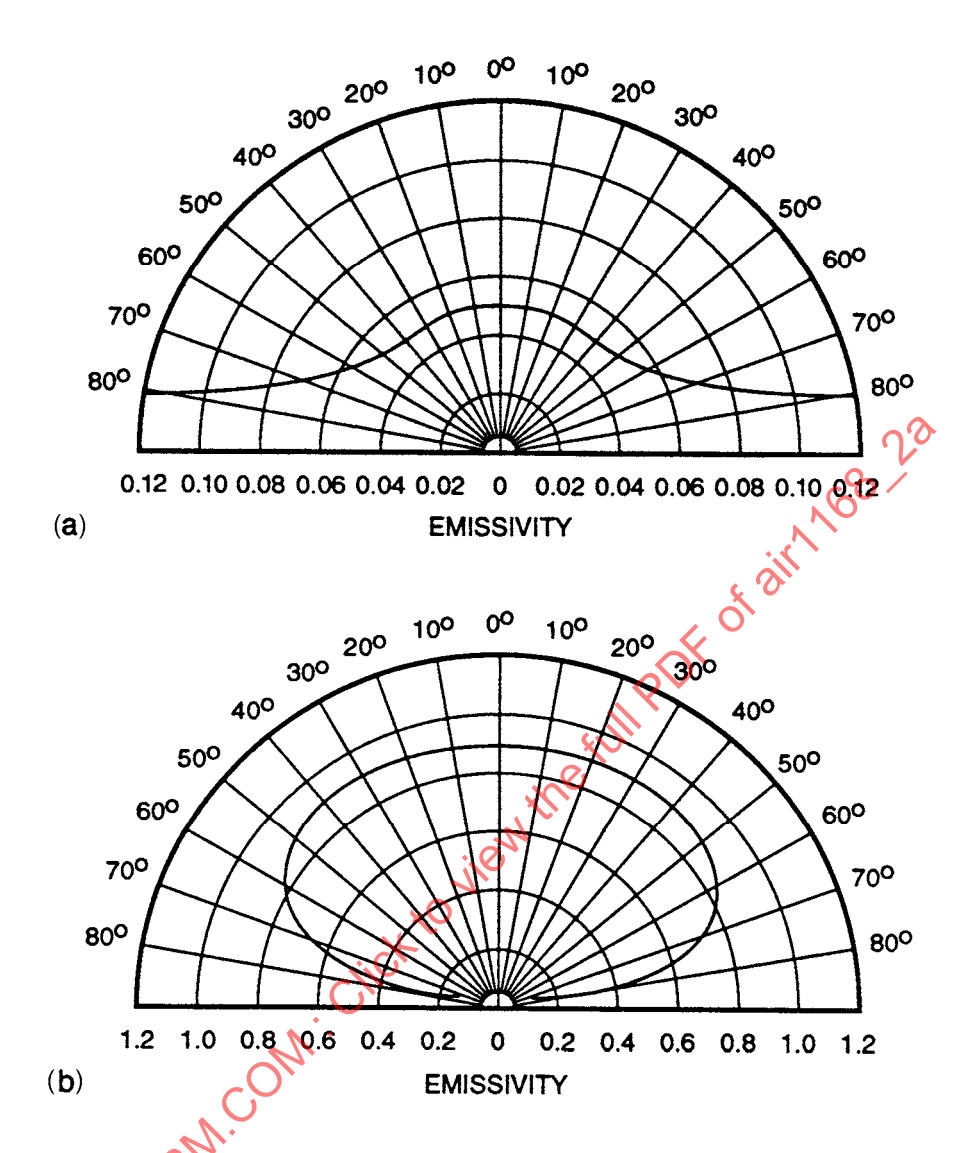
where:

I_n = Intensity of radiation in the normal direction, Btwh-ft²

Integrating the intensity over all angles gives the total radiation as given by the Stefan-Boltzmann law. Thus, the normal intensity I_n is given by

$$I_{n} = \frac{\sigma T^{4}}{\pi}$$
 (Eq. 333)

Not all surfaces obey Lambert's cosine law. Figure 79 illustrates the directional radiation of typical metal and nonconducting surfaces compared to a Lambert surface.



(a) and of Electrically Nonconducting (Non-metal) Surfaces (b) Compared to a Lambert Surface

- 4.7 Radiation Between Solids:
- 4.7.1 Elemental Black Surfaces: The net transfer of energy from one elemental black surface to another as shown in Figure 80 is given by

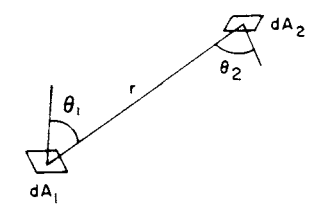


FIGURE 80 - Sketch Showing Transfer of Energy From One Surface to Another

4.7.1 (Continued):

$$dQ_{1 \Leftrightarrow 2} = \frac{I_1 - I_2}{r^2} (dA_1 \cos \theta_1) (dA_2 \cos \theta_2)$$
 (Eq. 334)

where:

 I_1 and I_2 = Intensities of radiation in the direction of r

For a surface obeying Lambert's cosine law,

$$dQ_{1 \Leftrightarrow 2} = \frac{\sigma(T_1^4 - T_2^4)(dA_1\cos\theta_1)(dA_2\cos\theta_2)}{\pi r^2}$$
 (Eq. 335)

4.7.2 Finite Black Surfaces: Integration of Equation 335 over finite surfaces leads to the total exchange of energy:

$$Q_{1 \Leftrightarrow 2} = \int_{A_1}^{\infty} \int_{A_2}^{\sigma(T_1^4 - T_2^4)} \cos\theta_1 \cos\theta_2 dA_1 dA_2$$
 (Eq. 336)

For two surfaces, each at uniform temperature,

$$Q_{1 \Leftrightarrow 2} = \sigma(T_1^4 - T_2^4) \int_{A_1} \int_{A_2} \frac{\cos \theta_1 \cos \theta_2}{\pi r^2} dA_1 dA_2$$
 (Eq. 337)

or

$$Q_{1 \Leftrightarrow 2} = F_{12}A_1\sigma(T_1^4 - T_2^4)$$
 (Eq. 338)

4.7.2 (Continued):

where:

$$F_{12} = \int_{A_1} \int_{A_2} \frac{\cos\theta_1 \cos\theta_2}{A_1 \pi r^2} dA_1 dA_2$$
 (Eq. 339)

 F_{12} is called the configuration factor and is a function of geometry only. The subscripts 1 and 2 signify that the configuration factor is from surface 1 to surface 2.

The reciprocity theorem is shown by inspection of Equation 339 to be

$$A_1F_{12} = A_2F_{21}$$
 (Eq. 340)

By definition of the configuration factor,

$$F_{12} + F_{13} + F_{14} + \dots = 1$$
 (Eq. 341)

4.7.3 Gray Body Radiation: Gray body radiation heat transfer is most easily treated by the network method outlined by A. K. Oppenheim (Reference 16). The three body radiation problem in Figure 81 illustrates the method.

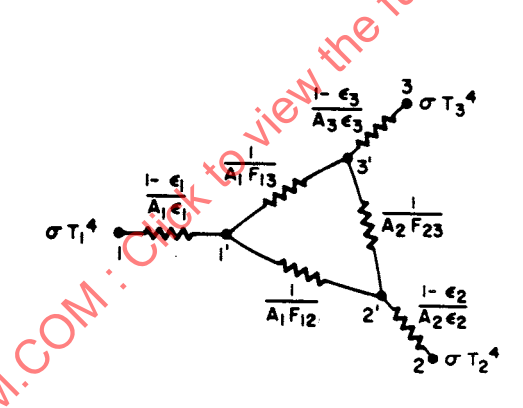


FIGURE 81 - Three Body Radiation

In Figure 81 the nodes 1, 2, and 3 represent the three isothermal gray surfaces. Nodes 1', 2', and 3' are floating nodes that are interconnected by the black body thermal resistance between the respective surfaces (1/AF). The thermal resistance connecting the floating node to the surface node is a function of the surface emissivity $(1 - \epsilon)/A\epsilon$. The heat transfer potential at the surface nodes is simply σT^4 , where σ is the Stefan-Boltzmann constant. The heat transfer between the various nodes can be obtained from simple circuit theory or from computer techniques.

This method of gray body analysis may be extended to any number of isothermal bodies, provided the black body configuration factors are known (see 4.7.5). The original work of Oppenheim (Reference 16) extends the analyses to the case of gray gases.

4.7.4 Radiation Heat Transfer Coefficient: For the special case of two bodies with configuration factor equal to 1.0, the exchange of radiant energy is

$$\begin{aligned} Q_{1 \Leftrightarrow 2} &= A_1 \sigma (T_1^4 - T_2^4) \\ &= A_1 \sigma (T_1^2 + T_2^2) (T_1^2 - T_2^2) \\ &= h_r A (T_1 - T_2) \end{aligned} \tag{Eq. 342}$$

where:

h_r = Radiation heat transfer coefficient (see Figure 82), and

= Radiation heat transfer coefficient (see Figure 82), and
$$h_r = 0.173 \times 10^{-8} \, \frac{T_1^4 - T_2^4}{T_1 - T_2} \qquad (Eq. \, 343)$$

$$(Eq. \, 343)$$

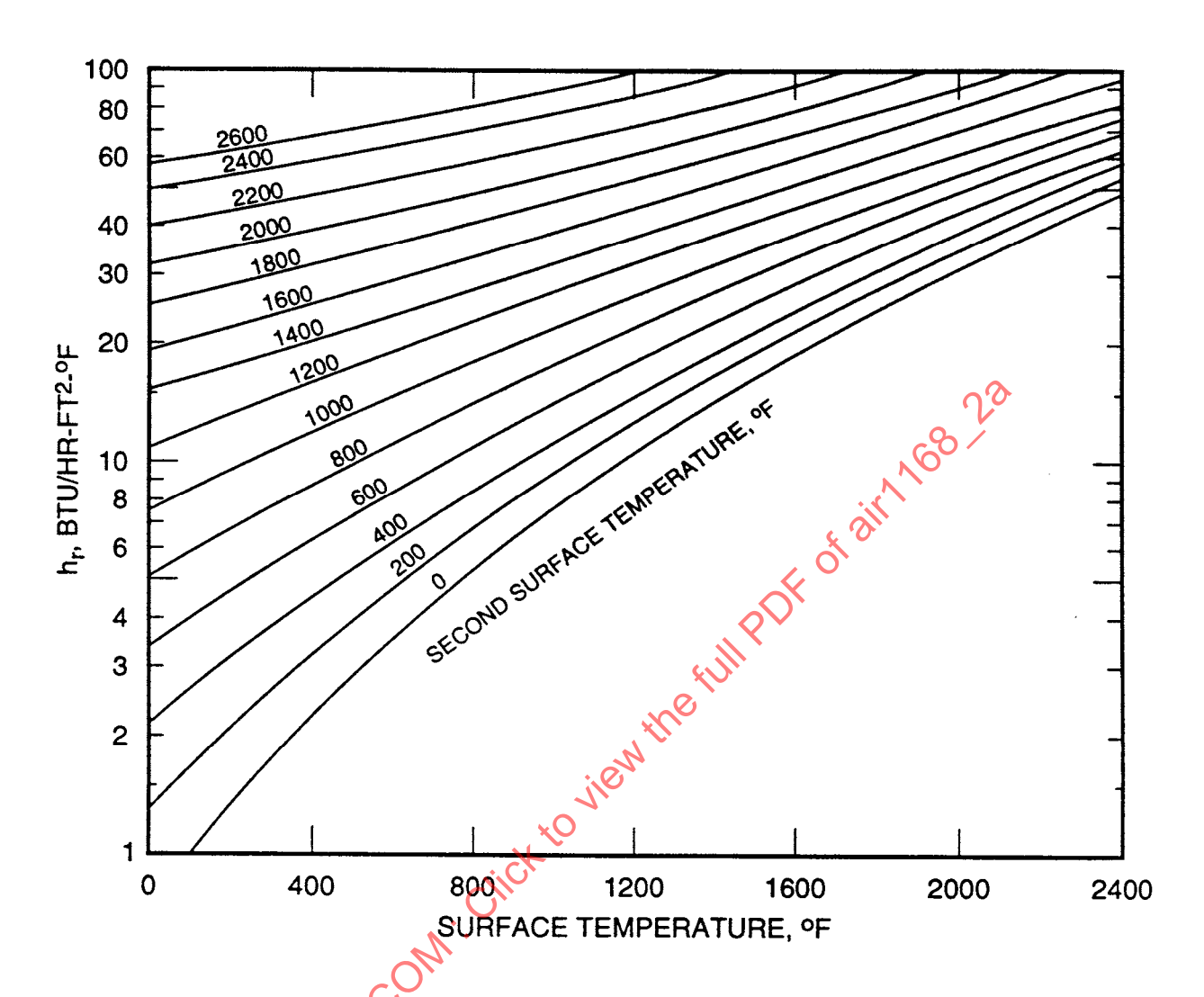


FIGURE 82 - Radiation Heat Transfer Coefficient for Black Body Radiation

- 4.7.5 Configuration Factors: The following configuration factors are for two black isothermal points, lines, or surfaces separated by a nonabsorbing medium.
- 4.7.5.1 Two Infinite Parallel Planes:

$$F_{12} = 1.0$$
 (Eq. 344)

For two infinite parallel gray planes, the overall configuration and emissivity factor F_{12} may be derived from the network analysis to be simply

$$F_{12} = \frac{1}{(1/\epsilon_1) + (1/\epsilon_2) - 1}$$
 (Eq. 345)

4.7.5.2 A Plane Point Source and Plane Rectangle Parallel to dA₁: The normal to dA₁ passes through one corner of A₂. See Figures 83 and 84.

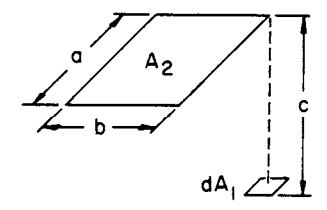


FIGURE 83 - Plane Point Source and Plane Rectangle

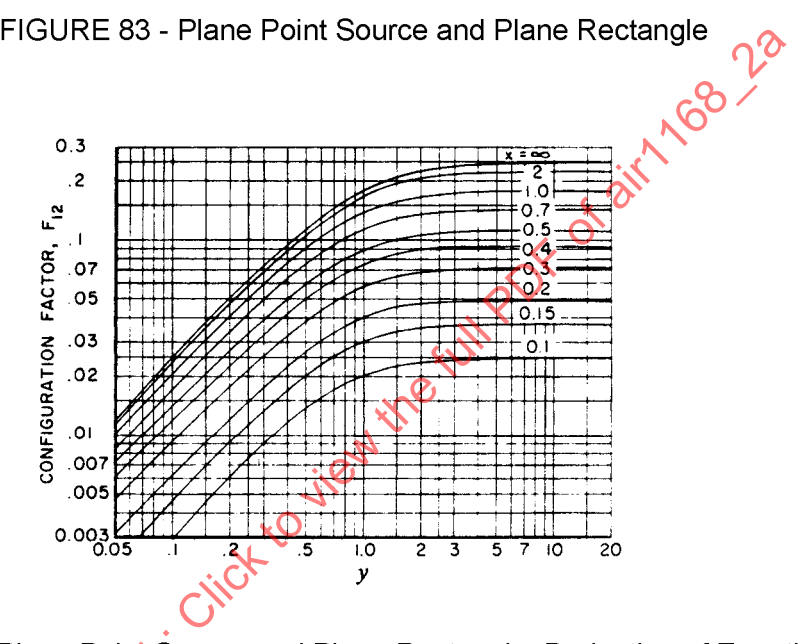


FIGURE 84 - Plane Point Source and Plane Rectangle; Derivation of Equation 346

$$F_{12} = \frac{1}{2\pi} \left[\frac{x}{\sqrt{1+x^2}} \tan^{-1} \left(\frac{y}{\sqrt{1+x^2}} \right) + \frac{y}{\sqrt{1+y^2}} \tan^{-1} \left(\frac{x}{\sqrt{1+y^2}} \right) \right]$$
 (Eq. 346)

for which

$$\lim_{y \to \infty} F_{12} = \frac{x}{4\sqrt{1+x^2}}$$
 (Eq. 347)

$$\lim_{x \to \infty} F_{12} = \frac{y}{4\sqrt{1+y^2}}$$
 (Eq. 348)

4.7.5.2 (Continued):

where:

$$x = \frac{a}{c}$$
 (Eq. 349)

$$y = \frac{b}{c}$$
 (Eq. 350)

4.7.5.3 A Plane Point Source and Plane Rectangle: The planes of dA_1 and A_2 intersect at an angle ϕ . See Figure 85.

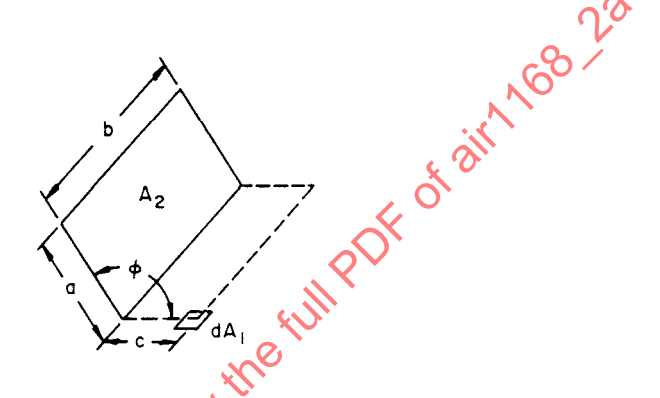


FIGURE 85 - Plane Point Source and Plane Rectangle Intersecting at Angle ϕ

$$F_{12} = \frac{1}{2\pi} \left\{ tan^{-1} \left(\frac{1}{L} \right) + V(N\cos\phi - L)tan^{-1}V + \frac{\cos\phi}{W} tan^{-1} \left(\frac{N - L\cos\phi}{W} \right) + tan^{-1} \left(\frac{L\cos\phi}{W} \right) \right] \right\}$$
(Eq. 351)

for which

$$\lim_{N \to \infty} F_{12} = \frac{1}{2\pi} \left\{ \tan^{-1} \left(\frac{1}{L} \right) + \frac{\cos \phi}{W} \left[\frac{\pi}{2} + \tan^{-1} \left(\frac{L \cos \phi}{W} \right) \right] \right\}$$
 (Eq. 352)

$$\lim_{L \to \infty} F_{12} = 0 \tag{Eq. 353}$$

$$\lim_{L \to 0} F_{12} = \frac{1}{4} (1 + \cos \phi)$$
 (Eq. 354)

$$\lim_{N,L\to\infty} F_{12} = 0 \tag{Eq. 355}$$

4.7.5.3 (Continued):

where:

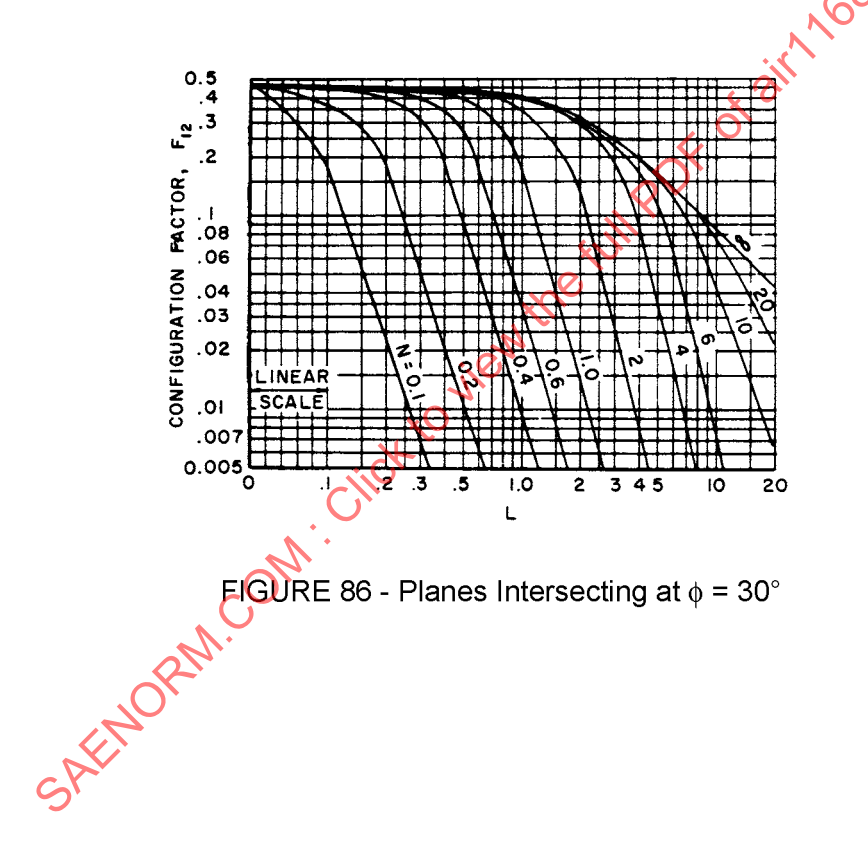
$$V = \frac{1}{\sqrt{N^2 + L^2 - 2NL\cos\phi}}$$
 (Eq. 356)

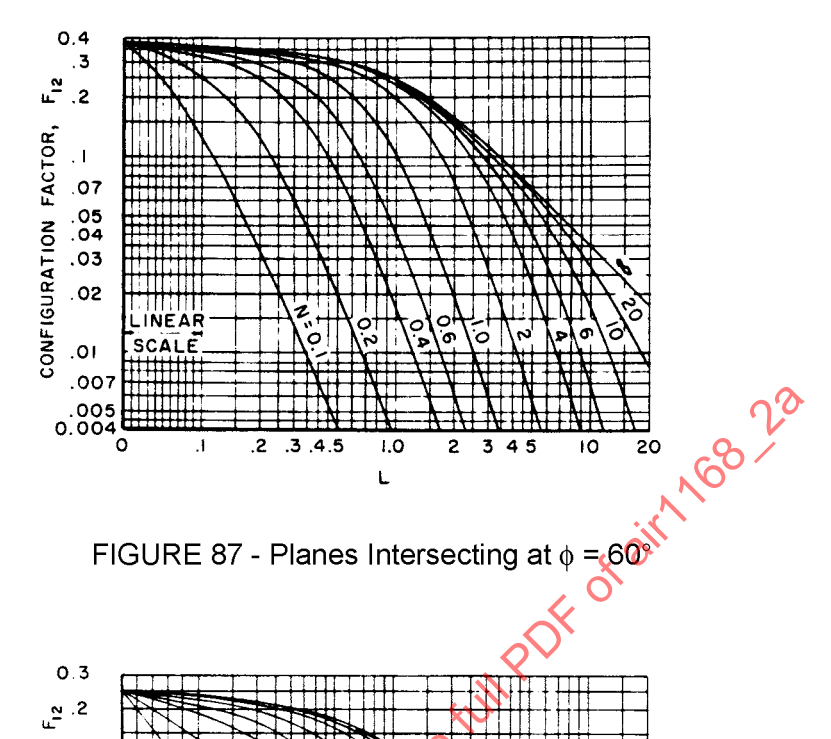
$$W = \sqrt{1 + L^2 \sin^2 \phi}$$
 (Eq. 357)

$$N = a/b$$
 (Eq. 358)

$$L = c/b$$
 (Eq. 359)

See Figures 86 through 90.





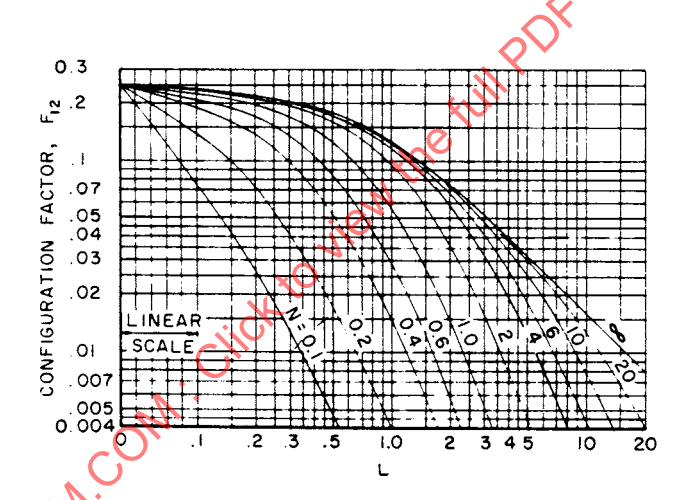
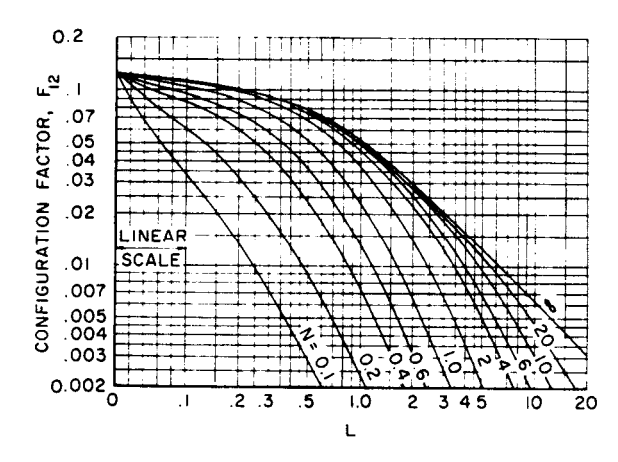
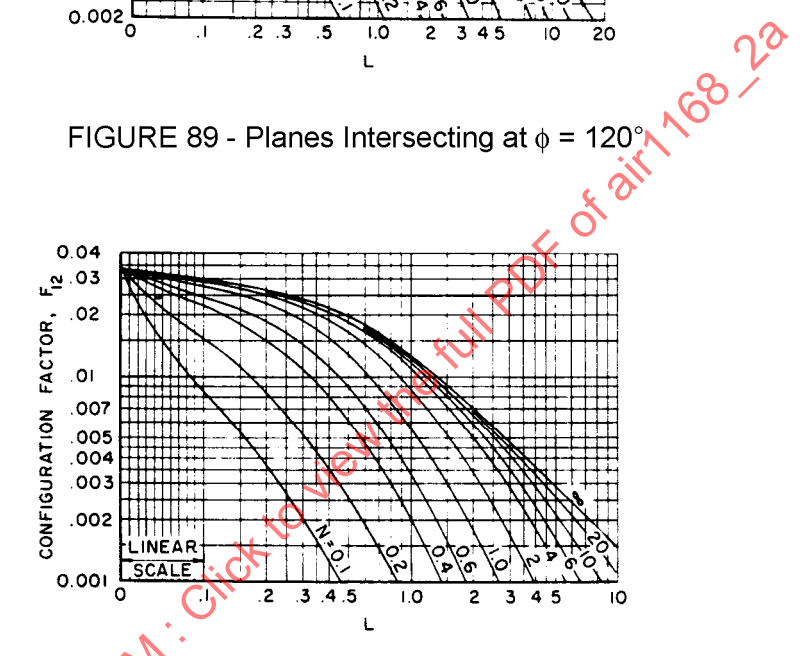


FIGURE 88 - Planes Intersecting at ϕ = 90°





FTGURE 90 - Planes Intersecting at $\phi = 150^{\circ}$

A Spherical Point Source dA_1 and a Plane Rectangle A_2 : The point source is located at one corner of a rectangle that has one common side with A_2 . The planes of the two rectangles 4.7.5.4 intersect at an angle ϕ as shown in Figure 91.

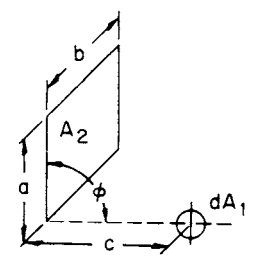


FIGURE 91 - Spherical Point Source and Plane Rectangle With One Common Side

4.7.5.4 (Continued):

Rectangle With One Common Side
$$F_{12} = \frac{1}{4\pi} \left\{ tan^{-1} \left[\frac{x(y - \cos\phi)}{\sqrt{1 + x^2 + y^2 - 2y\cos\phi}} \right] + tan^{-1} \left(\frac{x\cos\phi}{\sqrt{1 + x^2}} \right) \right\}$$
 (Eq. 360) see Figure 92):

For $\phi = 90^{\circ}$ (see Figure 92):

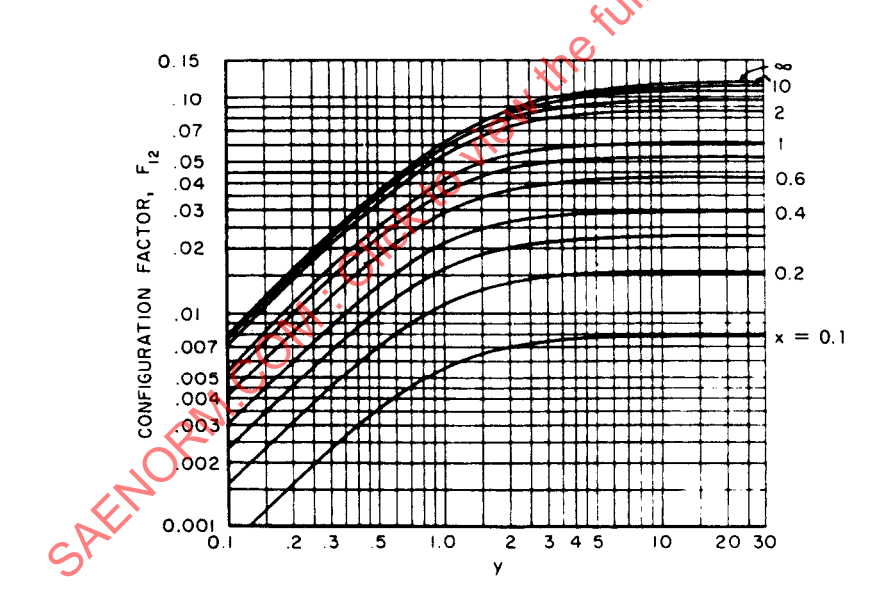


FIGURE 92 - Two Angles Intersecting at $\phi = 90^{\circ}$; Derivation of Equations 360 and 361

$$F_{12} = \frac{1}{4\pi} tan^{-1} \left(\frac{xy}{\sqrt{1 + x^2 + y^2}} \right)$$
 (Eq. 361)

4.7.5.4 (Continued):

for which

$$\lim_{x \to \infty} F_{12} = \frac{1}{4\pi} tan^{-1} y$$
 (Eq. 362)

$$\lim_{x,y\to\infty} F_{12} = \frac{1}{8}$$
 (Eq. 363)

where:

$$x = \frac{b}{c}$$
 (Eq. 364)

$$y = \frac{a}{c}$$
 (Eq. 365)

4.7.5.5 A Plane Point Source dA_1 and a Plane Circular Disk A_2 : The plane of dA_1 is parallel to the plane of dA_2 ; the point source is located at a distance dA_1 from the normal to the center of dA_2 , as shown in Figure 93.

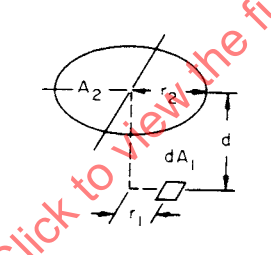


FIGURE 93 Plane Point Source and Plane Circular Disk

$$F_{12} = \frac{1}{2} \left(1 - \frac{x - 2E^2D^2}{\sqrt{x^2 - 4E^2D^2}} \right)$$
 (Eq. 366)

where:

$$x = 1 + (1 + E^2)D^2$$
 (Eq. 367)

$$E = r_2/d$$
 (Eq. 368)

$$D = d/r_1 \tag{Eq. 369}$$

See Figure 94 for a graphical solution of F₁₂ (Equation 366).

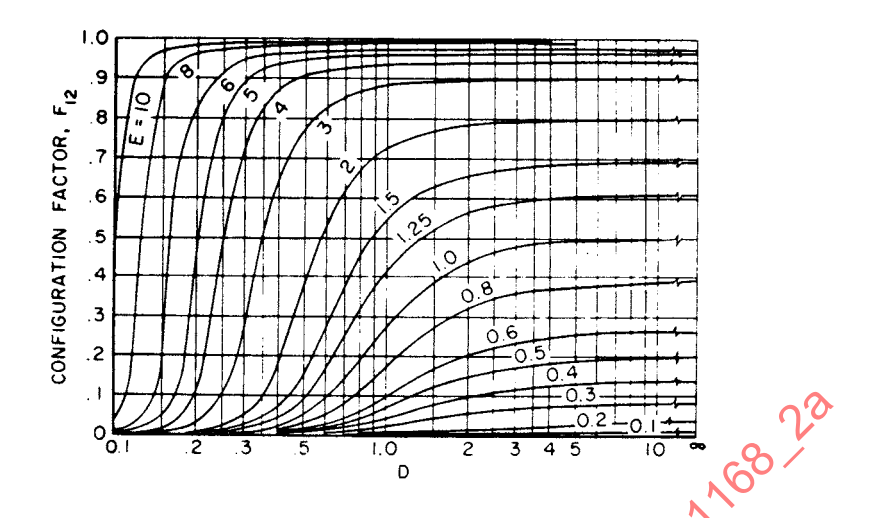


FIGURE 94 - Plane Point Source and Plane Circular Disk; Derivation of Equation 366

4.7.5.6 A Plane Point Source dA₁ and Any Surface A₂ Generated by an Infinitely Long Line Moving Parallel to Itself and the Plane of dA₁: This is shown in Figure 95.



FIGURE 95 - Line Moving Parallel to Itself and Plane at Point Source dA₁

FIGURE 95 - Line Moving Parallel to Itself and Plane at Point Source
$$dA_1$$

$$F_{12} = \frac{1}{2}(\cos\theta - \cos\omega) \tag{Eq. 370}$$

4.7.5.7 A Plane Point Source dA_1 and Any Infinite Plane A_2 With Planes of dA_1 and A_2 Intersecting at an Angle θ : Figure 96 illustrates this.

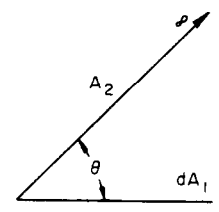


FIGURE 96 - Intersection of a Plane of Point Source dA₁ and an Infinite Plane A₂

$$F_{12} = \frac{1}{2}(1 + \cos\theta)$$
 (Eq. 371)

4.7.5.8 A Plane Point Source dA_1 and a Plane Disk A_2 , the Planes of dA_1 and A_2 Intersecting at an Angle of 90°: The centers of A_2 and dA_1 lie in a plane perpendicular to the two planes (see Figure 97).

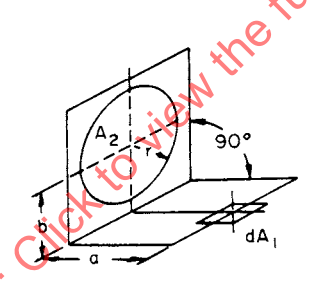


FIGURE 97 Untersection of Planes of a Point Source and a Disk

$$F_{12} = \frac{D}{2} \left[\frac{1 + R^2 + D^2}{\sqrt{(1 + R^2 + D^2)^2 - 4R^2}} \right] - 1$$
 (Eq. 372)

for which

$$\lim_{R \to 1} F_{12} = \left(\frac{1}{2} \frac{D^2 + 2}{\sqrt{D^2 + 4}} - D \right)$$
 (Eq. 373)

4.7.5.8 (Continued):

where:

$$R = \frac{r}{b}$$
 (Eq. 374)

$$D = \frac{a}{b}$$
 (Eq. 375)

4.7.5.9 A Plane Point Source dA₁ and a Right Circular Cylinder A₂ of Length I: The normal to dA₁ passes through the center of one end of the cylinder and is perpendicular to the axis of the cylinder, as in Figure 98.

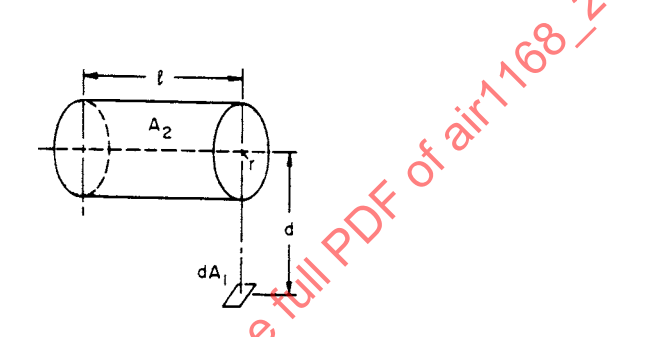


FIGURE 98 - Plane Point Source and Right Circular Cylinder

$$F_{12} = \frac{1}{\pi D} tan^{-1} \left(\frac{L}{\sqrt{D^2 - 1}} \right) + \frac{L}{\pi} \left[\frac{A - 2D}{D\sqrt{AB}} \cdot tan^{-1} \sqrt{\frac{A(D - 1)}{B(D + 1)}} - \frac{1}{D} \cdot tan^{-1} \sqrt{\frac{D - 1}{D + 1}} \right]$$
 (Eq. 376)

where:

$$A = (D+1)^2 + L^2$$
 (Eq. 377)

$$B = (D-1)^{2} + L^{2}$$
 (Eq. 378)

$$D = d r$$
 (Eq. 379)

$$L = r$$
 (Eq. 380)

See Figure 99 for a graphical solution of F_{12} (Equation 376).

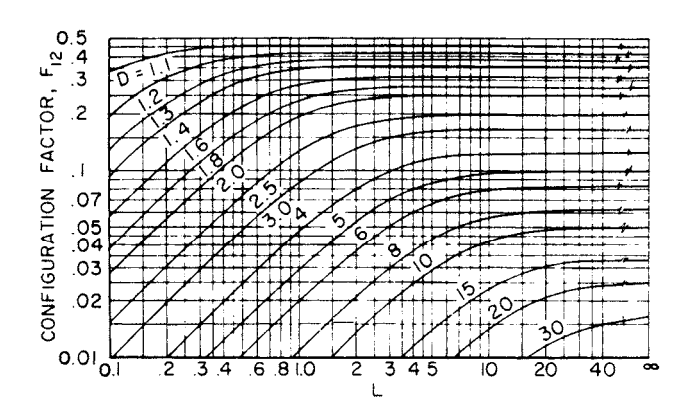


FIGURE 99 - Plane Point Source and Right Circular Cylinder; Derivation of Equation 376

4.7.5.10 Two Concentric Cylinders of Radius r and d and Length I With a Point Source dA₁ on the Inside of the Larger Cylinder at One End: The configuration factor is from the point source dA₁ on A₁ to A₂; A₁ does not include the ends of the annulus. See Figure 100.

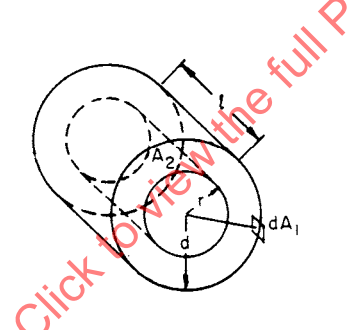


FIGURE 100 - Concentric Cylinders With the Larger Having an Inside Point Source

$$F_{12} = \frac{1}{2} \frac{1}{4D} + \frac{1}{\pi D} \left\{ L \tan^{-1} \sqrt{D^2 - 1} - \frac{1}{2} \tan^{-1} \left[\frac{L^2 - 4(D^2 - 1)}{4L\sqrt{D^2 - 1}} \right] - \left(\frac{L^2 + 2D^2}{\sqrt{L^2 + 4D^2}} \right) \tan^{-1} \left[\frac{\sqrt{(D^2 - 1)(L^2 + 4D^2)}}{L} \right] \right\}$$
(Eq. 381)

4.7.5.10 (Continued):

where:

$$D = \frac{d}{r}$$
 (Eq. 382)

$$L = \frac{1}{r}$$
 (Eq. 383)

See Figure 101 for a graphical solution of F_{12} (Equation 381).

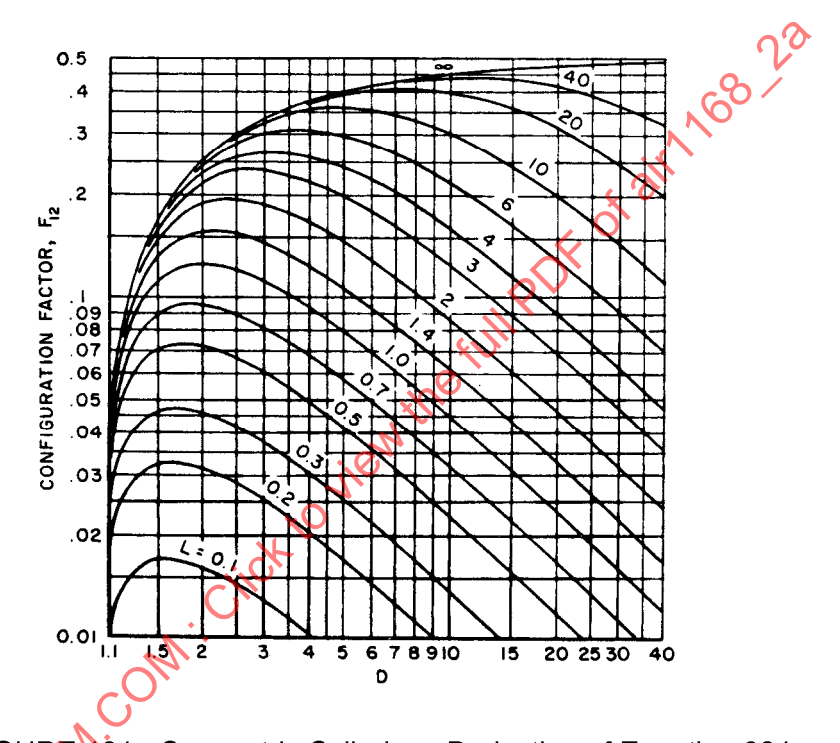


FIGURE 101 - Concentric Cylinders; Derivation of Equation 381

4.7.5.11 A Plane Point Source dA_1 and a Plane Trapezoid A_2 , the Planes of dA_1 and A_2 Intersecting at Angle ϕ : The source dA_1 lies on the side of the short leg of the trapezoid, as shown in Figure 102.

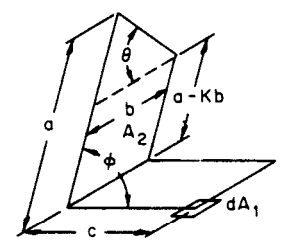


FIGURE 102 - Plane Point Source and a Plane Trapezoid

4.7.5.11 (Continued):

$$F_{12} = \frac{1}{2\pi} \left[\tan^{-1} \left(\frac{1}{L} \right) + \frac{N\cos\phi - L}{A} \left\{ \tan^{-1} \left[\frac{(K^2 + 1) + K(N - L\cos\phi)}{A} \right] \right\} - \tan^{-1} \left[\frac{K(N - L\cos\phi)}{A} \right] \right\} + \frac{\cos\phi}{B} \left[\tan^{-1} \left(\frac{L\cos\phi}{B} \right) + \tan^{-1} \left(\frac{N + L\cos\phi + K}{B} \right) \right] \right]$$

$$E:$$

$$A = \sqrt{(K^2 + 1)L^2 \sin^2\phi + (N - L\cos\phi)^2}$$

$$B = \sqrt{1 + L^2 \sin^2\phi}$$

$$N = a/b$$

$$L = c/b$$

$$\theta = \tan^{-1} K$$
(Eq. 386)
(Eq. 387)
(Eq. 388)

where:

$$A = \sqrt{(K^2 + 1)L^2 \sin^2 \phi + (N - L\cos \phi)^2}$$
 (Eq. 385)

$$B = \sqrt{1 + L^2 \sin^2 \phi}$$
 (Eq. 386)

$$N = a/b \tag{Eq. 387}$$

$$L = c/b$$
 (Eq. 388)

$$\theta = \tan^{-1} K \tag{Eq. 389}$$

See Figure 103 for a graphical solution of F_{12} (Equation 384).

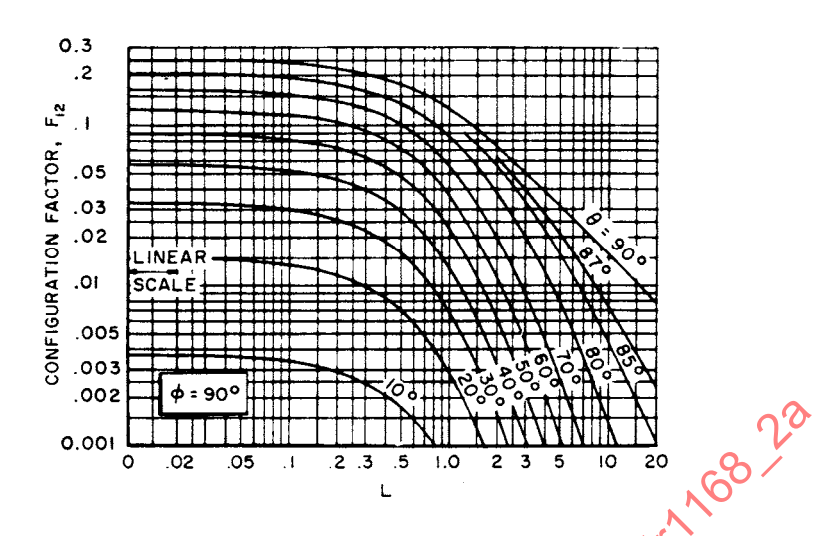


FIGURE 103 - Plane Point Source and a Plane Trapezoid; Derivation of Equation 384; φ = 90°

4.7.5.12 A Plane Point Source dA_1 and a Plane Trapezoid A_2 , the Planes of dA_1 and A_2 Intersecting at Angle ϕ : The source dA_1 lies on the side of the long leg of the trapezoid. See Figure 104.

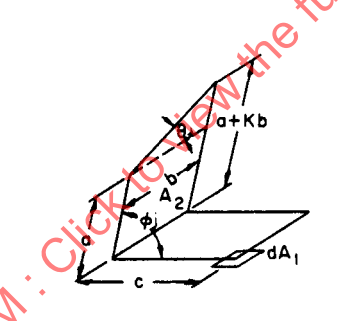


FIGURE 104-Intersecting Planes of a Point Source and a Trapezoid

$$F_{12} = \frac{1}{2\pi} \left(\tan \left(\frac{1}{L} \right) + \frac{\cos\phi}{B} \cdot \left[\tan^{-1} \left(\frac{N - L\cos\phi}{B} \right) + \tan^{-1} \left(\frac{L\cos\phi}{B} \right) \right]$$

$$\left(\frac{N + K)\cos\phi - L}{A} \left\{ \tan^{-1} \left[\frac{1 - K(N - L\cos\phi)}{A} \right] + \tan^{-1} \left[\frac{K(N + K - L\cos\phi)}{A} \right] \right\}$$
(Eq. 390)

4.7.5.12 (Continued):

where:

$$A = \sqrt{(K^2 + 1)L^2 \sin^2 \phi + (N + K - L \cos \phi)^2}$$
 (Eq. 391)

$$B = \sqrt{1 + L^2 \sin^2 \phi}$$
 (Eq. 392)

$$N = a/b \tag{Eq. 393}$$

$$L = c/b \tag{Eq. 394}$$

$$\theta = \tan^{-1}(K) \tag{Eq. 395}$$

See Figure 105 for a graphical solution of F_{12} (Equation 390).

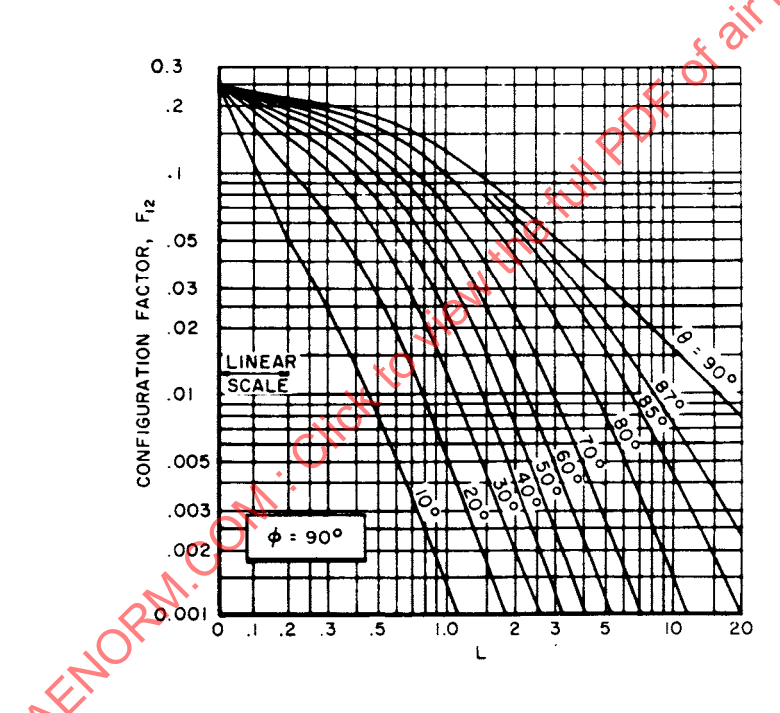


FIGURE 105 - Intersecting Planes of a Point Source and a Trapezoid; Derivation of Equation 390; φ = 90°

4.7.5.13 A Line Source dA_1 and a Plane Rectangle A_2 Parallel to the Plane of dA_1 With dA_1 Opposite One Edge of A_2 : Figure 106 illustrates this case.

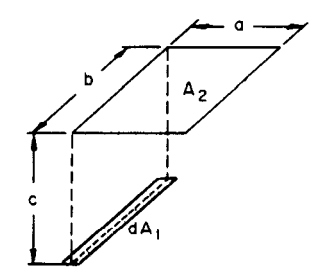


FIGURE 106 - Parallel Line Source Plane and Rectangle Plane, With One Opposite Edge

4.7.5.13 (Continued):

$$F_{12} = \frac{1}{\pi x} \left[\sqrt{1 + x^2} \tan^{-1} \left(\frac{y}{\sqrt{1 + x^2}} \right) - \tan^{-1} y + \frac{xy}{\sqrt{1 + y^2}} \cdot \tan^{-1} \left(\frac{x}{\sqrt{1 + y^2}} \right) \right]$$
 (Eq. 396)

for which

$$\lim_{x \to \infty} F_{12} = \frac{x}{2\sqrt{1 + y^2}}$$
 (Eq. 397)

$$\lim_{y \to \infty} F_{12} = \frac{1}{2} \left(\sqrt{1 + \frac{1}{x^2}} - \frac{1}{x} \right)$$
 (Eq. 398)

where:

$$x = \frac{b}{c} \tag{Eq. 399}$$

$$y = \frac{a}{c}$$
 (Eq. 400)

See Figure 407 for a graphical solution of F₁₂ (Equation 396).

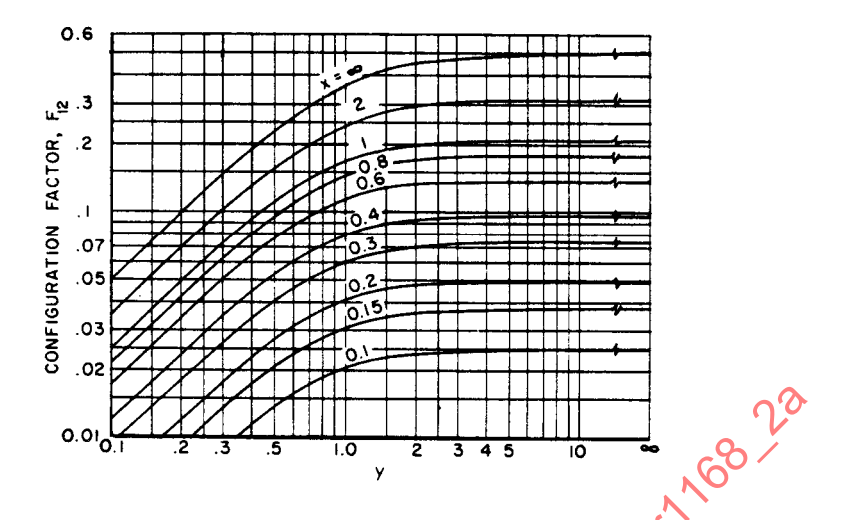


FIGURE 107 - Line Source and Rectangle Planes; Plot of Equation 396

4.7.5.14 A Line Source dA_1 and a Plane Rectangle A_2 That Intersects the Plane of dA_1 at an Angle ϕ : Refer to Figure 108.

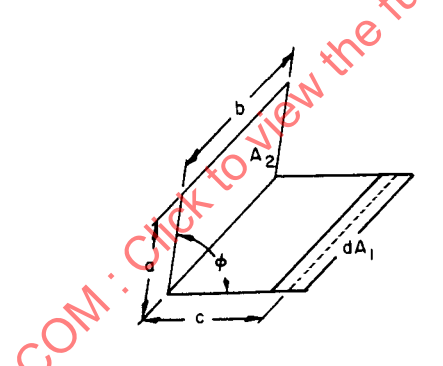


FIGURE 108 - Intersection of Planes of a Line Source and Rectangle

4.7.5.14 (Continued):

$$\begin{split} F_{12} &= \frac{1}{\pi} \bigg\{ tan^{-1} \bigg(\frac{1}{L} \bigg) + L \frac{sin^2 \phi}{2} ln \bigg[\frac{L^2 (L^2 - 2NL \cos \phi + 1 + N^2)}{(1 + L^2)(L^2 - 2NL \cos \phi + N^2)} \bigg] \\ &- L sin \phi \cos \phi \bigg[\frac{\pi}{2} - \phi + tan^{-1} \bigg(\frac{N - L \cos \phi}{L \sin \phi} \bigg) \bigg] \\ &+ cos \phi \sqrt{1 + L^2 sin^2 \phi} \cdot \bigg[tan^{-1} \bigg(\frac{N - L \cos \phi}{\sqrt{1 + L^2 sin^2 \phi}} \bigg) + tan^{-1} \bigg(\frac{L \cos \phi}{\sqrt{1 + L^2 sin^2 \phi}} \bigg) \bigg] \\ &+ \frac{N \cos \phi - L}{\sqrt{L^2 - 2NL \cos \phi + N^2}} \cdot tan^{-1} \bigg(\frac{1}{\sqrt{L^2 - 2NL \cos \phi + N^2}} \bigg) \bigg\} \end{split}$$

for which

$$\frac{1}{\sqrt{L^{2} - 2NL\cos\phi + N^{2}}} \cdot \tan^{-1}\left(\frac{1}{L^{2} - 2NL\cos\phi + N^{2}}\right)$$

$$\lim_{N \to \infty} F_{12} = \frac{1}{\pi} \tan^{-1}\left(\frac{1}{L}\right) + \frac{L\cos\phi}{\pi} \cdot \left\{\frac{\sin^{2}\phi}{2\cos\phi} \ln\left(\frac{L^{2}}{1 + L^{2}}\right) - \sin\phi(\pi - \phi)\right\}$$

$$+ \frac{\sqrt{1 + L^{2}\sin^{2}\phi}}{L} \cdot \left[\frac{\pi}{2} + \tan^{-1}\left(\frac{L\cos\phi}{1 + L^{2}\sin^{2}\phi}\right)\right]$$
(Eq. 402)

$$\lim_{L \to \infty} F_{12} = 0 \tag{Eq. 403}$$

$$\lim_{t \to 0} F_{12} = \frac{1}{2} (1 + \cos \phi)$$
 (Eq. 404)

$$\lim_{N \to 0} F_{12} = 0$$
 (Eq. 405)

where

$$\lim_{L \to \infty} F_{12} = 0$$

$$\lim_{L \to \infty} F_{12} = 0$$

$$\lim_{L \to 0} F_{12} = \frac{1}{2}(1 + \cos\phi)$$

$$\lim_{L \to 0} F_{12} = 0$$
(Eq. 404)
(Eq. 405)
(Eq. 405)
(Eq. 406)
(Eq. 407)

$$L = \frac{c}{b}$$
 (Eq. 407)

See Figures 109 through 113.

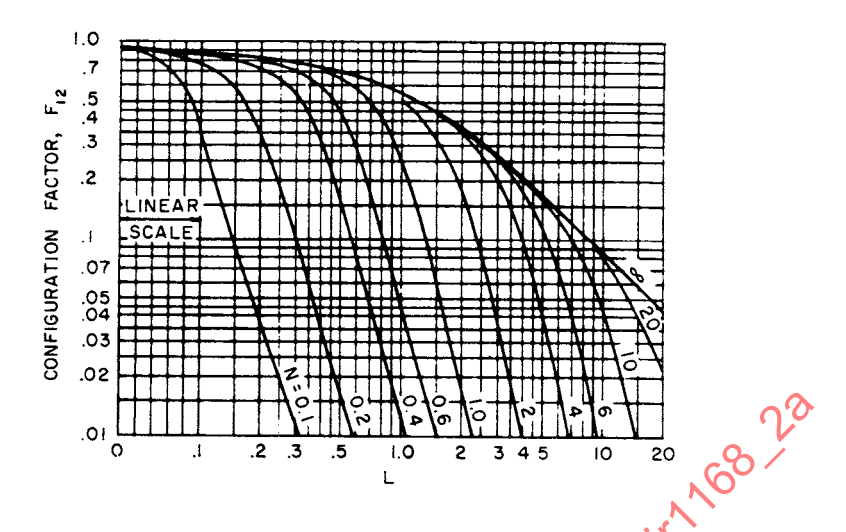


FIGURE 109 - Line Source and Rectangle Planes; Intersection at $\phi = 30^{\circ}$

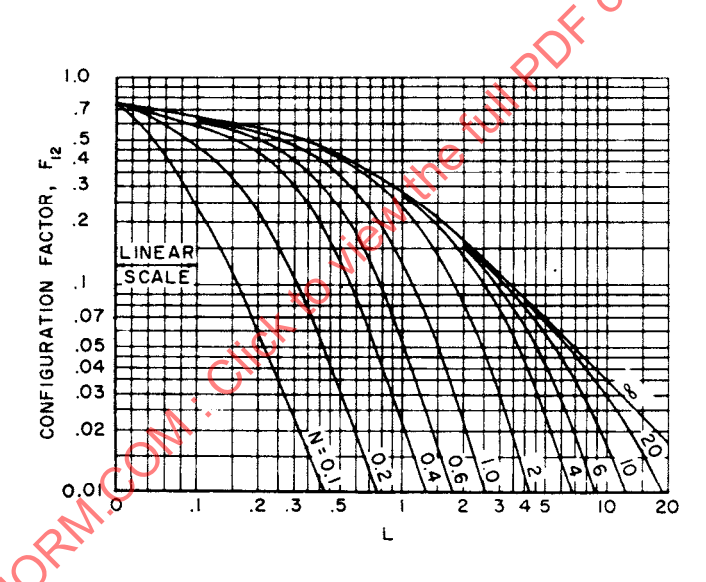


FIGURE 110 - Line Source and Rectangle Planes; Intersection at φ = 60°

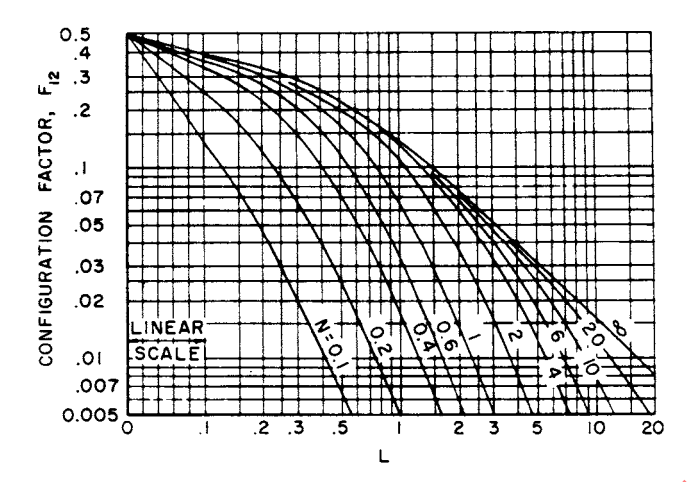


FIGURE 111 - Line Source and Rectangle Planes; Intersection at \$\phi = 90^\circ\$ (See Figure 108)

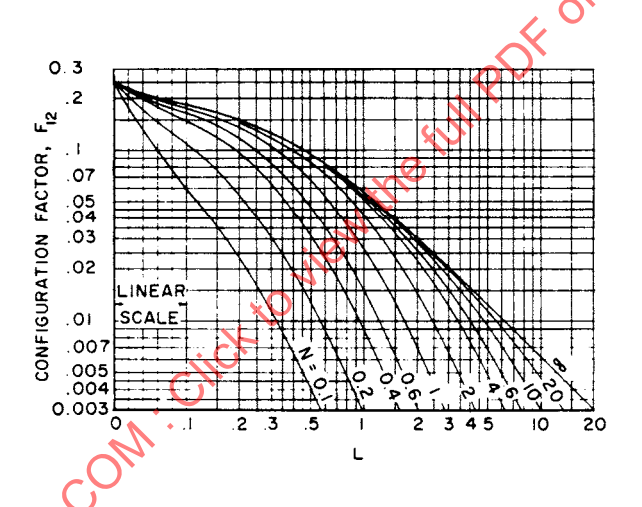


FIGURE 112 - Line Source and Rectangle Planes; Intersection at ϕ = 120 $^{\circ}$ (See Figure 108)

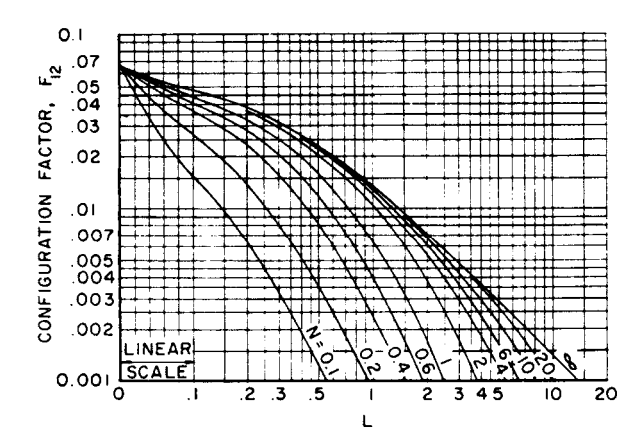
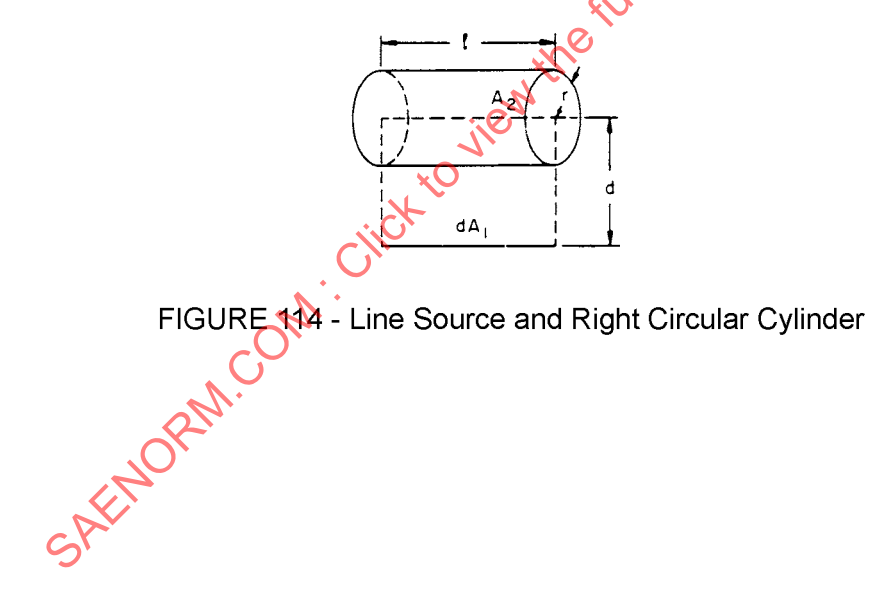


FIGURE 113 - Line Source and Rectangle Planes; Intersection at φ = 150° (See Figure 108)

4.7.5.15 A Line Source dA₁ and a Right Circular Cylinder A₂, Both of Length I: The normal through each end of the source passes through and is normal to the centerline of the cylinder at the ends. See Figures 114 and 115, where D = d/r and L = I/r.



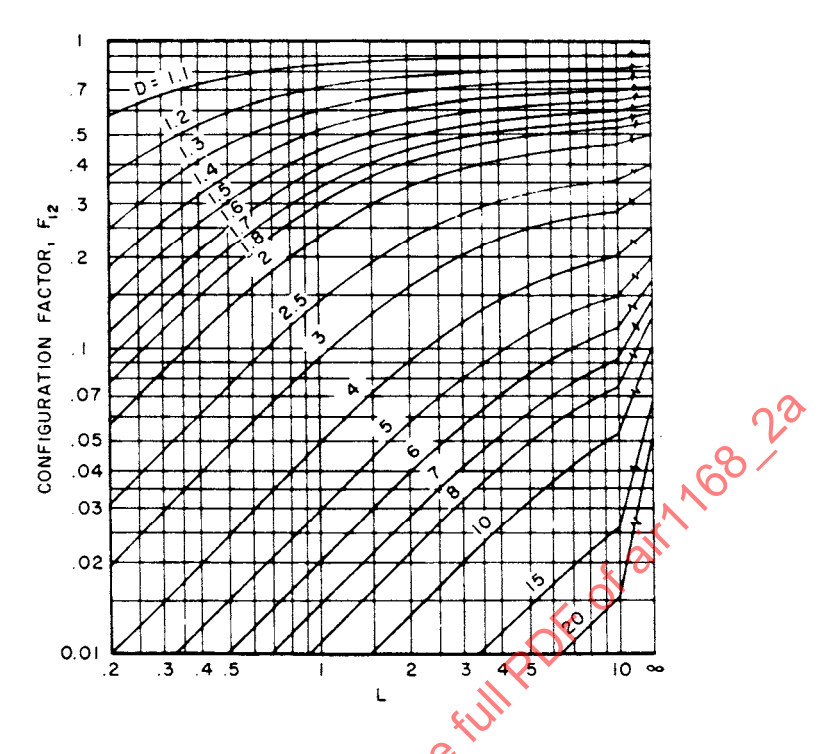


FIGURE 115 - Line Source and Right Circular Cylinder

4.7.5.16 Two Concentric Cylinders of Radii r and d and Length I With a Line Source dA₁ on the Inside of the Large Cylinder: A₁ is the area of the inner surface of the large cylinder (shown in Figure 116 with zero wall thickness), A₂ is the area of the outer surface of the small cylinder (zero wall thickness), and A₃ is the cross sectional area at the ends of the cylinders, as shown in Figure 116. See Figure 117 for F₁₁ where D = d/r and L = I/r.

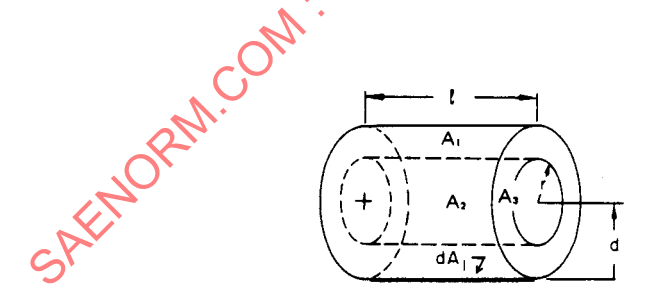
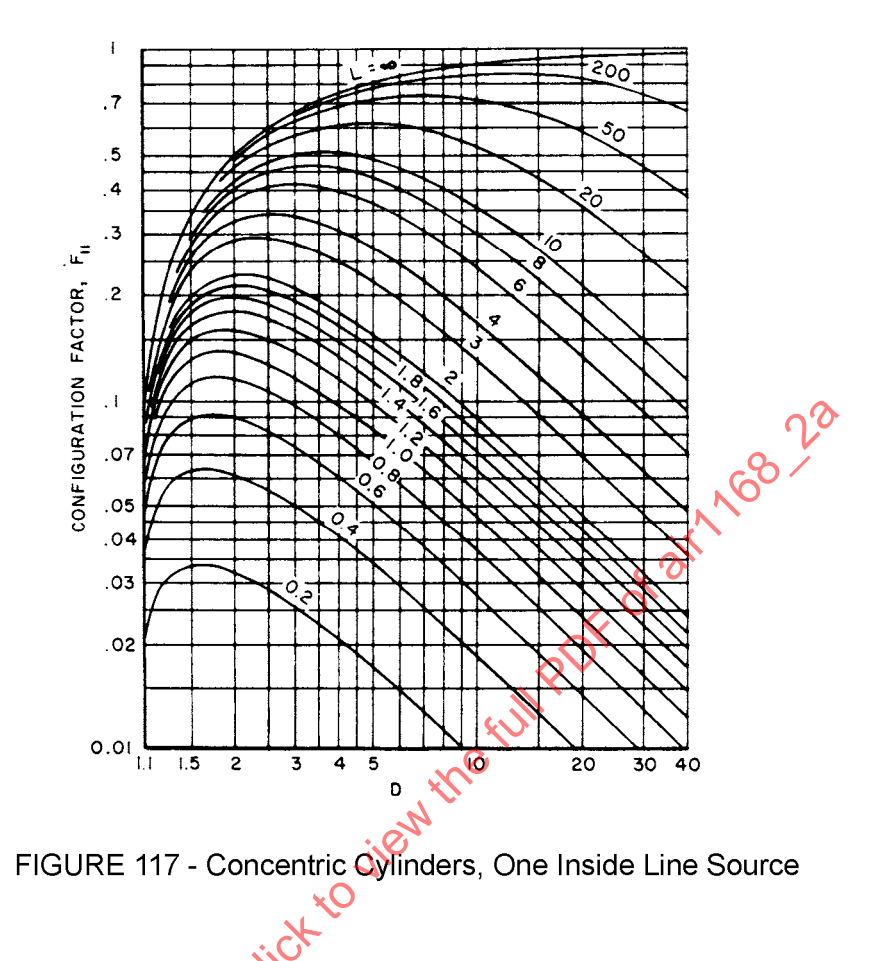


FIGURE 116 - Concentric Cylinders With Line Source Inside the Larger One A₁ = $2\pi dl$, A₂ = $2\pi rl$, A₃ = $\pi (d^2-r^2)$



4.7.5.16 (Continued):

$$F_{dA-3} = \frac{1}{2}(1 - F_{11} - F_{12})$$
 (Eq. 408)

where:

F₁₂ is obtained from Figure 115

4.7.5.17 An Infinitely Long Cylinder A₁ and an Infinite Plane A₂, Mutually Parallel: See Figure 118.

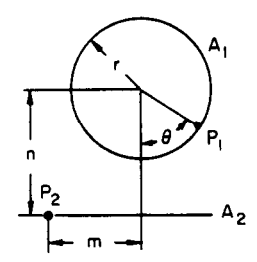


FIGURE 118 - Infinitely Long Cylinder and Infinite Plane, Mutually Parallel

$$F_{P_1 - A_2} = \frac{1}{2}(1 + \cos\phi)$$
 (Eq. 409)

$$F_{P_2-A_1} = \frac{N}{(N^2-M^2)}$$
 (Eq. 410)

where:

$$M = \frac{m}{r}$$
 (Eq. 411)

$$N = \frac{n}{r}$$
 (Eq. 412)

4.7.5.18 Identical, Parallel, Directly Opposed Rectangles A₁ and A₂: See Figure 119.

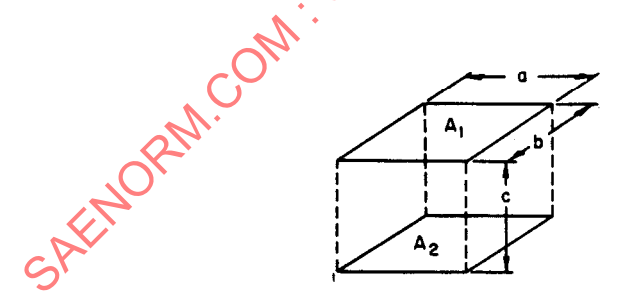


FIGURE 119 - Identically Parallel, Directly Opposed Rectangles

4.7.5.18 (Continued):

$$F_{12} = \frac{2}{\pi x y} \left\{ \ln \left[\frac{(1+x^2)(1+y^2)}{1+x^2+y^2} \right]^{1/2} + y \sqrt{1+x^2} \tan^{-1} \left(\frac{y}{\sqrt{1+x^2}} \right) + x \sqrt{1+y^2} \tan^{-1} \left(\frac{x}{\sqrt{1+y^2}} \right) - y \tan^{-1} y - x \tan^{-1} x \right\}$$
(Eq. 413)

for which

$$\lim_{x \to \infty} F_{12} = \sqrt{1 + \frac{1}{y^2}} - \frac{1}{y}$$
 (Eq. 414)

$$\lim_{y \to \infty} F_{12} = \sqrt{1 + \frac{1}{x^2}} - \frac{1}{x}$$
 (Eq. 415)

$$\lim_{x,y\to\infty} F_{12} = 1$$
 (Eq. 416)

where:

$$\lim_{x \to \infty} F_{12} = \sqrt{1 + \frac{1}{y^2} - \frac{1}{y}}$$

$$\lim_{y \to \infty} F_{12} = \sqrt{1 + \frac{1}{x^2} - \frac{1}{x}}$$

$$\lim_{x,y \to \infty} F_{12} = 1$$

$$\lim_{x,y \to \infty} F_{12} = 1$$
(Eq. 416)
$$x = \frac{b}{c}$$
(Eq. 417)
$$y = \frac{a}{c}$$
(Eq. 418)
$$(Eq. 418)$$

$$y = \frac{a}{c}$$
 (Eq. 418)

See Figure 120.

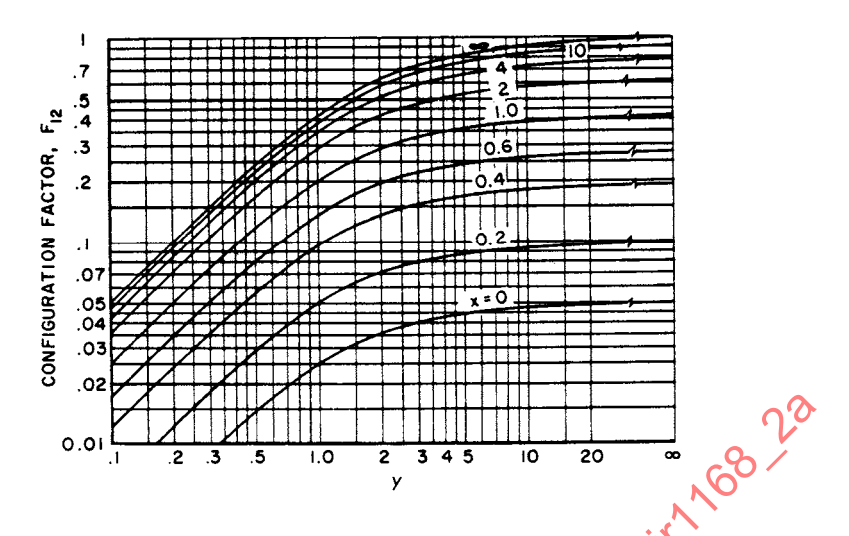


FIGURE 120 - Parallel, Opposed Rectangles; Per Equation 413

4.7.5.19 Two Rectangles A_1 and A_2 With One Common Edge and Included Angle ϕ : See Figure 121.

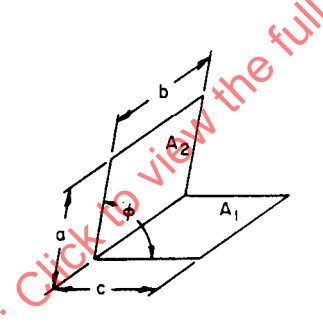


FIGURE 121 - Two Rectangles With Common Edge and Included Angle

For $\phi = 90^{\circ}$:

$$F_{12} = \frac{1}{\sqrt{L}} \left(L tan^{-1} \left(\frac{1}{L} \right) + N tan^{-1} \left(\frac{1}{N} \right) - \sqrt{N^2 + L^2} tan^{-1} \left(\frac{1}{\sqrt{N^2 + L^2}} \right) + \frac{1}{4} ln \left\{ \left[\frac{(1 + L^2)(1 + N^2)}{(1 + L^2 + N^2)} \right] \left[\frac{L^2(1 + L^2 + N^2)}{(1 + L^2)(L^2 + N^2)} \right]^{L^2} \left[\frac{N^2(1 + L^2 + N^2)}{(1 + N^2)(L^2 + N^2)} \right]^{N^2} \right\} \right)$$
(Eq. 419)

4.7.5.19 (Continued):

for which

$$\lim_{L \to \infty} F_{12} = 0 \tag{Eq. 420}$$

$$\lim_{N \to \infty} F_{12} = \frac{1}{\pi} \left[tan^{-1} \left(\frac{1}{L} \right) + \frac{1}{4L} \cdot ln(1 + L^2) - \frac{L}{4} ln \left(\frac{1 + L^2}{L^2} \right) \right]$$
 (Eq. 421)

where:

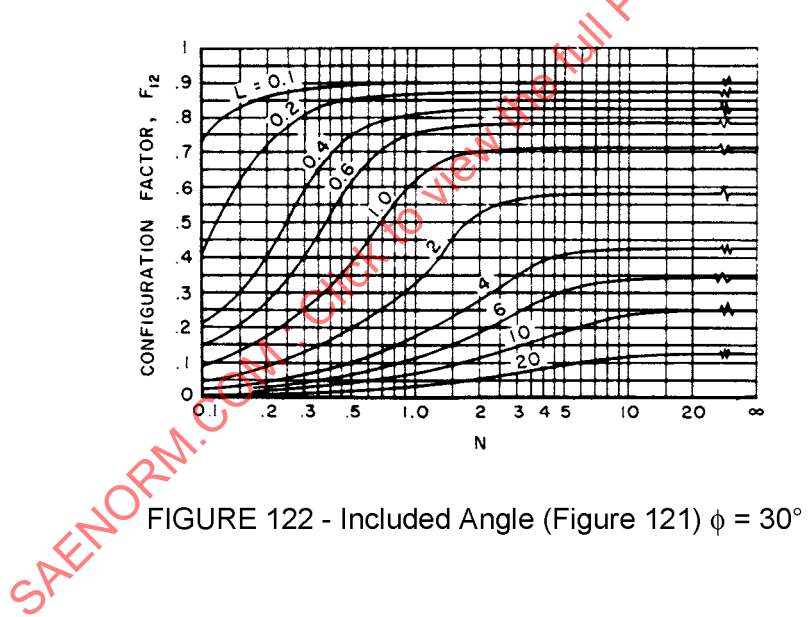
$$N = \frac{a}{b}$$
 (Eq. 422)

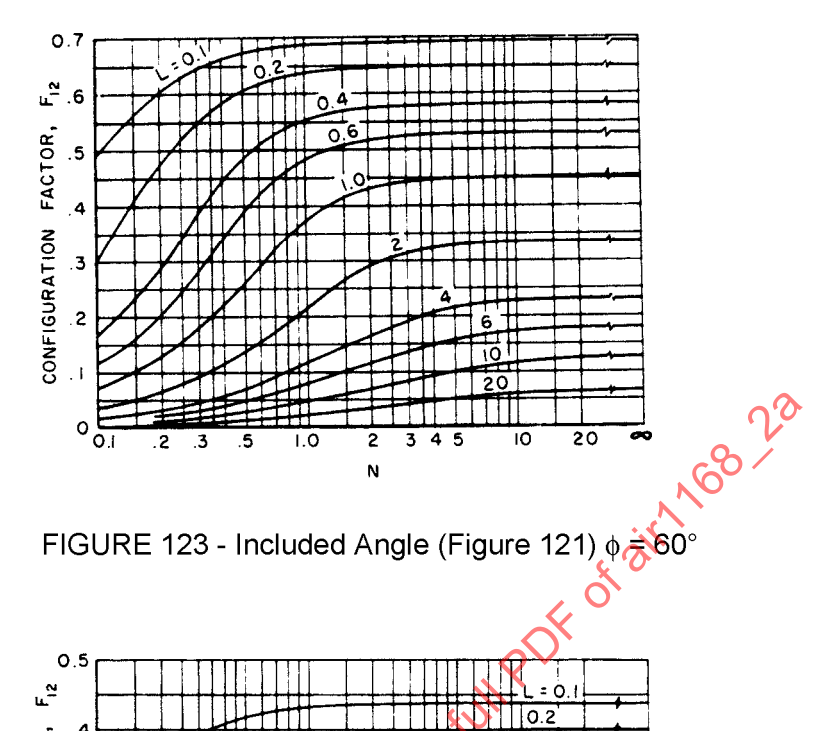
 $L = \frac{c}{b}$ (Eq. 423)

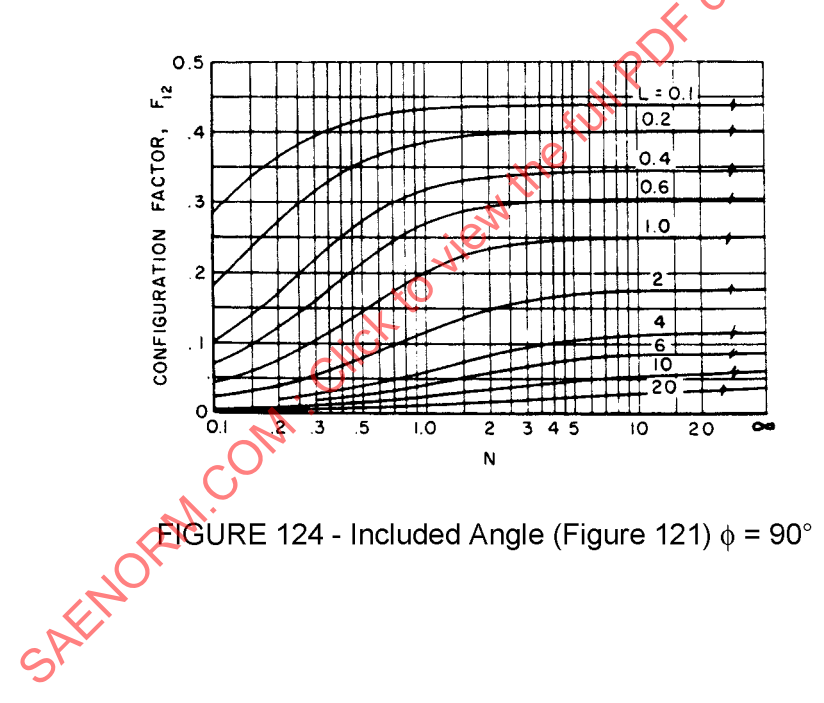
ures 122 through 126.

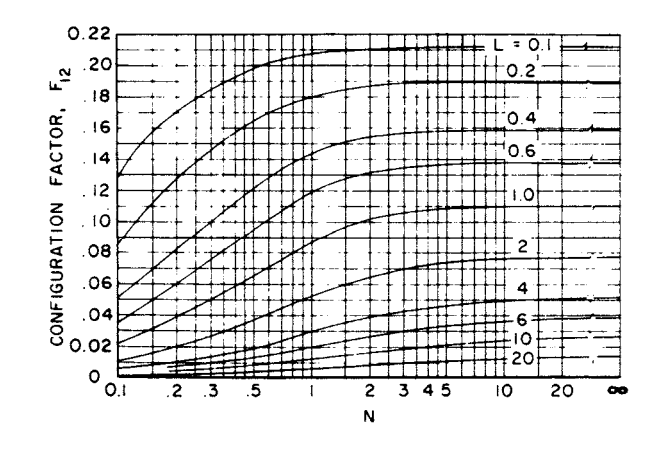
$$L = \frac{c}{b}$$
 (Eq. 423)

See Figures 122 through 126.









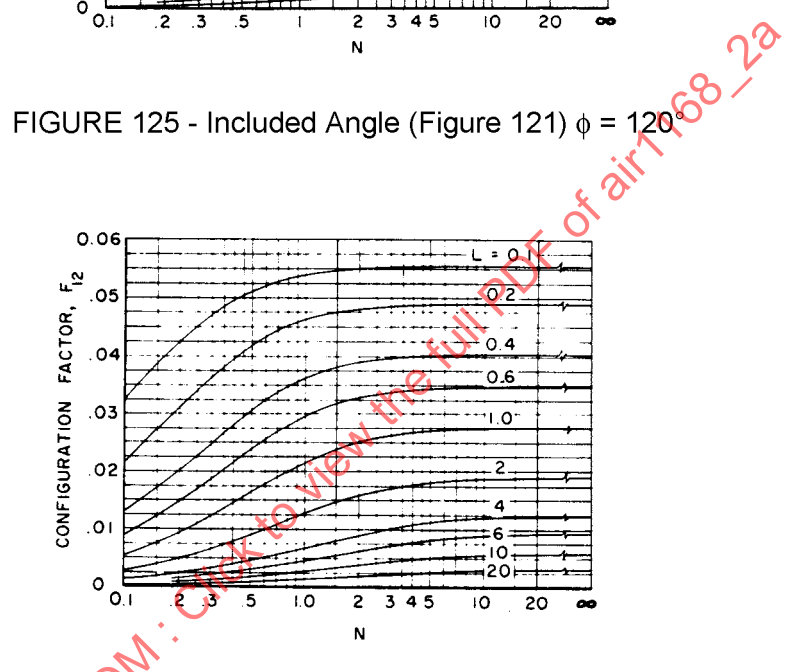


FIGURE 126 - Included Angle (Figure 121) $\phi = 150^{\circ}$

4.7.5.20 Parallel, Directly Opposed, Plane Circular Disks: Figure 127 illustrates this case.

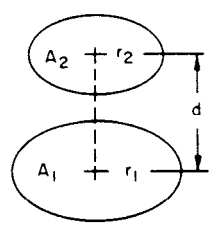


FIGURE 127 - Parallel, Directly Opposed, Plane Circular Disks

4.7.5.20 (Continued):

$$F_{12} = \frac{1}{2}(x - \sqrt{x^2 - 4E^2D^2})$$
 (Eq. 424)

where:

$$x = 1 + (1 + E^2)D^2$$
 (Eq. 425)

$$E = r_2/d (Eq. 426)$$

$$D = d/r_1 \tag{Eq. 427}$$

See Figure 128.

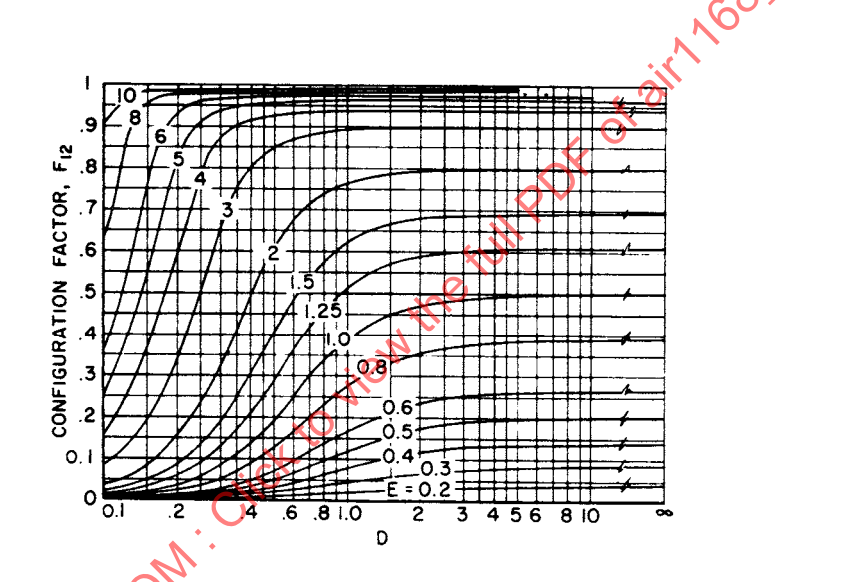


FIGURE 128 - Parallel, Opposed Plane Circular Disks; Per Equation 424

4.7.5.21 Two Parallel, Concentric Cylinders A₁ and A₂ of Radii r₁ and r₂ and Infinite Length: See Figure 129

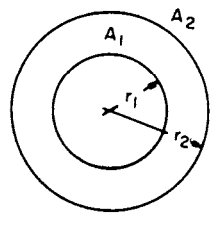


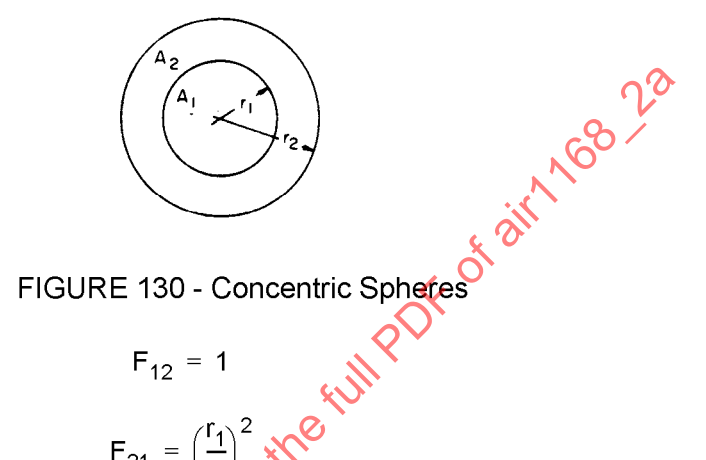
FIGURE 129 - Parallel, Concentric Cylinders

4.7.5.21 (Continued):

$$F_{12} = 1$$
 (Eq. 428)

$$F_{21} = \frac{r_1}{r_2}$$
 (Eq. 429)

4.7.5.22 Two Concentric Spheres A_1 and A_2 of Radii r_1 and r_2 : See Figure 130.



$$F_{12} = 1$$
 (Eq. 430)

F₁₂ = 1 (Eq. 430)
$$F_{21} = \left(\frac{r_1}{r_2}\right)^2$$
(Eq. 431)
Plane of an Infinitely Long Rectangle of Width I – m:

4.7.5.23 An Infinite Cylinder Parallel to the Plane of an Infinitely Long Rectangle of Width I – m: See Figure 131.

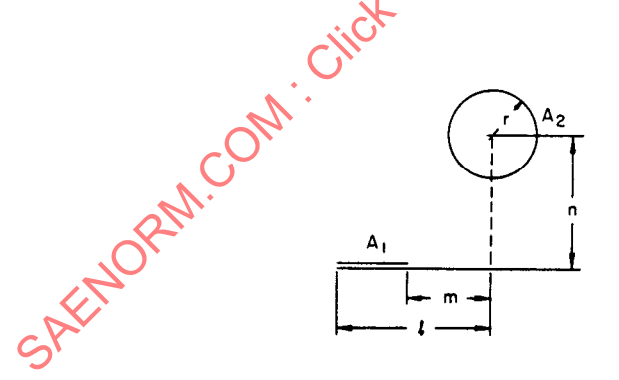


FIGURE 131 - Cylinder Parallel to Plane of Rectangle

$$F_{12} = \left[\frac{1}{(L-M)}\right] \tan^{-1}\left(\frac{L}{N}\right) - \tan^{-1}\left(\frac{M}{N}\right)$$
 (Eq. 432)

4.7.5.23 (Continued):

For M = 0,

$$F_{12} = \left(\frac{1}{L}\right) \tan^{-1}\left(\frac{L}{N}\right)$$
 (Eq. 433)

where:

$$N = \frac{n}{r}$$
 (Eq. 434)

$$M = \frac{m}{r}$$
 (Eq. 435)

$$L = \frac{1}{r}$$
 (Eq. 436)

4.7.6 Celestial Radiation: The solar heating flux outside the earth's atmosphere varies from 406 to 442 Btu/h-ft². The albedo (or reflectivity) of the earth for solar radiation averages approximately 0.39 over the earth's surface. If it is assumed that the earth is in near-equilibrium with all space, the effective average temperature of the earth is given by

Solar energy absorbed = Energy radiated
$$S(1-\rho)\pi R^2 = 4\pi R^2 \epsilon \sigma T_{earth}^4$$
 (Eq. 437) arth, ft

where:

R = Radius of earth, ft

S = Solar heating flux, Btu/h-ft2

 ρ = Albedo, dimensionless

 ε = Radiation emittance, dimensionless

Solution of the relation yields T_{earth} = 444 °R, which is the atmospheric temperature at approximately 22,000 ft.

4.7.7 Radiation from Luminous Gases: One of the most common problems in this category occurs in industrial furnace design, in which (1) a portion of the enclosure constitutes a heat source or sources (such as a fuel bed, a carborundum muffler, or a row of electrical resistors), (2) another portion is a heat sink or sinks (such as the surface of a row of billets, the tubes of a tube still, or boiler furnace), and (3) another portion is an intermediate refractory connecting wall system, which is a heat sink only to the extent that it loses heat by conduction through its walls to the furnace exterior.

4.7.7 (Continued):

If the convection from gases on the outside of the refractory walls is approximately equal to the loss by conduction through the walls, the net radiant heat interchange of the inside surface of the walls with the rest of the furnace interior is zero. Since the radiation incident upon the refractory walls is generally so enormous compared with the difference between gas convection and wall conduction, the assumption that the net radiant heat transfer at the wall surface is zero is an excellent one. It simplifies enormously the problem of heat transfer from source to sinks and the effect thereon of the refractory sources.

The configuration factors F_{12} discussed previously in this section may be used or a more complete set of factors can be found in Chapter 4 of Reference 6.

4.7.8 Radiation from Nonluminous Gases: If black body radiation passes through a gas mass containing, for example, carbon dioxide, absorption occurs in certain regions of the infrared spectrum. Conversely, if the gas mass is heated, it radiates in those same wavelength regions. Of the gases encountered in heat transfer equipment, carbon monoxide, the hydrocarbons, water vapor, carbon dioxide, sulfur dioxide, ammonia, hydrogen chloride, and the alcohols are among those with emission bands of sufficient magnitude to merit consideration. Curves showing the emissivity of these gases are found in Reference 6.

The treatment of radiation from powdered coal or atomized oil flames, from dust particles in flames, and from flames made luminous by the thermal decomposition of hydrocarbons to soot involves the evaluation of radiation from clouds of particles.

The combustion process by which soot luminosity is produced is a complex one, far from being completely understood. It is presently not possible to predict the flame luminosity in a proposed furnace, but a simpler approach is often feasible.

The significant property of a flame is its emission rate, separable into its temperature and emissivity. If a furnace for a given operation exists for study, measurements can be made with an optical pyrometer and a total radiation pyrometer, which are of assistance in improving performance or in designing a new furnace of different capacity or shape. For a complete discussion of this method, see Reference 6.

5. REFERENCES:

- 1. R. V. Churchill, Introduction to Complex Variables and Applications, McGraw-Hill, 1948.
- 2. H. S. Carslaw and J. C. Jaeger, Conduction of Heat in Solids, Oxford Press, 1947.
- 3. M. Jakob, Heat Transfer, John Wiley, 1949.
- 4. L. R. Ingersoll, O. J. Zobel, and A. C. Ingersoll, Heat Conduction, McGraw-Hill, 1948.
- 5. L. M. K. Boelter, V. H. Cherry, H. H. Johnson, and R. C. Martinelli, Heat Transfer Notes, University of California Press, 1948.
- 6. W. H. McAdams, Heat Transmission (3rd ed.), McGraw-Hill, 1954.
- H. Schlichting, Boundary Layer Theory, McGraw-Hill, 1955.
- 8. E. R. G. Eckert, Heat and Mass Transfer (2nd ed.), McGraw-Hill, 1959.
- 9. E. R. G. Eckert, "Survey on Heat Transfer at High Speeds," WADC TR 54-70, April, 1954.
- J. A. Fay, F. R. Riddell, and N. H. Kemp, "Stagnation Point Heat Transfer in Dissociated Air Flow," Jet Propulsion, June, 1957.
- 11. J. A. Fay and F. R. Riddell, "Theory of Stagnation Point Heat Transfer in Dissociated Air," J. Aero. Sciences, February, 1958.
- 12. S. C. Sommer and B. J. Short, "Free-Flight Measurements of Turbulent Boundary Layer Skin Friction in the Presence of Severe Aerodynamic Heating at Mach Numbers from 2.8 to 7.0," NACA TN 3391, 1955.
- 13. L. Lees, "Laminar Heat Transfer over Blunt Bodies at Hypersonic Speeds," Jet Propulsion, April, 1956.
- E. R. G. Eckert and J. N. B. Livingood, "Method for Calculation of Laminar Heat Transfer in Air Flow Around Cylinders of Arbitrary Cross Section (Including Large Temperature Differences and Transpiration Cooling)," NACA Report 1118, 1953.
- 15. J. P. Hartnett, E. R. G. Eckert et al., "Simplified Procedures for the Calculation of Heat Transfer to Surfaces with Non-Uniform Temperatures," WADC Technical Report 56-373, December, 1956.
- A. K. Oppenheim, "Radiation Analysis by the Network Method," ASME Trans., May, 1956.
- 17. D. C. Hamilton and W. R. Morgan, "Radiant-Interchange Configuration Factors," NACA TN 2836, December, 1952.

- 5. (Continued):
 - 18. AICHE, Sept. 1958, p. 330.
 - 19. W. M. Kays and A. L. London, Compact Heat Exchangers, National Press, 1955.
 - 20. M. Jakob and W. N. Dow, "Heat Transfer from Cylindrical Surfaces to Air in Parallel Flow With and Without Unheated Starting Section," ASME Trans. Vol. 68, 1946, pages 123-134.

Chen the full PDF of air 1,68 28 Chen the full PDF of air 1,68 28

SECTION 1D - MASS TRANSFER

1. INTRODUCTION:

1.1 Scope:

1.1.1 Relationship Between Convection and Evaporation: For a liquid evaporating into a gaseous atmosphere (see Figure 132) it can be shown that there is a relationship between the mass transfer that takes place by evaporation and the heat transfer between the liquid and the gas. It is convenient to express this relationship as a dimensionless ratio, that is, h_o/k_mS which is the Lewis number N_{Le} (symbols are defined in 2.1.1), where:

$$h_o = \frac{q}{A(t_s - t_\infty)}$$
 (Eq. 438)

$$k_{\rm m} = \frac{W}{A(\omega_{\rm s} - \omega_{\infty})}$$
 (Eq. 439)

S = Specific humid heat
=
$$c_{pB} + c_{pA}\omega$$
 (Eq. 440)

For air-water mixtures,

$$S = 0.24 + 0.45\omega$$
 (Eq. 441)

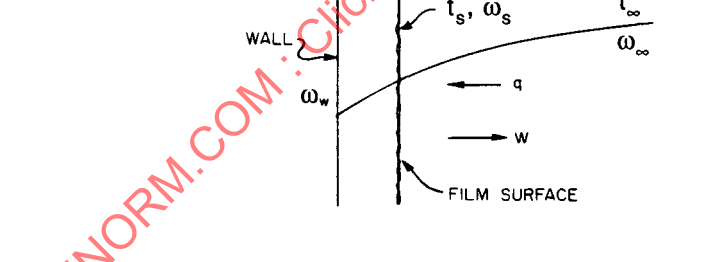


FIGURE 132 - Diagram of a Liquid Evaporating Into a Gaseous Atmosphere

Figure 133 gives values of h_o/k_mS for various liquids evaporating into air as a function of $kM_A/D_{AB}(\rho g)_AM_BS$. For air-water mixtures at low humidities, $h_o/k_mc_p = 0.89$.

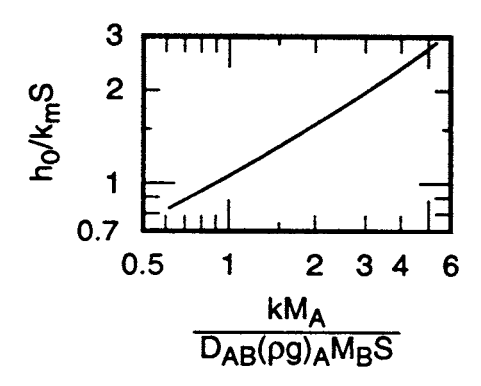


FIGURE 133 - Dimensionless Relationship Between Evaporation and Convection (Reference 1)

2. SURFACE EVAPORATION INTO A GAS ATMOSPHERE:

2.1 Diffusion:

Diffusion is the transport of molecules of a given substance through another substance, due solely to the concentration gradients of the given substance. Only gaseous diffusion of a vapor through a noncondensing gas is considered here.

2.1.1 Nomenclature:

A = Area, ft^2

c_p = Specific heat of dry gas at constant pressure, Btu/lb-°F

c_{pA} = Specific heat of component A, Btu/lb-°F c_{pB} = Specific heat of component B, Btu/lb-°F

 D_{AB} = Diffusivity of component A into noncondensable component B, ft²/h

d_p = Diameter of the sphere ft G_m = Mass velocity, lb-mole/h-ft²

 h_0 = Convective heat transfer coefficient, Btu/h-ft²-°F

K = Boltzmann constant, ft-lb/°R

 $\begin{array}{lll} k & = Thermal\ conductivity\ of\ mixture,\ Btu-ft/h-ft^2-°F \\ k_g & = Mass\ transfer\ coefficient,\ lb-mole/h-ft^2-atm \\ k_m & = Mass\ transfer\ coefficient,\ lb\ dry\ gas/ft^2-h \end{array}$

L_e = Latent heat of evaporation, Btu/lb L_s = Latent heat of sublimation, Btu/lb

M = Molecular weight, lb/lb-mole

M_A = Molecular weight of component A, lb/lb-moleM_B = Molecular weight of component B, lb/lb-mole

N_{Le} = Lewis number, dimensionless
 N_{Sc} = Schmidt number, dimensionless
 P = Absolute pressure of mixture, psia

P_{A1} = Partial pressure of component A at point 1, psia

2.1.1 (Continued):

 P_{A2} = Partial pressure of component A at point 2, psia P_{B} = Barometric pressure, psia = Log mean effective pressure differential of component B, psia P_{BM} = Partial pressure of component B at point 1, psia P_{B1} = Partial pressure of component B at point 2, psia P_{B2} = Vapor pressure at the surface, psia P_{∞} Vapor pressure of final mixture, psia = Heat transferred, Btu/h q = Heat absorbed by evaporation, Btu/h view the full PDF of air 168 28 = Total heat transferred by convection and evaporation, Btu/h q_{tot} = Mol distance parameter, angstrom r = Mol separation factor, dimensionless r_{AB} = $(r_A + r_B)/2$, where r_A and r_B are obtained from Table 5 = Universal gas constant R = 0.729 ft³-atm/lb-mole-°F = Specific humid heat, Btu/lb-°F S $= c_{pB} + c_{pA}\omega$ Т = Temperature, °R $\mathsf{T}_{\mathsf{crit}}$ = Critical temperature, °R = Normal boiling point temperature, °R T_{NBP} = Surface temperature, °F = Wall temperature. °F t_{w} = Final mixture temperature, °F t_{∞} = Specific volume, ft³/lb = Weight of liquid evaporated, lb/h W W_A = Weight of vapor diffused, lb/h-ft² Χ = Correlation factor for evaporation and convection, dimensionless Ζ = Distance of travel of component, ft $f(\theta)$ = Collision function obtained from Figure 134, dimensionless = Density of component A, lb/ft³ $(\rho g)_A$ = Energy mol interaction, ft-lb = Energy mol interaction ϵ_{AB} $= \sqrt{\varepsilon_{\Delta}\varepsilon_{B}}$, ft- $|b\rangle$ = Absolute humidity, lb-vapor/lb-dry gas ω = Absolute humidity at film surface, lb-vapor/lb-dry gas ω_{s} Absolute humidity at wall, lb-vapor/lb-dry gas ω_{w} = Absolute humidity remote from surface, lb-vapor/lb-dry gas ω_{∞}

2.1.2 Diffusion in Laminar Flow: The diffusion of component A through the noncondensing component B is given by

$$W_{A} = \frac{D_{AB}P}{RTZP_{BM}}(P_{A1} - P_{A2})\frac{M_{A}}{14.7}$$
 (Eq. 442)

where:

 P_{BM} = Log mean effective pressure differential of component B between points 1 and 2

$$= (P_{B1} - P_{B2})/[ln(P_{B1}/P_{B2})]$$
 (Eq. 443)

$$P_{B1} = P - P_{A1}$$
 (Eq. 444)

$$P_{B2} = P - P_{A2}$$
 (Eq. 445)

and

$$[\ln(P_{B1}/P_{B2})] \qquad (Eq. 443)$$

$$(Eq. 444)$$

$$(Eq. 445)$$

$$P_{BM} = \frac{(P-P_{A1}) - (P-P_{A2})}{\ln[(P-P_{A1})/(P-P_{A2})]}$$

$$= \frac{P_{A2} - P_{A1}}{\ln[(P-P_{A1})/(P-P_{A2})]} \qquad (Eq. 446)$$

$$= \frac{P_{A2} - P_{A1}}{\ln[(P-P_{A1})/(P-P_{A2})]} \qquad (Eq. 446)$$

$$= 0.02195 T^{3/2} (\frac{1}{1} + \frac{1}{1})^{1/2}$$

The diffusivity of the system (D_{AB}) is given by

$$D_{AB} = \frac{0.02195 \text{ T}^{3/2} \left(\frac{1}{M_A} + \frac{1}{M_B}\right)^{1/2}}{P(r_{AB})^2 [f(\theta)]}$$
 (Eq. 447)

The values of $f(\theta)$ can be found from Figure 134, using values of ε/K from Table 5; values of r are also given in Table 5.

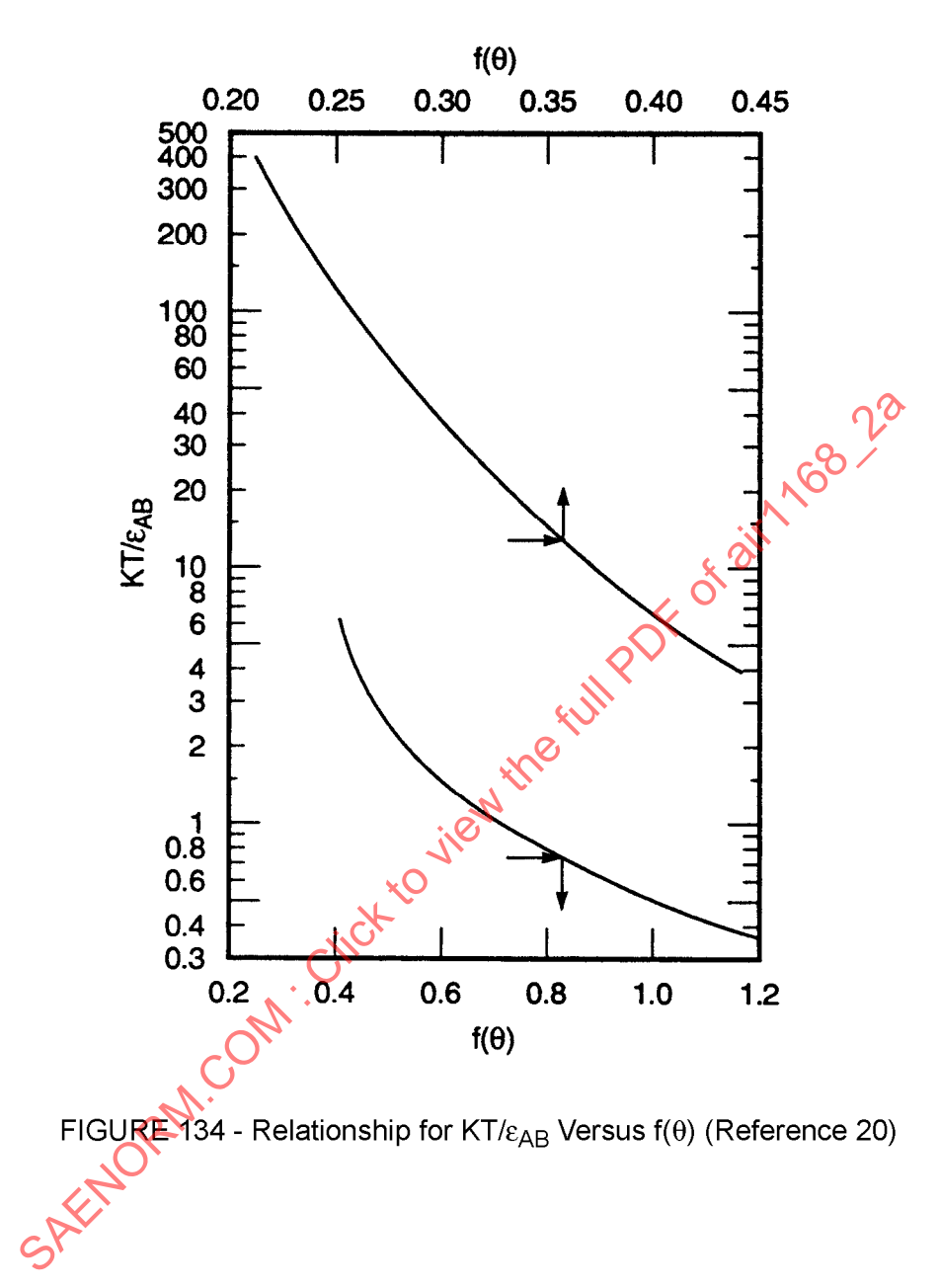


TABLE 5 - Values of Diffusion Factors¹

Gas	(ε/K), °R	r
Air	174.4	3.617
H ₂	60.0	2.968
N ₂	164.5	3.681
CO₂	342.0	3.996
N₂O	396.0	3.879
NO	214.0	3.470
CH₄	246.0	3.882
O2	204.0	3.433
co	198.5	3.590
Α	223.0	3.418
Ne	64.25	2.800
He	10.85	2.700

¹Ref. 2.

2.1.2 (Continued):

If necessary, values of ϵ/K and r can be estimated, using the following empirical relationships:

$$\varepsilon/K = 0.75T_{crit}$$
 (Eq. 448)

$$\varepsilon/K = 1.39T_{NBP} \tag{Eq. 449}$$

$$r = 0.833 \left(\frac{\text{vM}}{62.428} \right)^{1/3}$$
 (Eq. 450)

Illustrative Example of Diffusion in Laminar Flow: Estimate the diffusivity of O_2 through CO at 14.7 2.1.3 psia and 492 °R.

Solution:

$$M_{\odot} = 32$$

$$M_{\rm B} = 28$$

From Table 5 for O

$$(\epsilon/K)_A = 204 \, ^{\circ}R \text{ and } r_A = 3.433$$

and for CO,

$$(\epsilon/K)_B = 198.5 \, ^{\circ}R$$
 and $r_B = 3.590$

2.1.3 (Continued):

Then

$$\begin{split} \frac{\epsilon_{AB}}{K} &= \sqrt{\left(\frac{\epsilon}{K}\right)_{A} \left(\frac{\epsilon}{K}\right)_{B}} \\ &= \sqrt{(204)(198.5)} = 202 \\ \frac{KT}{\epsilon_{AB}} &= \frac{492}{202} = 2.43 \end{split}$$

From Figure 134, $f(\theta) = 0.504$; therefore

$$r_{AB} = \frac{r_A + r_B}{2} = \frac{3.433 + 3.590}{2}$$

= 3.512

$$D_{AB} = \frac{(0.02195)(492)^{3/2}(1/32 + 1/28)^{1/2}}{(14.7)(3.512)^2(0.504)}$$
$$= 0.683 \text{ ft}^2/\text{h}$$

 $r_{AB} = \frac{r_A + r_B}{2} = \frac{3.433 + 3.590}{2}$ = 3.512 and substitution into Equation 447 yields $D_{AB} = \frac{(0.02195)(492)^{3/2}(1/32 + 1/28)^{1/2}}{(14.7)(3.512)^2(0.504)}$ = 0.683 ft²/h Alternately, the critical properties of the gases might have been used to estimate the quantities. Thus, for O_2 , Thus, for O_2 ,

$$T_{crit}$$
 = 278 °R and v_{crit} = 145.5 ft³/lb

Therefore

$$(\epsilon/K)_A = (0.75)(278) = 208 \,^{\circ}R$$

$$r_A = (0.833) \left[\frac{(145.5)(32)}{62.428} \right]^{1/3}$$

$$= 3.50$$

Similarly, for CO,

$$T_{crit} = 242 \,^{\circ}\text{R}$$
 and $v_{crit} = 200 \,^{\circ}\text{ft}^3/\text{lb}$ $(\epsilon/\text{K})_A = (0.75)(242) = 182 \,^{\circ}\text{R}$ $r_B = (0.833) \left\lceil \frac{(200)(28)}{62.428} \right\rceil^{1/3} = 3.72$

These values lead to D_{AB} equal to 0.647 ft²/h as opposed to 0.683 ft²/h.